A NEW DIMENSION IN FLUORINE CHEMISTRY: FLUORINE IN CLOSE INTERACTIONS

by

Mark D. Struble

A dissertation submitted to Johns Hopkins University in conformity with the requirements for the degree of Doctor of Philosophy

Baltimore, Maryland
July, 2016

Abstract

This work attempts to shed some light on some of the fundamental chemistry utilized by C-F bonds in organofluorine compounds, with special care to noncovalent interactions. A fluorinated sesquinorbornane scaffold was the template for the majority of the studies owing to its rigid conformation and ability to be modified. Thanks to those two attributes, the properties of C-F bonds were observed under various conditions in a multitude of different conformations. Through that work, the C-F bond was observed to take part in S_N1 reactions through anchimeric assistance. Even more interesting is the anchimeric assistance is facilitated through a positively charged fluoronium intermediate. In addition, the conformation of the scaffold, allows other functional groups to be placed in close proximity to the C-F bond. After making a series of molecules with different functional groups, the through-space interaction of the C-F bond with the proximal C-H was investigated. A correlation between proton-fluorine coupling constants and the interaction's strength was observed. The positioning also allowed the observation of a strong hydrogen bonding interaction between the fluorine and an alcohol. While the hydrogen bond appears strong by most spectroscopic methods, IR spectroscopy shows little to no shift when compared to a control molecule. This appears to be a rare case of bond compression from steric strain cancelling out bond relaxation from hydrogen bonding, a so called "no-shift" bond. In an attempt to be sure our system can be used to generate hydrogen bonds, a hydrogen bond between an alcohol and a nonconjugated π-system was investigated. Owing to the reduction of steric strain in the molecule a strong hydrogen bond was observed accompanied by a characteristic red shift in the IR spectrum. Interestingly the red shift was nearly 189 cm^{-1}, which is much larger than other observed examples of this type of interaction. In order to bolster our claims about a fluoronium ion intermediate, an in depth investigation into the reactivity of the fluoronium system was reported. This was done through several rate studies, control reactions and isotopic labeling experiments. All of which indicate that the fluoronium is the most likely intermediate. Finally another example of fluorine acting as a directing group was investigated. Specifically, a C-F bond was found to influence a Diels-Alder reaction between a fluorinated dienophile and a borole so that one product was favored to a substantial degree.

Advisor: Professor Thomas Lectka

Reader: Professor Chris Falzone

Reader: Professor John P. Toscano

For My Family

Acknowledgements

I would first like to thank my advisor, Professor Thomas Lectka, for all of his patience and assistance during my time at JHU. He has been an endless font of advice and unique stories that have helped me along throughout my graduate career. I am especially envious of his ability to spot interesting chemical transformations in experiments that at first appeared to be dead ends. I would also like to thank Professors Chris Falzone and John Toscano for serving on my committee as well as being readers for this dissertation. I have had many meaningful conversations with both and their advice has greatly helped me on the path to my future career. I would also like to thank Professor Gary H. Posner for his generosity, whether it was for lending a chemical that we didn't have or letting us use an apparatus.

I am very thankful for the many members of the Lectka group that I have had the chance to get to know during my time here. I would like to thank Dr. Jeremy Erb for his patience in training me back when I knew next to nothing about chemical synthesis. Thanks are also due to Dr. Mike Scerba for laying the groundwork for my first project as well as graciously answering any questions I had. I would especially like to thank Dr. Steve Bloom and Cody Pitts who I worked with for the majority of my time here. They were there for all the highs and lows and have been great friends. For the more recent additions of Max Holl, Desta Bume and Liangyu Guan I am happy to have gotten to know you and I can leave knowing the lab is in good hands. I would also like to extend a thank you to the numerous undergraduates who have worked for me these last five years. You all have given me a great deal of experience training others and forced me to improve my own methods so I could lead by example. For financial support I must thank the JHU chemistry department for providing me with Gary H. Posner and Rudolph Sonneborn fellowships.

Most importantly I want to thank my family for their endless support during my time here. I could not wish for a better one. It is to them that this dissertation is dedicated.

Publications Drawing Upon this Dissertation

1) Struble, M. D.; Scerba, M. T.; Siegler, M.; Lectka, T. "Evidence for a Symmetrical Fluoronium Ion in Solution" *Science* **2013**, *340*, 57-60.

2) Struble, M. D.; Strull, J.; Patel, K.; Siegler, M. A.; Lectka, T. "Modulating "Jousting" C-F---H-C Interactions with a Bit of Hydrogen Bonding" *J. Org. Chem*. **2014**, *79*, 1-6.

3) Struble, M. D.; Kelly, C.; Siegler, M. A.; Lectka, T. "Search for a Strong, Virtually "No-Shift" Hydrogen Bond: A Cage Molecule with an Exceptional OH···F Interaction" *Angew. Chem. Int. Ed.* **2014**, *53*, 8924-8928.

4) Struble, M. D.; Holl, M. G.; Coombs, G.; Siegler, M. A.; Lectka, T. "Synthesis of a Tight Intramolecular OH---Olefin Interaction, Probed by IR, ^{1}H NMR, and Quantum Chemistry" *J. Org. Chem.* **2015**, *80*, 4803-4807.

5) Struble, M. D.; Holl, M. G.; Scerba, M. T.; Siegler, M. A.; Lectka, T. "Search for a Symmetrical C-F-C Fluoronium Ion in Solution: Kinetic Isotope Effects, Synthetic Labeling, and Computational, Solvent, and Rate Studies" *J. Am. Chem. Soc.* **2015**, *137*, 11476-11490.

6) Struble, M. D.; Liangyu Guan.; Siegler, M. A.; Lectka, T. "A C-F Bond Directed Diels-Alder Reaction" *J. Org. Chem.* **2016**, (in review).

Publications not Included in this Dissertation

1) Holl, M. G.; Struble, M. D.; Singal, P.; Siegler, M. A.; Lectka, T. "Positioning a Carbon-Fluorine Bond over the π Cloud of an Aromatic Ring: A Different Type of Arene Activation" *Angew. Chem. Int. Ed.* **2016,** *55*, 8266-8269.

2) Holl, M. G.; Struble, M. D.; Siegler, M. A.; Lectka, T. "The Close Interaction of a C-F Bond with a Carbonyl π-System: Attractive, Repulsive, or Both?" *J. Fluorine Chem.* **2016,** *188*, 126-130.

Table of Contents

Chapter 1: Generation of a Symmetrical Fluoronium Ion in Solution

Chapter 2: Through-space "Jousting" Interactions

Chapter 3: A Strong "No-Shift" O-H---F Interaction

List of Tables

List of Figures

List of Schemes

List of Abbreviations

Å	Angstroms
asym	asymmetrical
aq	aqueous
B3	B3LYP/6-311++G**
B97	ωB97XD/6-311+G**
BCP	bond critical point
°C	degrees Celsius
CCl_4	carbon tetrachloride
CCSD	coupled cluster with a full treatment singles and doubles
$CDCl_3$	deuterated chloroform
CN	cyano
cm^{-1}	wavenumbers
Cy	cyclohexyl
CSD	Cambridge Structural Database
DA	Diels-Alder
DAST	diethylaminosulfur trifluoride
DCM	dichloromethane
DFT	density functional theory
DMAD	dimethylacetylene dicarboxylate
DMAP	4-dimethylaminopyridine
DMF	N,N-dimethylformamide
DTBP	2,6-di-*tert*-butylpyridine
EtOAc	ethyl acetate
EtOH	ethanol
equiv	equivalent
ΔG_{act}	Gibbs Free Energy of activation

h	hours
ΔH_{act}	enthalpy of activation
H-bond	hydrogen bond
HF	Hartree-Fock method
HFIP	1,1,1,3,3,3-hexafluoro-2-propanol
HRMS	high-resolution mass spectroscopy
Hz	Hertz
iPr	isopropyl
IR	Infrared
kcal	kilocalorie
kcal/mol	kilocalorie per mole
KIE	kinetic isotope effect
LAH	lithium aluminium hydride
M	molarity
Me	methyl
MeCN	acetonitrile
MeOH	methanol
mp	melting point
MP2	second order Møller–Plesset perturbation theory
NMR	nuclear magnetic resonance
OH	alcohol
ρ	electron density
PCC	pyridinium chlorochromate
PFTB	perfluoro-*tert*-butyl alcohol
Ph	phenyl
ppm	parts per million
QTAIM	quantum theory of atoms in molecules
RDS	rate determining step

ΔS_{act}	entropy of activation
S_N1	unimolecular nucleophilic substitution reaction
S_N2	bimolecular nucleophilic substitution reaction
$S_N2(e)$	extended bimolecular nucleophilic substitution reaction
S_Ni	internal nucleophilic substitution reaction
sym	symmetrical
Tf	triflate (trifluoromethanesulfonate)
TFAA	trifluoroacetic anhydride
TFE	2,2,2-trifluoroethanol
THF	tetrahydrofuran
TLC	thin-layer chromatography
TS	transition state
v/v	volume to volume

Chapter 1

Generation of a Symmetrical Fluoronium Ion in Solution

1.1 Introduction.

To new students of organic chemistry, the story of the halonium ions is almost magical; these strange species seem to be counterintuitive to everything that was previously taught about bonding by such electronegative atoms. Perhaps the most familiar of the haloniums is the bromonium ion; in its formation, bromine, an electronegative atom that normally attaches itself to carbon through a single bond, becomes instead a formally positively charged member of a bromocyclopropane ring.[1] The first hint of its existence came through stereochemical studies, namely the strong preference for *trans*-addition of dibromine to double bonds. Analogous behavior was documented in chlorination reactions as well.[2] In a short span of time, the viability of symmetrical chloronium, bromonium and iodonium[3] ions, whose stability increases in that order, became well established. However, there was a notable absence; namely, it was not clear that fluorine, the most electronegative atom by most measures, could form a fluoronium ion in which equal bonding exists between carbon atoms, i.e. $[C—F—C]^+$. Given the explosive growth in the importance of fluorine to synthetic chemistry,[4] the pharmaceutical industry,[5] and biochemistry[6] of late, the problem is especially timely – that is, to what extent can divalent fluorine be compelled to withstand a formally positively charged environment in solution?

Assuming that the fluoronium would share similar properties with other halonium ions, it should be able to engage in analogous modes of bonding. For example, bromonium ions can form three-membered rings, they can be acyclic, or the bromine can be part of a larger ring. Thus, the fluorine atom also can be imagined as a part of a fluoracyclopropane, with similar bonding interactions (Figure 1.1). We also note that the system may not be symmetric (i.e. both C-F interactions equivalent) depending on substituents; at some point, the asymmetrical fluoronium can devolve into an electrostatic interaction. Such a scenario can be anticipated when the C-F bond approaches its normal length.

Herein we document the previous work we built upon and our thought processes leading up to our system designed to observe the fluoronium species. In addition we lay out our evidence for the conclusions we have reached. Overall, our guiding principle derives from the saying that a strong claim must be met by

similar evidence – and as the ions we report herein are not directly observed, as much indirect evidence as possible has been amassed.

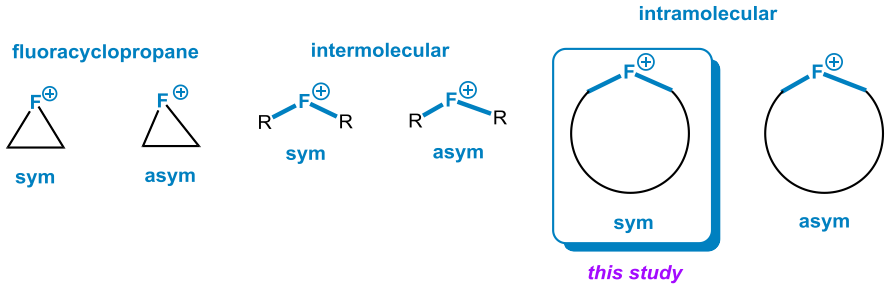

Figure 1.1 Putative fluoronium configurations.

1.2 Precedents.

Due to their unique nature, research on fluoronium ions is supported by a diverse foundation of precedents. In the gas phase, Morton et al. have generated a cationic fluoracyclopropane whose existence was confirmed by a neutral product study (Figure 1.2).[7] In more recent work, Dopfer and Solca characterized F-protonated fluorobenzene **2** by IR spectroscopy, also in a gas phase study.[8] Moving to solution phase chemistry, Gabbai et al. have reported the synthesis of a carbocation engaging in an interaction with a neighboring C-F bond in the 1,8-disubstituted naphthalene system **3**.[9] Although not a fluoronium per se, this remarkable species undergoes rapid fluoride shifts as witnessed by NMR equilibration at elevated temperatures. The disilane analog **4** reported by Müller et al., on the other hand, possesses equivalent distances between Si and F.[10] These works stand in contrast to a notable paper by Olah et al. in which the authors demonstrated that cation **6** isomerizes in solution strictly through methyl group shifts rather than the putative fluoronium shift depicted in **5**; this result suggests that achieving a reversible fluoride-shifting system in a small ring would be a challenge.[11] In loose regard to the intramolecular asymmetrical case (Figure 1.1), we reported a system that undergoes irreversible fluoride shifts that are initiated by aryl cations.[12] More recently Erdélyi et al. were able to observe a unique, asymmetric $[N\text{-}F\text{—}N]^+$ interaction by trapping it as its bispyridine complex.[13] Peterson et al.[14] have observed a fluoride shift initiated by a vinylic cation; whether this shift occurred through asymmetric fluoronium transition states or intermediates is unclear. There are also claims in the literature of putative

symmetrical diarylfluoronium ions (**7**), although considerations of theory and stability would seem to rule both out.[15]

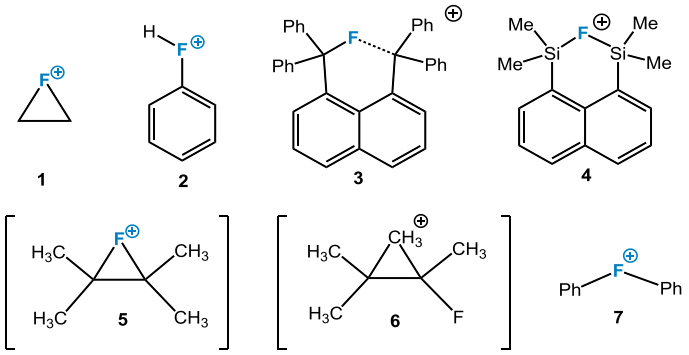

Figure 1.2 Previously reported bridged fluorine species.

1.3 Our design process.

Whenever one has to design a new system it pays to start simple. However, although the simplest system – $[Me\text{-}F\text{-}Me]^+$ - was a stable minimum computationally, the idea that it could exist in solution under any circumstances is far-fetched. In order to imagine a viable system that could at least be generated as a reactive intermediate, certain design constraints must be considered: i) the fluoronium ion should form intramolecularly;[16] ii) the fluorine atom should be positioned between secondary carbons (primary would render a system very unstable, whereas tertiary carbons are less likely to form a symmetrical fluoronium);[17] iii) we posit that if an ether linkage can fit comfortably between the two carbon atoms, the isoelectronic, formally positively-charged fluorine should as well.

Bearing these conditions in mind, we determined that a cage hydrocarbon[18] would be an ideal framework to anchor a fluoronium interaction. Initially, we screened commonly occurring cages that could be modified to become a fluoronium ion. Figure 1.3 shows the theoretical fluoronium molecules as energetic minima (vacuum at B3LYP/6-311++G** [abbrev. "B3"] or ωB97XD/6-311+G** ["B97"] levels). The structures had to match our original criteria, along with providing identical C-F bond lengths at the energetic minimum. Structure **8** is based on cubane,[19] **9** on adamantane,[20] the more fanciful **10** is a distorted dodecahedrane dicationic cage, in which the fluorine engages in interactions with three carbon atoms;[21] two equivalently, the third more distantly. The tetracation **11**, derived from a gaslamp-type skeleton, of course, would likely live only in imagination, confirming that theory can only guide us so far.

On the other hand, the most synthetically reasonable in our eyes was the basic sesquinorbornane structure **12**, which we imagined (substituted with an anhydride) could be constructed through a series of diastereoselective Diels-Alder reactions.

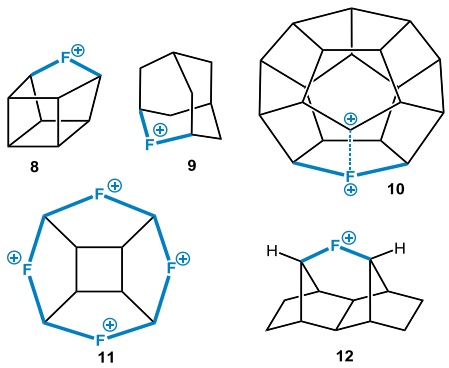

Figure 1.3 Possible fluoronium ion cages.

Why was our first choice to ensconce a fluoronium within a cage? Perhaps by releasing the restraints that the cage imposes, piece by piece, we can gain insight (Figure 1.4). For example, fluoronium **13** is stable relative to kinetically accessible isomers at all HF, MP2, and DFT based levels of theory investigated. Likewise, if we remove the anhydride group, the fluoronium interaction appears to be sustained. However, if we eliminate the ethano-bridges, thus removing strain from the system and increasing potential degrees of freedom, we see that classical isomer **15** becomes more stable relative to fluoronium **14**, which is still a defined intermediate and not a transition state (B97, H_2O solvent dielectric).

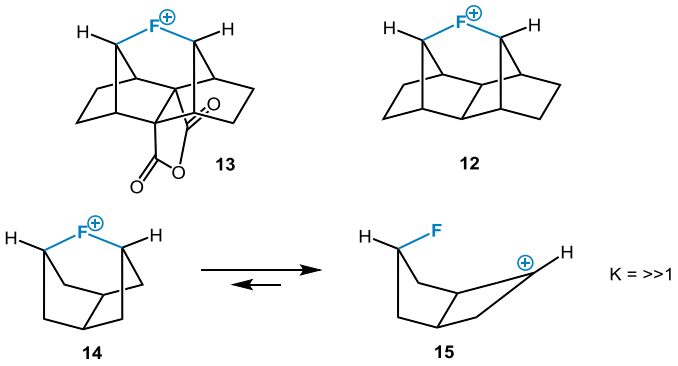

Figure 1.4 Loosening restraints in the fluoronium system.

Another insight was provided by calculations on the intermolecular model, $[\text{i-Pr-F-i-Pr}]^+$ (B97, vacuum). Fully optimized, the C-F-C angle is 125°, and the C-F bond distances are equivalent (1.61 Å); the C-C distance is 2.86 Å.

(1.1)

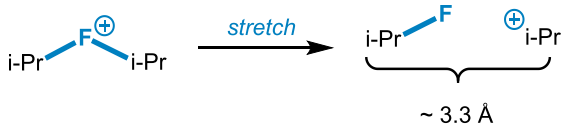

As this C-C distance is stretched, the symmetrical structure is retained until the C-C distance reaches ~ 3.2 Å. At 3.3 Å, a "classical," equilibrating structure is predicted (Equation 1.1). Thus there are limits to the size of C-C distances within a preferred cage, and the framework provided by **13** seems to be closer to optimal if not a bit tight (2.66 Å). Another virtue of this cage is that intramolecular hydride shifts of virtually any type are precluded. For example, a hydride shift could potentially lead to an α-fluorocarbenium ion, as seen in Equation 1.2.[22] Not only is such a shift sterically impossible in our system, but the calculated energy of the α-fluoro cation is higher than the fluoronium at several DFT levels (e.g. B3, B97), in contrast to the expected trend.

(1.2)

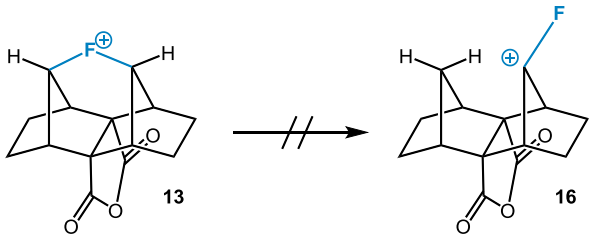

The next logical step was to compare the calculated energy of the fluoronium ion to some well-known carbocations. We chose to employ isogyric[23] equations (B97) to estimate the stability of fluoronium **13** with respect to more common carbocations (Scheme 1.1). In an aqueous dielectric, cation **13** is less stable than t-butyl[24] and 2-norbornyl,[25] but more stable than the isopropyl and 7-norbornyl.[26] Note that the isopropyl cation has a debatable independent existence in aqueous solution.[27] On the other hand, comparison with similarly strained cage systems may be more germane. Whereas theory predicts that the

fluoronium is more stable than the μ-hydrido-bridged species **18**, the chloronium, not surprisingly, is quite a bit more stabilized.

Table 1.1 Optimizations of cation **13** at various levels of theory.

Method/Basis Set	d(Å) C-F	C--F—C angle (degrees)
B3LYP/6-311++G**	**1.60**	**115**
B3LYP/6-311++G**	**1.58**	**116**[a]
B3LYP/cc-pVTZ	**1.59**	**115**
EDF2/6-311++G**	**1.59**	**115**
MP2/6-311++G**	**1.57**	**115**
PBEPBE/6-311++G**	**1.61**	**114**
mPW1PW91/cc-pVTZ	**1.55**	**116**[a]
HCTH/cc-pVTZ	**1.57**	**114**[a]
ωB97XD/cc-pVTZ	**1.55**	**116**[a]
B3PW91/cc-pVTZ	**1.57**	**115**
ωB97XD/6-311+G**	**1.56**	**116**[a]
BPV86/cc-pVTZ	**1.59**	**114**[a]
M06/cc-pVTZ	**1.56**	**116**
TPSSTPSS/cc-pVTZ	**1.60**	**114**

[a]Calculations were performed with the default Gaussian solvation model for water.

Various widely-used levels of theory (DFT and MP2) are in basic agreement on cation **13**'s structure (Table 1.1). The C-F bond length average is 1.58 Å among the methods chosen in the table; the C-F-C bond angle averages about 115°. A QTAIM[29] analysis (B97) shows that each C-F interaction constitutes a little less than half of a normal C-F covalent bond (electron density at BCP ρ = 0.14), in the roughest sense.

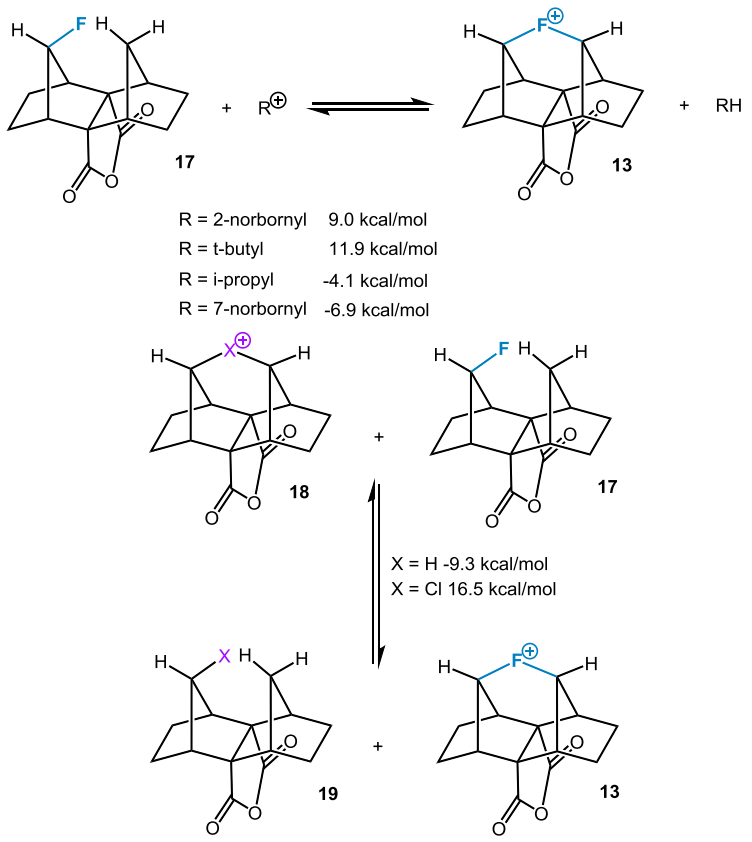

Scheme 1.1 Isogyric comparisons of fluoronium **13** versus common cations (B97, aqueous dielectric).

1.4 Previous synthetic approaches.

As a test, the first approach to the basic skeleton involved the thermal Diels-Alder reaction of fluorinated dienophile **20**[28] with 1,3-cyclopentadiene (Equation 1.3). This reaction, conducted in a sealed tube, produced two diastereomers in comparable amounts (**21**, 30%; **22**, 40%). As easy as the reaction proved to be, compound **21** turned out to be a dead end (other than the interesting through-space interaction between bridgehead H and F it displays).[29] All attempts to functionalize **21** at the methano-bridge by oxidation invariably failed.

(1.3)

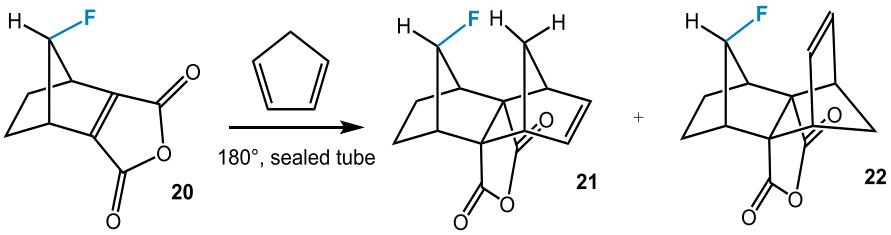

Next we turned our attention to alkene **22**, in which the fluorine interacts closely with the double bond on the opposing bridge. Following the well-established precedents of Paddon-Row et al.[30] and Winstein et al.[31] on similarly configured carbon frameworks, we expected that bromination of **22** would result in rearrangement of the carbon skeleton to provide product **23** that could then be further elaborated. However, to our surprise, this did not occur (Scheme 1.2). Thinking that the poor migratory ability of the electron deficient carbon vicinal to the anhydride group was partly responsible, we employed a reduced version in the form of cyclic ether **24**, but this more promising substrate also failed to rearrange upon bromination.

With this result in hand, we reasoned that addition of an electrophile to this unusual alkene **22** must involve anchimeric assistance from the lone pairs on the fluorine atom, which would thereby reduce the impetus for rearrangement. In fact, reaction of **22** with Br_2 affords the *cis*-dibrominated product **25** exclusively. The crystal structure of **25** determined from single-crystal X-ray diffraction reveals some interesting features, including a close interaction of the *in*-F with two H atoms on the ethano-bridge. A through-space ^{1}H-^{19}F coupling of 4.4 Hz was detected; weaker than the interaction of the two methano-bridges but still notable. Although highly selective *cis*-dibrominations are rare (especially in simple, unsubstituted cycloalkenes), similar reactions are precedented.[32] *Cis*-products can be observed in cases where a bromonium isomerizes to a carbocation that can undergo free rotation. In our case this is not possible, but a "double inversion" involving assistance from the fluorine would also explain the *cis* stereochemistry, thereby implicating fluorine in an anchimeric role (Scheme 1.3).

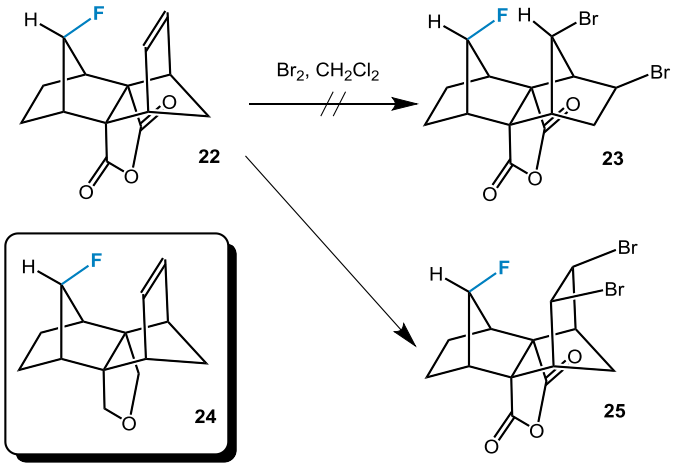

Scheme 1.2 Putative rearrangement of **22** upon bromination.

One could argue that the fluorine is merely a steric impediment to the reaction of a *trans*-bromide ion, but we may well expect the aforementioned skeletal rearrangement to resolve this problem. We turned to computations to provide some guidance; calculation of bromonium ion **26** at (B97, CH_2Cl_2 dielectric) shows a significant interaction of both carbon atoms with fluorine through a QTAIM analysis (ρ at the BCP = 0.020). However, lying slightly lower in energy (0.76 kcal/mol) is the (not quite symmetrical) fluoronium **28**, which can then be trapped by bromide ion through an internal S_N2 reaction to provide the product. Something along these lines may indeed happen, as ion **26** should not normally engage in frontside trapping of bromide. Although the explanation is attractive, it does not provide solid proof. However, the fluorine should not be immediately dismissed as just a blocking group, as a number of examples show.

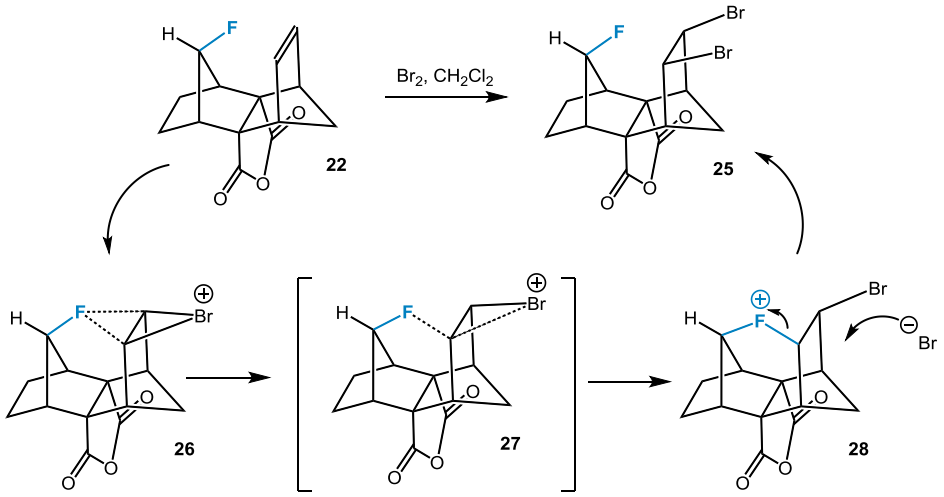

Scheme 1.3 Proposed *cis*-dibromination mechanism.

An especially beautiful parallel to the fluorine participation in system **25** can be seen in the work of Prinzbach et al.,[33] who treated olefin **29** with Br_2 and isolated tetrabromide **30**. The "backside" aromatic ring evidently participates in the bromination to form a σ-complex that is in turn trapped by bromide; further bromination then yields **30**. The newly-formed C-C bond provides compelling evidence for anchimeric assistance, allowing the observer to conclude that the aromatic ring provides more than just steric hindrance. Another example[34] involves putative participation of an ether oxygen as an anchimeric assistor in an olefin whose two faces are sterically hindered. Last is a case[35] that involves postulated

backside anchimeric assistance of a sulfone group to produce a 1:1 mixture of diastereomers in the bromination of cyclobutene **33** (Scheme 1.4).

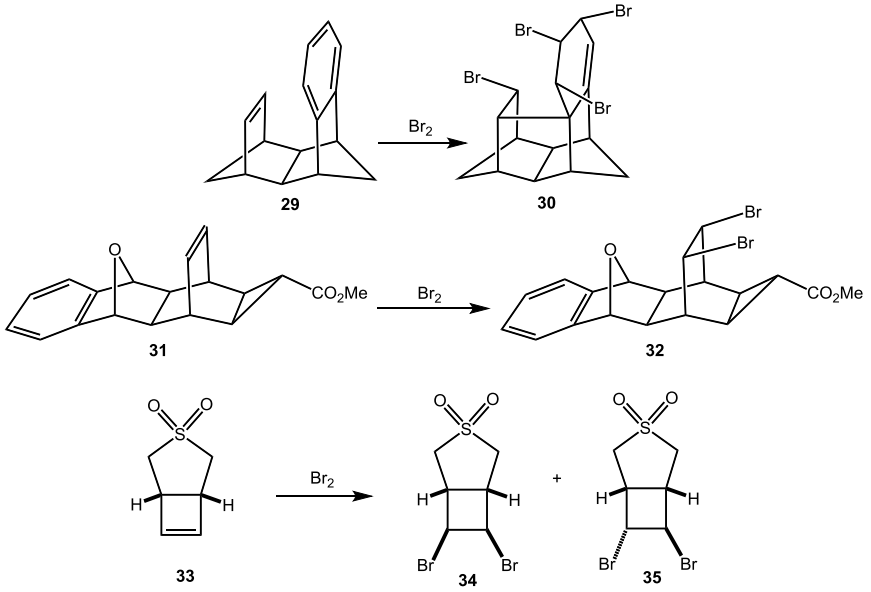

Scheme 1.4 Anchimeric assistance in bromination and notable *cis*-dibromination reactions that may utilize it.

1.5 New synthetic approach.

Ironically, premature fluorine participation in these initial attempts may have thwarted the synthesis of **23**. Our next approach for system **13** instead involved the use of a 5-trialkylsilyl-substituted cyclopentadiene. Silane **40**[36] was chosen as the precedent existed that the silyl substituent would be amenable to the stereoselective Fleming-Tamao oxidation[37] in a subsequent step. We were optimistic about this approach thanks to several transition state calculations, whose relative energies we have found to be quite accurate for fairly nonpolar cycloaddition reactions.[38] At the B97 level, the two most favorable diastereomeric transition states lie close together in energy. The desired isomer **36** is calculated to be lowest in energy, with **37** only 0.03 kcal/mol higher in energy. The other two possible isomers are unlikely to form as the transition states are considerably higher in energy (3.5 and 3.9 kcal/mol). At the very least, this calculation led us to believe that the Diels-Alder reaction would have an excellent chance of producing at least some of the desired diastereomer.

To begin the synthesis, cyclopentadiene **40** was made by the reaction of sodium cyclopentadiene with 1-chloro-1-methylsilacyclobutane.[36] Unfortunately, all attempts at a thermal or Lewis acid catalyzed Diels-Alder reaction using diene **40** and dienophile **20** utterly failed. The diene, it appeared, was very susceptible to rearrangement[39] and decomposition; a finding not surprising in light of the migratory aptitude of electropositive silicon groups.

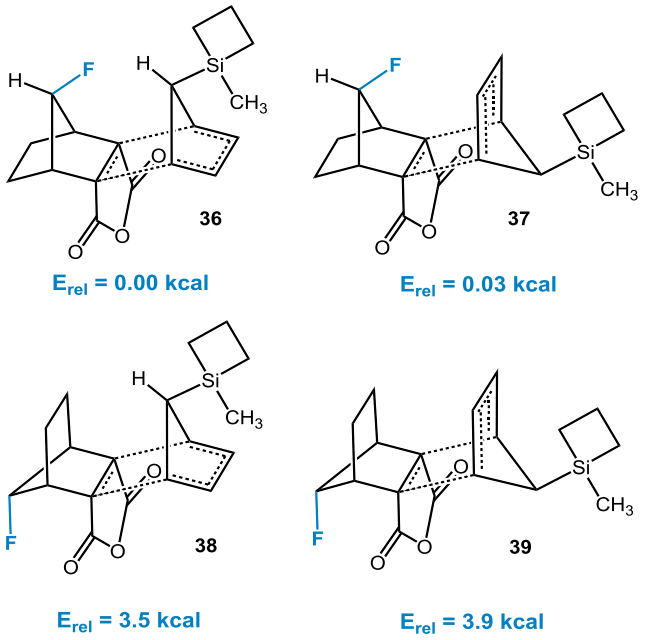

Figure 1.5 Transition state calculations for the Diels-Alder reaction of **20** and **40** (B97, vacuum).

At this juncture our approach to system **13** appeared to be in serious jeopardy. As a last resort, we tried a reaction under very high pressure; the literature is filled with examples of failed Diels-Alder reactions whose fortunes were transformed by a high-pressure apparatus.[40] The reaction was conducted in a 10 mL syringe (1:3 mixture of **20**:**40**; 3M in CH_2Cl_2) for 3 days at 12 kbar. The crude ^{19}F NMR showed the presence of two major diastereomers whose structures we presumed to be those favored by calculation. Based on the prediction of ^{19}F chemical shifts (δ = -0.914i + 142.63; i = isotropic shielding at B3),[41] the desired diastereomer was produced in a slightly higher yield than **37**, as expected. The crude mixture was then subjected to Fleming-Tamao oxidation; separation of the crude products by column chromatography on silica (yielding the desired alcohol in 36%) was followed by hydrogenation with palladium on carbon at 2 bar (99% yield) and triflation (97% yield). Our synthetic approach is detailed in Scheme 1.5.

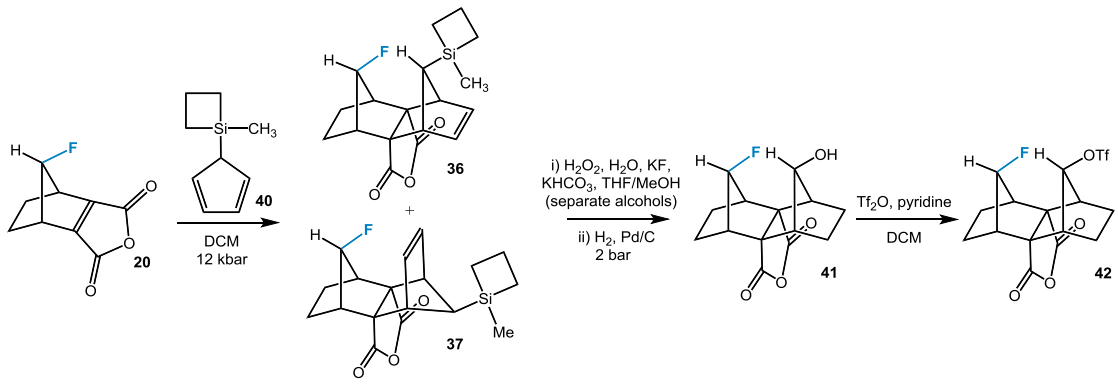

Scheme 1.5 Synthetic approach to **42**.

We chose to use a triflate as a leaving group as it is a good candidate for the generation of very reactive cationic intermediates.[42] We obtained a crystal structure of triflate **42**, revealing the close interaction of F and the *in*-H (1.86 Å) at its estimated position.[43] With that in mind, we surmised that hydrolysis of **42** would release a fair amount of strain energy. This triflate proved to be the key molecule for our studies - however, due to the bottleneck created by the low throughput high pressure reaction and Fleming-Tamao oxidation, making it in large quantities proved impossible - thus very judicious choices of its use were in order.

Initially, the hydrolysis of **42** was attempted in several different solvent systems (due to its low solubility in pure water). A particularly well-behaved example was a combination of the polar, ionizing TFE[44] and water. In 70/30 v/v TFE/water, **42** smoothly hydrolyzed to afford **41** in almost quantitative yield (98%). This indicated to us that we had a remarkably stable system with no apparent propensity to rearrange; however the identity of the product provided little useful information about the mechanism of the substitution reaction. We considered a number of mechanistic scenarios (Scheme 1.6), such as S_N1, an S_N2 reaction that is "extended" to involve fluorine [S_N2(e)], an S_N1 "frontside" reaction (S_Ni),[45] a garden-variety S_N2, or cleavage of an S-O bond. The penultimate mechanism, somewhat less plausible S_N2 variant can immediately be ruled out as we do not isolate this particular diastereomer, but the others cannot be distinguished on the basis of the product, which is the same in all of the cases.

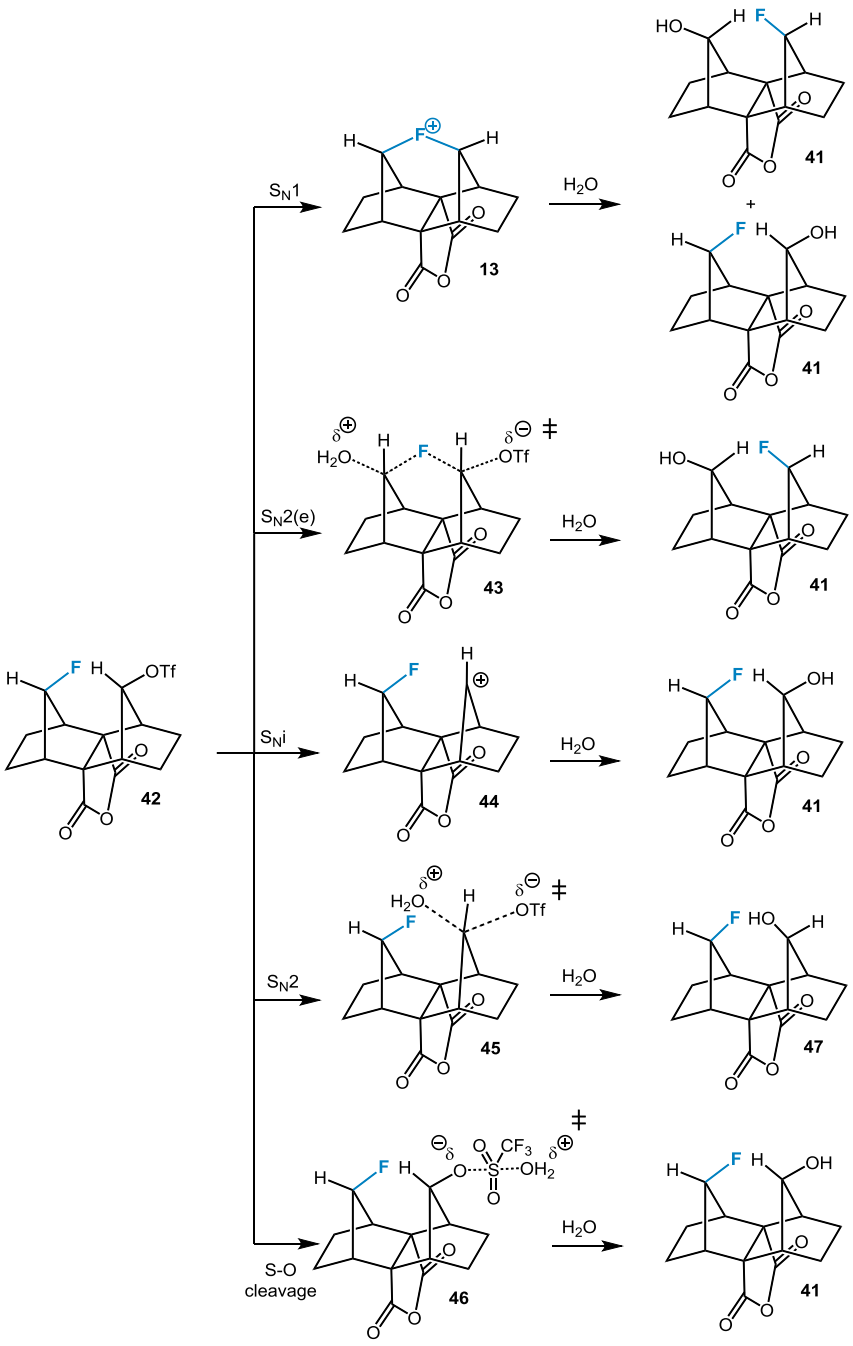

Scheme 1.6 Probable mechanistic pathways for the hydrolysis of **42**.

1.6 Isotopic Labeling Study.

We then turned to an isotopic labeling experiment, which allowed differentiation between various mechanistic alternatives; scrambling between positions is a classic indication of a cloaked symmetrization

process. We went about labeling our compounds by replacing the hydrogenation step in Scheme 1.5 with a deuterated diimide reduction, which upon triflation affords d_2-isotopomer **48**. When this labeled substrate is subjected to hydrolysis in TFE/water 70/30 v/v, we obtain an approximate (1:1) mixture of isotopomeric products **54** and **55** (Figure 1.6). The situation is now greatly clarified (Scheme 1.7). Were the reaction proceeding through an S_N2 or the S_Ni, a 1:1 ratio would not be expected. The 1:1 ratio is thus the likely result of equal trapping on both electrophilic sites of a symmetrical intermediate. Although highly suggestive, without direct characterization the case is obviously circumstantial. Circumstantial evidence is most compelling when it is overwhelming – thus we sought to accumulate as much evidence for the nature of this symmetrical intermediate as we could. In addition, we thoroughly investigated the mechanistic properties and capabilities of this sesquinorbornane system.

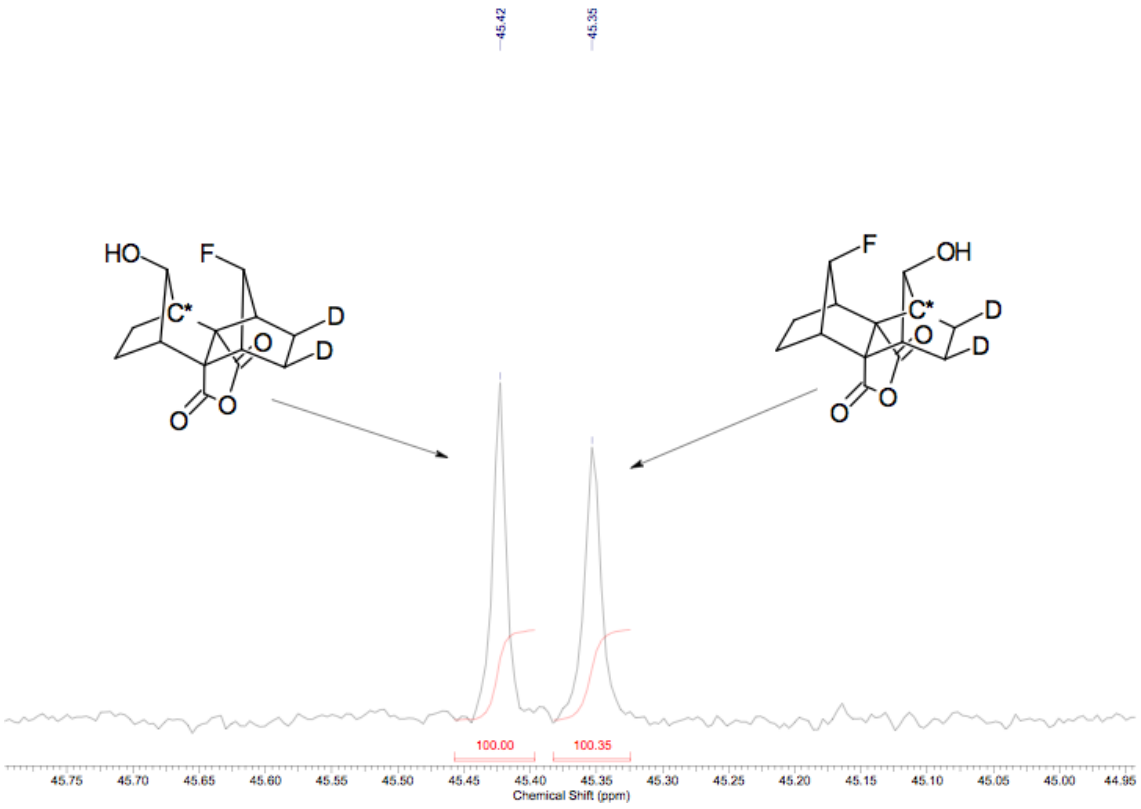

Figure 1.6 Sample integration of isomeric bridgehead carbons in alcohols **54** and **55**, ^{13}C spectrum in $CDCl_3$. Zero filling and exponential line broadening (0.4 Hz) were used (calculated 46.3 ppm).

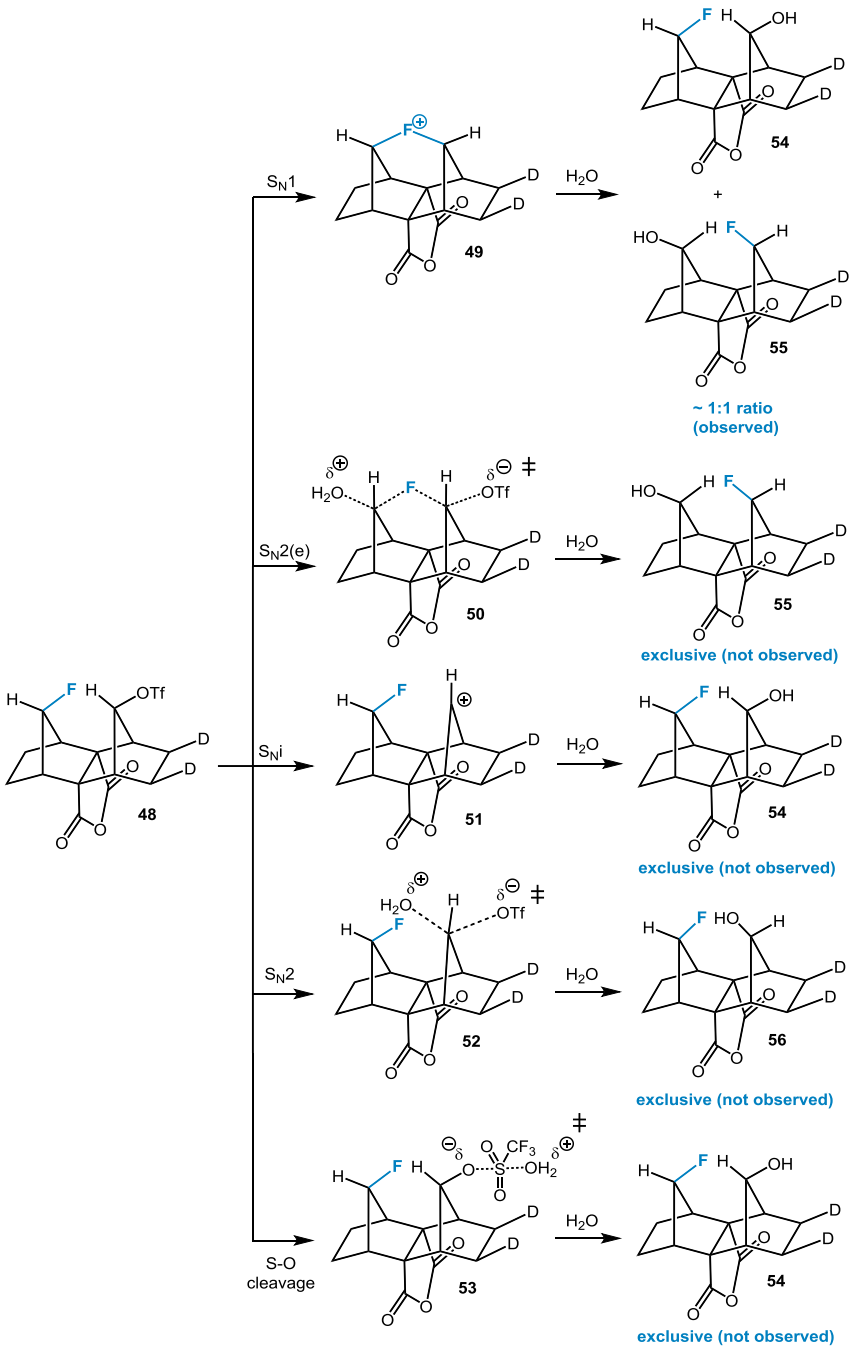

Scheme 1.7 Mechanistic outcomes for the hydrolysis of **48**.

1.7 Conclusion.

In a nutshell, evidence for the generation of a fluoronium ion in solution is as follows: i) The equivalent ratio of labeled isomers **54** and **55** is consistent with a scenario in which the predominant solvolytic pathway results from nucleophilic attack on either bridge of a symmetrical ionic intermediate in

which counterions do not interfere. ii) The conditions of the reaction are consistent with what we would expect for the S_N1 process (relatively nonnucleophilic medium and high dielectric constant).[46] Schneider and Schmidt have used HFIP to observe pure S_N1 reactions on cyclohexyl tosylates;[47] we performed a hydrolysis in similar conditions, but results were less accurate due to difficulties experienced in the integration of small quantities of the product alcohols. iii) The alternative pathways, shown in Schemes 1.6 and 1.7, operate only to a very small extent, if at all. The fact that strictly 1:1 ratios of labeled isomeric products were obtained in various mixtures of water and cosolvents argues for a pure S_N1 reaction as well. iv) As stated, ion **13** is computationally stable at all suitable levels of theory, whereas the conceptual nonfluoronium (asymmetric, or nonbridging) isomer, with all its attendant strain and steric hindrance to nucleophile trapping, is not stable at any suitable level of theory. While it is clear the system reacts with S_N1-like chemistry, the exact nature of the mechanism and the system's reactivity need to be more thoroughly investigated.

1.8 References.

[1] a) Olah, G. A. *Halonium Ions* Wiley, New York, 1975. b) Olah, G. A.; Rasul, G.; Hachoumy, M.; Burrichter, A.; Prakash, G. K. S. *J. Am. Chem. Soc.* **2000**, *122,* 2737–2741. c) Brown, R. S.; Nagorski, R. W.; Bennet, A. J.; McClung, R. E. D.; Aarts, G. H. M.; Klobukowski, M.; McDonald, R.; Santarsiero, B. D. *J. Am. Chem. Soc.* **1994**, *116,* 2448–2456. d) Boldyrev, A. I.; Simons, J. *J. Chem. Phys.* **1992**, *97*, 4272–4281. e) Damrauer, R.; Leavell, M. D.; Hadad, C. M. *J. Org. Chem.* **1998**, *63,* 9476–9485. f) Teberekidis, V. I.; Sigalas, M. P. *Tetrahedron* **2003**, *59,* 4749–4756.

[2] Stoyanov, E. S.; Stoyanova, I. V.; Tham, F. S.; Reed, C. A. *J. Am. Chem. Soc.* **2010,** *132,* 4062-4063.

[3] For a review of iodonium ion chemistry, see: Grushin, V. V. *Chem. Soc. Rev.* **2000,** *29,* 315-324.

[4] Neumann, C. N.; Ritter, T. *Angew. Chem. Int. Ed.* **2015** *54*, 3216-3221.

[5] Bégué, J.; Bonnet-Delpon, D. *J. Fluorine Chem.* **2006**,*127*, 992-1012.

[6] Ojima, I. *J. Org. Chem.* **2013**, *78*, 6358-6383.

[7] Nguyen, V.; Cheng, X. H.; Morton, T. H. *J. Am. Chem. Soc.* **1992**, *114,* 7127-7132.

[8] Solca, N.; Dopfer, O. *J. Am. Chem. Soc.* **2003**, *125,* 1421-1430.

[9] Wang, H.; Webster, C. E.; Pérez, L. M.; Hall, M. B.; Gabbaï, F. P. *J. Am. Chem. Soc.* **2004,** *126*, 8189-8196.

[10] Panisch, R.; Bolte, M.; Müller, T. *J. Am. Chem. Soc.* **2006**, *128,* 9676-9682.

[11] Olah, G. A.; Prakash, G. K. S.; Krishnamurthy, V. V. *J. Org. Chem.* **1983**, *48,* 5116-5117.

[12] Ferraris, D.; Cox, C.; Anand, R.; Lectka, T. *J. Am. Chem. Soc.* **1997**, *119*, 4319-4320.

[13] Karim, A.; Reitti, M.; Carlsson, A. C.; Gräfenstein, J.; Erdélyi, M. *Chem. Sci.* **2014**, *5*, 3226-3233.

[14] Peterson, P. E.; Bopp, R. J. *J. Am. Chem. Soc.* **1967**, *89,* 1283-1284.

[15] a) Shchepina, N. E.; Badun, G. A.; Nefedov, V. D.; Toropova, M. A.; Fedoseev, V. M.; Avrorin, V. V.; Lewis, S. B. *Tetrahedron Lett.* **2002**, *43,* 4123-4124. b) Nefedov, V. D.; Toropova, M. A.; Shchpina, N. E.; Avrorin, V. V.; Zhuzavlev, V. E.; Trofimova, N. I. *Radiokhimiya* **1989**, *31,* 69-70.

[16] a) Menger, F. M. *Acc. Chem. Res.* **1985**, *18,* 128-134. b) Kalesky, R.; Zou, W. *J. Phys. Chem. A* **2014**, *118*, 1948−1963.

[17] Recently, however, the utility of the triquinane framework for stabilizing tertiary-tertiary C—F—C cations has also been put forth: Gunbas, G.; Mascal, M. *J. Org. Chem.* **2013**, *78*, 9579−9583.

[18] Most often, the term "cage hydrocarbon" is employed in the context of rigid diamondoids: Gunawan, M. A.; Hierso, J-C.; Poinsot, D.; Fokin, A.; Fokina, N. A.; Tkachenko, B. A.; Schreiner, P. A. *New J. Chem.* **2014**, *38,* 28-41.

[19] Eaton, P. E.; Cole, T. W. *J. Am. Chem. Soc.* **1964**, *86,* 3157-3158.

[20] Fort, R. C.; Schleyer, P. v. R. *Chem. Rev.* **1964**, *64,* 277-300.

[21] Schneider and Werz have proposed tetracoordinate halonium ions in a theoretical investigation: Schneider, T. F.; Werz, D. B. *Org. Lett.* **2010**, *12,* 4844-4847.

[22] Olah, G. A.; Prakash, G. K. S.; Rasul, G. *Proc. Nat. Acad. Sci.* **2013**, *110,* 8427-8430.

[23] Wheeler, S. E.; Houk, K. N.; Schleyer, P. v. R.; Allen, W. D. *J. Am. Chem. Soc.* **2009,** *131,* 2547-2560.

[24] Deno, N. C.; Turner, J. O.; Hodge, J. D.; Pittman, C. U.; Boyd, D. B. *J. Am. Chem. Soc.* **1964**, *86,* 1745-1748.

[25] For studies on 2-norbornyl cation solvolysis, see: Schreiner, P. R.; Schleyer, P. v. R.; Schaefer, H. F. III *J. Org. Chem.* **1997**, *62,* 4216-4228.

[26] For a notable study on the 7-norbornyl cation: Sunko, D. E.; Vancik, H.; Deljac, V.; Milun, M. *J. Am. Chem. Soc.* **1983**, *105,* 5364-5368.

[27] The isopropyl cation is known to possess a short lifetime in solution in TFE: Pezacki, J. P.; Shukla, D.; Lusztyk, J.; Warkentin, J. *J. Am. Chem. Soc.* **1999**, *121,* 6589-6598.

[28] Scerba, M. T.; Bloom, S.; Haselton, N.; Siegler, M.; Jaffe, J.; Lectka, T. *J. Org. Chem.* **2012**, *77*, 1605-1609.

[29] For examples of through space H-F interactions, see: a) Mallory, F. B.; Mallory, C. W.; Ricker, W. M. *J. Am. Chem. Soc.* **1975,** *97,* 4770-4771. b) Mallory, F. B.; Mallory, C. W.; Ricker, W. M. *J. Org. Chem.* **1985**, *50,* 457-461.

[30] a) Paddon-Row, M. N.; Cotsaris, E.; Patney, H. K. *Tetrahedron* **1986**, *42,* 1779-1788. b) Chau, D. D.; Paddon-Row, M. N.; Patney, H. K. *Aust. J. Chem.* **1983**, *36,* 2423-2446.

[31] Svensson, T.; Winstein, S. *J. Am. Chem. Soc.* **1972**, *94,* 2336-2347.

[32] For examples of *cis*-brominations, see: a) Berson, J. A.; Swidler, R. *J. Am. Chem. Soc.* **1954**, *76,* 4060-4069. b) Steinfeld, G.; Lozan, V.; Kersting, B. *Angew. Chem. Int. Ed.* **2003**, *42,* 2261-2263.

[33] Fessner, W-D.; Sedelmeier, G.; Spurr, P. R.; Rihs, G.; Prinzbach, H. *J. Am. Chem. Soc.* **1987**, *109,* 4626-4642.

[34] Menzek, A.; Altundas, A.; Coruh, U.; Akbulut, N.; Vazquez Lopez, E. M.; Hokelek, T.; Erdonmez, A. *Eur. J. Org. Chem.* **2004**, 1143-1148.

[35] Cadogan, J. I. G.; Cameron, D. K.; Gosney, I.; Highcock, R. M.; Newlands, S. F. *J. Chem. Soc. Chem. Commun.* **1985**, 1751-1752.

[36] Auner, N.; Grobe, J. *J. Organomet. Chem.* **1980**, *188,* 25-52.

[37] Fleming-Tamao: a) Tamao, K.; Ishida, N.; Tanaka, T.; Kumada, M. *Organometallics* **1983**, 2, 1694-1696. b) Fleming, I; Henning, R ; Plaut, H. *J. Chem. Soc. Chem. Commun.* **1984**, 29-31. c) Fleming, I.; Sanderson, P. E. J. *Tetrahedron Lett.* **1987**, *28*, 4229-4232.

[38] Goldstein, E.; Beno, B.; Houk, K. N. *J. Am. Chem. Soc.* **1996**, *118,* 6036-6043.

[39] Kennedy, J. P.; Carlson, G. M. *J. Poly. Sci.* **1983**, *21,* 2973-2986.

[40] For a classic example of a high pressure Diels-Alder reaction, see: Dauben, W. G.; Kessel, C. R.; Takemura; K. H. *J. Am. Chem. Soc.* **1980**, *102,* 6893-6894.

[41] Wu, A.; Zhang, Y.; Xu, X.; Yan, Y. J. *J. Comp. Chem.* **2007**, *28,* 2431-2442.

[42] a) Su, T. M.; Sliwinski, W. F.; Schleyer, P. v. R. *J. Am. Chem. Soc.* **1969**, *91,* 5386-5388. For another example, see the cubyl cation: b) Kevill, D. N.; D'Souza, M. J.; Mariarty, R. M.; Tuladhar, S. M.; Penmasta, R.; Awasthi, A. K. *J. Chem. Soc. Chem. Commun.* **1990**, 623-624.

[43] Ladd, M; Palmer, R. *Structure Determination by X-Ray Crystallography: Analysis by X-Rays and Neutrons*, 5th ed.; Springer: New York, 2013.

[44] For lead references on solvolyses in TFE, see: a) Kaspi, J.; Rappoport, Z. *J. Am. Chem. Soc.* **1980**, *102,* 3829-3837. b) Bentley, T. W.; Roberts, I. *J. Phys. Org. Chem.* **2005**, *18,* 96-100. c) Bentley, T. W.; Llewellyn, G.; Ryu, Z. H. *J. Org. Chem.* **1998**, *63,* 4654-4659.

[45] Kice, J. L.; Bartsch, R. A.; Dankleff, M. A.; Schwartz, S. L. *J. Am. Chem. Soc.* **1965**, *87,* 1734-1739.

[46] Bentley, T.; Carter, G. E. *J. Am. Chem. Soc.* **1982**, *104,* 5741-5747.

[47] Schneider, H. J.; Schmidt, G. *Chem. Ber.* **1986**, *119,* 65-73.

Chapter 2

Through-space "Jousting" Interactions

2.1 Introduction.

Over the last few decades there has been a marked increase in the use of fluorine in chemistry, whether it be for medical/biological applications,[1] materials development,[2] or synthetic methodology.[3,4] In particular, an estimated 20% of the current pharmaceuticals on the market contain fluorine, and there is a large amount of ongoing research investigating the effects of fluorination on the properties of natural products for drug discovery.[5,6] In a recent review, fluorine was called the "second-favorite heteroatom" after nitrogen for drug design.[7] It is perhaps a bit extreme to say that this explosion of interest has ushered in a "fluorine renaissance," but the new appreciation fluorine has recently gained from multiple fields of science is quite notable. Due to this fact, interest in the properties of organofluorine molecules has experienced a phenomenal growth with each passing year.[8] For fluorine to reach its potential, more information of its properties and how it acts in complex systems is desirable.[9] From both a medicinal and academic standpoint, an especially intriguing facet is the way that C-F bonds interact with other *extremely proximate functional groups*, especially intramolecularly.[10] With the noted success of fluorination in medicine, this information could help pave the way for designing new fluorinated drugs that interact better with biological systems.[11] In the realm of synthetic chemistry, exploitation of fluorine's unique acceptor properties has imparted stereoselectivity to new reactions.[12] Because of their ubiquity in organic chemistry and the lively debate surrounding the C-F bond's ability as a hydrogen bond acceptor, interaction with proximate, C-H bonds would be of special interest.[13,14]

Herein, we document the properties of a series of molecules in which the nature of a C-F---H-C interaction can be modulated by hydrogen bonding that is induced by the placement of functional groups geminal to the H-C bond. Electronic effects arising from these conditions are documented by X-ray crystallography, IR, ^{1}H and ^{19}F NMR spectroscopy. Depending on the nature of the functional group, both additional *red* and rarer *blue*-shifted hydrogen bonding interactions can be induced relative to a standard molecule. As a starting point for our study, we chose to utilize the easily modifiable organofluorine cage-system we designed for our fluoronium experiments (Figure 2.1).[15] The virtue of this system is that it

affords a rigid framework in which fluorine is positioned to interact closely with a nearby, conformationally immobile C-H bond. Now imagine the two σ-bonds pointing at each other in close proximity - they almost look like they are about to clash, like medieval jousters, in effect - a graphic description of close, non-bonded interactions between spatially proximate bonds such that one or both may experience evident bond compression or distortion. Although the implication is that such interactions are generally strain-inducing, a small bit of hydrogen bonding serves to make the best of a tight situation. We decided to observe if polarizing the "jousting" interaction in the manner of a stronger hydrogen bond would counteract the effect in interesting and heretofore unseen ways and enhance attraction. This is a chance to observe true conformationally locked C-F---H-C hydrogen bonding, which is a generally rare occurrence, and represents a timely problem in fluorine chemistry.[16]

2.2 Precedents and theory.

Our prototype molecule (X = H_a, **17**) is an interesting case in itself. From calculation (B3LYP/6-311++G**), an intra-bridgehead (H---F) distance of 1.94 Å can be estimated. This is a very close interaction indeed; compare the seminal study of Thalladi et al. on C-H---F interactions in crystalline fluorobenzenes, which indicate typical 2.41-2.78 Å H---F distances.[17] The authors concluded that these constitute weak, but clear, examples of H-bonding. A recent paper by Thakur et al. highlights several other molecules with H---F distances ranging from 2.23-2.35 Å.[18] As a point of reference, a basic, prototype C-H---F interaction between two aliphatic centers, methane and fluoromethane, is exceptionally weak as shown by an optimized bond distance in vacuum (2.68 Å at B3LYP/6-311++G**). One can also see that something unusual is going on by comparing the chemical shifts of the *in*-proton that interacts closely with F (H_a) vs. the *out* (H_b); in a sense, presenting us with an internal reference. The *out*-H resonates at δ 1.30, a standard value for methylene groups in hydrocarbons. The *in*-H resonates at δ 3.16, a downfield shift of almost 2 ppm from analogous systems. While this may appear to be clearly the work of a hydrogen bond, there are some subtleties. There is the extreme forced proximity between the fluorine and hydrogen, which we would expect to result in putative bond compression.[19] Hence we have a rarer situation in which a potential H-bonded species exhibits a significant blue-shifted C-H stretch (3108 cm^{-1}). Blue-shifted (or "improper") X-H---Y hydrogen bonds have become a spirited problem and subject of debate the past

decade or so.[20] Their existence is often attributed to an increase in s-character of the X-H hybrid orbital, as predicted by Bent's rule,[21,22] or, as Joseph and Jemmis have alternatively written, to the "electron affinity of X, which causes a net gain of electron density at the X-H bond region in the presence of Y."[21] Spin-spin coupling constants are also very illustrative; a primarily through-space (which could also be termed a "through hydrogen bond"[23]) H-F spin-spin coupling of 12 Hz was observed.[24] On the other hand, although electron density (ρ) calculations using the QTAIM program[25] indicate a BCP between H and F, its magnitude represents a borderline weak/moderate H-bonding interaction (ρ at BCP = 2.4 X 10^{-2}).[26,27,28] In this case, it may be that we have some interplay of weak hydrogen bonding and non-bonded repulsion (the jousting).

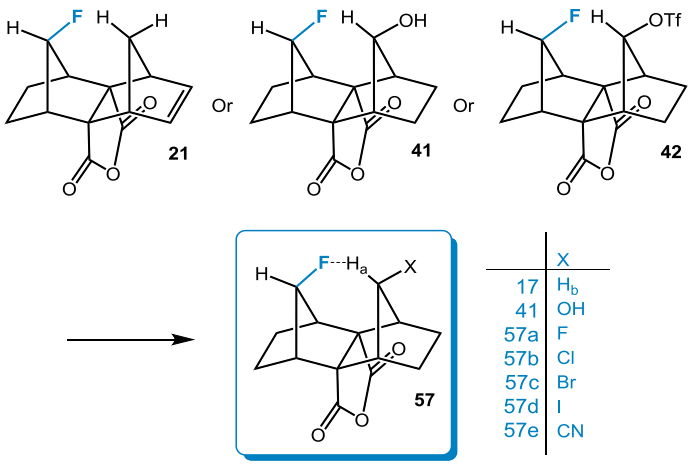

Figure 2.1 Molecules and their precursors for the study of through-space (or through-hydrogen bond) fluorine interactions.

2.3 Synthetic procedure.

At this point we sought to make a series of substituted cage molecules from previously characterized starting materials as points of comparison (see Figure 2.1). We chose substituents that were fairly non-sterically demanding yet homologous, namely halides and the hydroxyl group. Molecule **17** was synthesized by hydrogenation of **21**,[15b] alcohol **41**, itself a derivative of interest, served as the substrate for the synthesis of **57a** (treatment with DAST), and **57b**, **57c**, **57d**, and **57e** were all made through triflation of **41** followed by treatment with NaCl, NaBr, NaI, or NaCN in DMF or acetone. The S_N1 reactions of **57b-e**

proceeded with no discernible rearrangements to the molecule's structure, likely due to the effect of the electron-withdrawing capabilities of the anhydride ring.[29]

2.4 Spectroscopic/Theoretical data.

As can be seen in Table 2.1, the magnitude of J_{H-F}-coupling, which should correlate to the strength of the through-space interaction[30] (H_a---F), increases in the order: H < F ~ OH < Cl < Br < I, paralleling the increase in frequency of the IR stretch of C-H_a (which hybrid DFT calculations show is indeed heavily localized on the C-H_a bond). The largest shift in the IR spectrum occurred for X = I (**57d**), in which the H stretch resonates at 3156 cm^{-1}, representing a 48 cm^{-1} blue shift from the C-H_a stretch of **17** (and a ca. 190 cm^{-1} blue shift from the one carbon bridge of norbornane[31]). As it has been observed in other blue-shifted systems, the intensity of the IR stretches is generally low.[23] The large through-space coupling between the bridgeheads (J_{H-F} = 25.3 Hz) is also maximized for the halides in this molecule.

Table 2.1 Spectroscopic and calculational data.

X (**57**)	$J(^1H_a-^{19}F)$ Hz	δ ^1H_a NMR	ρ $(10^{-2})^a$	d(F-H) Å	%s C-H[c]	ν (C-H stretch, cm^{-1})	d(C-H)[c] Å	natural charge for H_a[c]	natural charge for C[c]
H (**17**)	12.2	3.16 (1.30[b])	2.4	1.906	26.1 (23.9)	3108	1.078 (1.094)	0.24 (0.20)	-0.39 (-0.39)
OH (**41**)	18.7	5.68	2.6	1.874	26.6 (24.5)	3134	1.078 (1.098)	0.21 (0.16)	0.11 (0.13)
F (**57a**)	17.5	6.32	2.6	1.885	27.6 (25.4)	3135	1.077 (1.093)	0.21 (0.17)	0.23 (0.24)
Cl (**57b**)	24.5	5.68	2.8	1.844	27.6 (25.5)	3146	1.074 (1.089)	0.25 (0.21)	-0.19 (-0.18)
Br (**57c**)	24.5	5.84	2.9	1.844	28.0 (25.9)	3152	1.073 (1.088)	0.25 (0.21)	-0.25 (-0.24)
I (**57d**)	25.3	5.85	2.9	1.842	28.4 (26.2)	3156	1.073 (1.088)	0.25 (0.22)	-0.33 (-0.32)
CN (**57e**)	30.7	4.56	3.0	1.826	24.8 (23.2)	3082	1.081 (1.094)	0.28 (0.244)	-0.35 (-0.35)

[a] ρ equals electron density at BCP (bond critical point). Optimizations performed at B3LYP/6-311++G** (B3LYP/DGDZVP on I). [b] Out hydrogen.
[c] Values in parenthases are for norbornanes in which X is placed in the 7-position.

In addition, we obtained a crystal structure of **57d** and compared it to the calculated equilibrium structure at the B3LYP/6-311++G** level (Figure 2.2). Owing to the low scattering power of the H atoms in X-ray diffraction the locations of the H atoms cannot be accurately determined, thus the C-H bond length

had to be constrained to 1.071(10) Å to match the calculated value obtained from DFT calculations. The F---H distances in both structures are close, with 1.837(18) Å for the crystal structure and 1.842 Å for the calculation, reflecting an anticipated downward trend in F---H distances with increasing J-coupling values. QTAIM calculations also show an upward trend of electron density (as well as a positive Laplacian of the electron density) at the bond critical points of the H---F interactions, surpassing the threshold for moderate hydrogen bonding.[32] A natural bond order analysis also provides some clues; for example, the percent s-character of the carbon-centered hybrid orbital of the C-H bond trends upward in line with the IR stretch, resulting in a stronger C-H bond. Larger halogens, engaging in longer bonds, are thus observed to impart additional s-character to the remaining hybrid orbitals, in concord with Bent's rule, thereby enhancing H-bonding and alleviating bond compression.[33] This trend is also present in parallel calculations on 7-substituted norbornanes, which can be seen as non-hydrogen bonded standards (see Table 2.1). However, one can also see that computed bond lengths are shortened in our study molecules relative to norbornanes, a consequence in part on bond compression; natural atomic charges also show a polarization of H_a relative to the norbornanes as well. Thus we have several more apparent cases of blue-shifted hydrogen bonds (relative to **17** and the norbornanes), the most dramatic of which is represented by the iodide **57d**, in which the shift can be attributed to an increase in the s-character of the C-H hybrid orbital from reference molecule **17**.

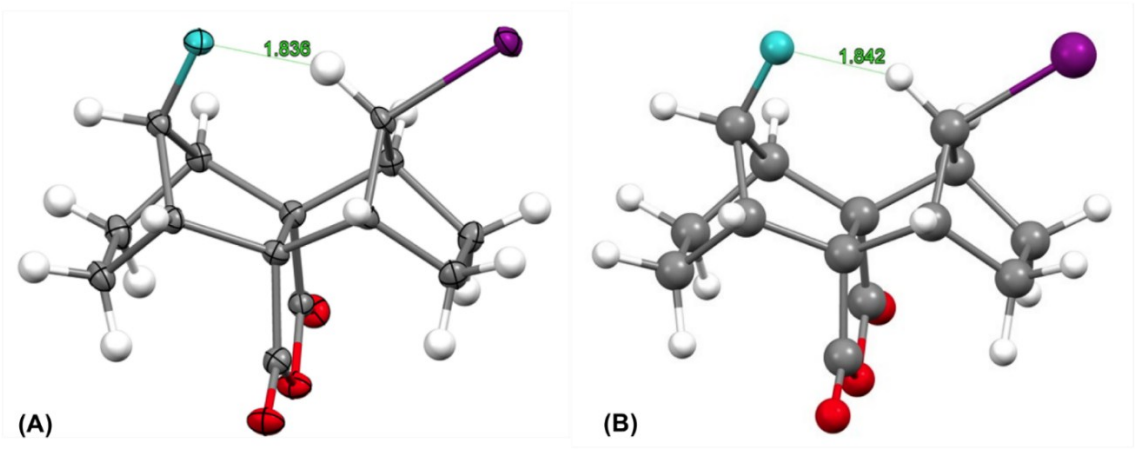

Figure 2.2 (a) Crystal structure of **57d** determined from single crystal X-ray diffraction. The C-H_a distance was constrained to the value calculated in the DFT equilibrium calculation (1.073 Å). (b) Equilibrium structure calculation of **57d** at B3LYP/6-311++G** (B3LYP/DGDZVP on I).

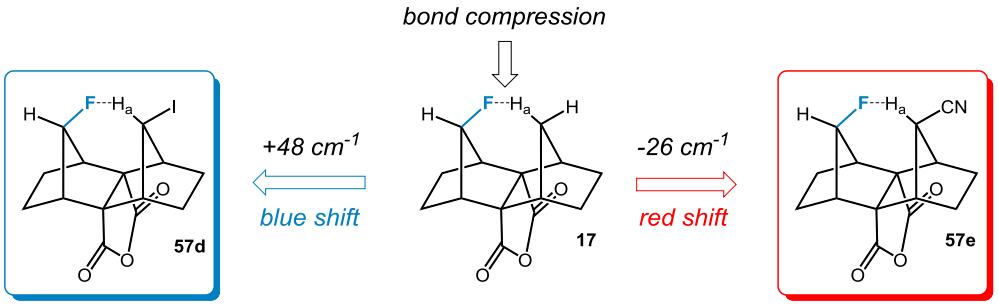

Figure 2.3 Blue versus red shifts in C-F---H-C interactions.

2.5 Electron withdrawing effects.

After exhausting the halides, we wondered: what would happen if we instead attached a sterically unencumbered resonance electron-withdrawing substituent to the C-H bond? To achieve the desired effect, we imagined the placement of a cyano group (R = CN) geminal to H_a as ideal. It is often thought of as being a "pseudo-halogen," and has a comparable steric demand (namely fairly low). Similarly, a QTAIM calculation indicates significantly enhanced electron density residing between H---F ($\rho = 3.0 \times 10^{-2}$). How should this translate spectroscopically? In fact, a significant *red* shift relative to the prototype molecule **17** (**57e**, 3082 cm^{-1}) was observed (but still blue-shifted relative to 7-norbornyl derivatives). H---F coupling is also large, as in **57d** (X = I) (30.7 Hz [calcd. At B3LYP/6-311++G** using the GIAO method in Gaussian 09[34] to be 26 Hz]), suggesting a more powerful interaction between H and F. Long-range spin-spin couplings between ^{13}C-H_a and ^{19}F are also very large – whereas for **17** (X = H) the coupling is 38 Hz, for X = I and CN (**57d** and **57e** respectively) it is 50 Hz. The C-H bond stretch is red-shifted relative to the iodide by 74 cm^{-1}, yet QTAIM predicts *comparable* ρ values at the BCP, correlating with the ^{19}F---H_a couplings. The s-character of the C-H hybrid has now dropped to 24.8%, revealing a trend in the opposite direction. Here the resonance electron withdrawing character of the cyano group plays a role through hyperconjugation with the C-H bond.[35] In Figure 2.3, we compare the effects of iodo (**57d**, blue shift) versus cyano (**57e**, red shift) substitution on the C-H_a stretches.

2.6 Conclusions.

We have found that a series of cage molecules, with their rigidity, forced proximity of H and F atoms as well as their versatility, provide ideal systems for the investigation of "jousting" interactions. Our

results show clear indications of both F---H hydrogen bonding interactions as well as C-H bond compression enforced by the cage framework of the study molecules. There also appears to be a clear correlation between percent s-character in C-H hybrids with the blue-shifted H-bond examples; this trend can be counteracted by the placement of a resonance electron-withdrawing cyano group on the cage system to afford a red-shifted interaction (relative to a standard molecule). Most importantly, in this series of molecules, the size of the through-space H---F spin-spin couplings may be indicative of the strength of the interactions; this conclusion is supported by QTAIM calculations.

2.7 References.

[1] Filler, R.; Saha, R. *Future Med. Chem.* **2009**, *5*, 777-791.

[2] Maienfisch, P.; Hall, R. G. *Chimia* **2004**, *58*, 93-99.

[3] Kitazume, T. *J. Fluorine Chem.* **2000**, *105*, 265-278.

[4] Shimizu, M.; Hiyama, T. *Angew. Chem. Int. Ed.* **2005,** *44,* 214-231.

[5] Bégué, J.; Bonnet-Delpon, D. *J. Fluorine Chem.* **2006**, *127*, 992-1012.

[6] Isanbor, C.; O'Hagan, D. *J. Fluorine Chem.* **2006**, *127*, 303-319.

[7] Ojima, I. *J. Org. Chem.* **2013**, *78*, 6358−6383.

[8] Müller, K.; Faeh, C.; Diederich, F. *Science* **2007**, *317*, 1881-1886.

[9] Kirk, K. L. *J. Fluorine Chem.* **2006**, *127*, 1013-1029.

[10] Nishide, K.; Hagimoto, Y.; Hasegawa, H.; Shiro, M.; Node, M. *Chem. Commun.* **2001**, 2394-2395.

[11] Wilcken, R.; Zimmermann, M. O.; Lange, A.; Joerger, A. C.; Boeckler, F. M. *J. Med. Chem.* **2013**, *56*, 1363-1388.

[12] a) Gold, B.; Shevchenko, N. E.; Bonus, N.; Dudley, G. B.; Alabugin, I. V. *J. Org. Chem.* **2012**, *77*, 75−89. b) Gold, B.; Dudley, G. B.; Alabugin, I. V. *J. Am. Chem. Soc.* **2013**, *135*, 1558−1569.

[13] Schneider, H. *Chem. Sci.*, **2012**, *3*, 1381-1394.

[14] Dunitz, J. D.; Taylor, R. *Chem. Eur. J.* **1997***, 3,* 89-98.

[15] a) Struble, M. D.; Scerba, M. T.; Siegler, M. A.; Lectka, T. *Science* **2013**, *340*, 57-60. b) The synthesis and very preliminary study of a prototype of this cage system was also reported: Scerba, M. T.; Bloom, S.; Haselton, N.; Siegler, M.; Jaffe, J.; Lectka, T. *J. Org. Chem*. **2012**, *77*, 1605-1609.

[16] a) Howard, J. A. K.; Hoy, V. J.; O'Hagan, D.; Smith, G. T. *Tetrahedron* **1996**, *52*, 12613-12622. b) Chan, M. C. W.; Kui, S. C. F.; Cole, J. M.; McIntyre, G. J.; Matsui, S.; Zhu, N.; Tam, K-H. *Chem. Eur. J.* **2006,** *12,* 2607-2619.

[17] Thalladi, V. R.; Weiss, H.; Bläser, D.; Boese, R.; Nangia, A.; Desiraju, G. R. *J. Am. Chem. Soc.* **1998**, *120*, 8702-8710.

[18] Thakur, T. S.; Kirchner, M. T.; Bläser, D.; Boese, R.; Desiraju, G. R. *CrystEngComm*, **2010**, *12*, 2079–2085.

[19] For more information on the effects of bond compression on NMR see a) Lawson, M. N.; Blanda, M. T.; Staggs, S. J.; Sederholm, L. N.; Easter, D. C. *J. Phys. Org. Chem.* **2009**, *22*, 1212–1224. b) Kleinpeter, E.; Szatmári, I.; Lázár, L.; Koch, A.; Heydenreich, M.; Fülöp, F. *Tetrahedron* **2009**, *65*, 8021-8027.

[20] Jemmis and Joseph have organized a nice discussion of the theory of blue-shifted, or "improper" H-bonds: Joseph, J.; Jemmis, E. D. *J. Am. Chem. Soc.* **2007**, *129,* 4620-4632.

[21] a) Alabugin, I. V.; Manoharan, M.; Peabody, S.; Weinhold, F. *J. Am. Chem. Soc.* **2003**, *125*, 5973-5987. b) Alabugin, I. V.; Manoharan, M. *J. Comput. Chem.* **2006**, *28*, 373-390.

[22] Bent, H. A. *Chem. Rev.* **1968**, *68*, 587-648.

[23] Bagno et al. have pointed out the equivalence of through-space and through-H-bond couplings, see: Bagno, A.; Saielli, G.; Scorrano, G. *Chem. Eur. J.* **2002**, *8,* 2047-2056.

[24] For pioneering examples of through-space H-F couplings, see: a) Adcock, W.; Rizvi, S. Q. A. *Aust. J. Chem.* **1973**, *26,* 2659-2663. b) Yamamoto, G.; Oki, M. *J. Org. Chem.* **1984**, *49,* 1913-1917.

[25] AIMAll (Version 13.05.06), Keith, T. A., TK Gristmill Software, Overland Park KS, USA, 2013 (aim.tkgristmill.com).

[26] Bader, R. F. W. *Acc. Chem. Res.* **1985,** *18***,** 9-15.

[27] The calculated Laplacian of the charge density at the bond critical point > 0 for **1a-1g**, consistent with a "charge shift" or weak-moderate hydrogen bond, see: Grabowski, S. J. *J. Phys. Chem. A* **2011**, *115*, 12789–12799.

[28] Parthasarathi, R.; Subramanian, V.; Sathyamurthy, N. *J. Phys. Chem. A* **2006**, *110,* 3349-3351.

[29] For a discussion of similar reactions involving solvolyses of **3** see reference 13a.

[30] Chaudhari, S. R.; Mogurampelly, S.; Suryaprakash, N. *J. Phys. Chem. B* **2013**, *117,* 1123-1129.

[31] NIST Mass Spec Data Center, Stein, S. E., director.

[32] Koch, U.; Popelier, P. L. A. *J. Phys. Chem.* **1995**, *99,* 9747-9754.

[33] Grabowski, S. J. *J. Phys. Chem. A* **2011**, *115*, 12340–12347.

[34] Gaussian 09, Revision A.1, Frisch, M. J. et al. Gaussian, Inc., Wallingford CT, 2009.

[35] Salzner, U.; Schleyer, P. v. R. *Chem. Phys. Lett.* **1992**, *190*, 401-406.

Chapter 3

A Strong "No-Shift" O-H---F Interaction

3.1 Introduction.

A key spectroscopic signature of a hydrogen bond (X--HY) is found in the IR spectrum wherein the YH stretch is generally red-shifted.[1] However, recent studies have revealed intriguing examples of hydrogen bonds in which the YH stretch is blue-shifted – a phenomenon that has become important in its own right.[2] In a nutshell, the red-shifted examples are often attributed largely to weakening of the YH bond due to overlap of lone pairs on X with σ*(YH).[3] Blue shifts, on the other hand, have been ascribed to the dominant influence of rehybridization-induced YH bond strengthening (in the manner of Bent's rule).[4]

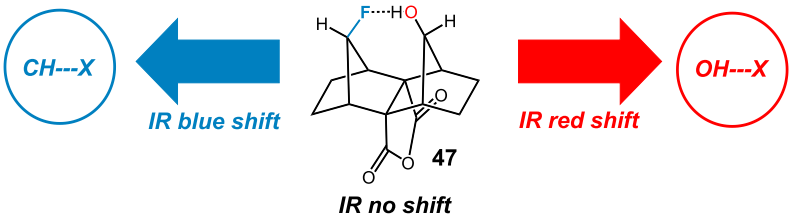

Figure 3.1 Blue, red, and no-shift H-bonds.

Blue shifts in the IR spectrum often involve the interactions of CH bonds with donors; on the other hand, OH groups that engage in H-bonding are generally red-shifted (Figure 3.1). A lively debate has surrounded the question of whether blue-shifted H-bonds represent a fundamentally different concept than their red-shifted counterparts, but the most common belief at the moment is that there exists no basic difference between red- and blue-shifted H-bonds, just a changing balance between hyperconjugative- and rehybridization-induced effects. If this is the case, what about the interesting possibility of a fairly strong H-bonding interaction in which no meaningful shift in the YH stretch can be observed in a non-interactive solvent due to canceling red- and blue-shifting tendencies?[5,6] There would be in fact no compelling rationale why such an H-bond could not exist. In this chapter, is reported a serendipitous but apparently rare example of a strong, virtually "no-shift" H-bond. The discovery was made during the investigation of a cage molecule that was specially designed to exhibit an intense F---HO interaction, thereby helping to clarify the controversy about whether such H-bonds can in fact exist in solution.[7] In our case, NMR studies

(coupling constants, isotopic chemical shift perturbations, and proton exchange rates) tell the tale of a strong H-bond that the IR spectra cannot, and would seem to confirm the emerging orthodoxy concerning the nature of blue- vs. red-shifted H-bonds.

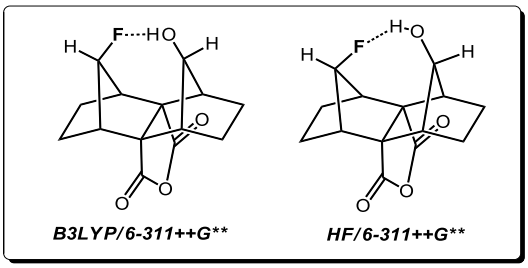

Figure 3.2 Structures of **47** generated at B3LYP/6-311++G** (F---H = 1.58 Å) and HF/6-311++G** (F---H = 2.01 Å).

3.2 Initial work.

Hydrogen bonding to fluorine as a covalent acceptor is a fascinating subject that has gained relevance recently as fluorinated molecules become more prevalent in medicine and biology, and the precise role that fluorine plays in medicinal chemistry assumes a central, if not urgent, role.[8] Whereas it is generally accepted nowadays that fluorine, as part of a C-F bond, is a competent H-bond acceptor, several outstanding questions remain, the most important of which involves the strength of the interaction. From a biochemical standpoint, the ubiquity of hydroxyl groups would indicate that the C-F---H-O interaction could be especially important.[9] On the other hand, periodic screens of the CSD indicate that significant interactions (< 2.2 Å H---F distance) are uncommon.[10] Rarer still are strong interactions between covalent fluorine and relatively non-acidic aliphatic alcohols,[11] and controversy has arisen over whether such interactions qualify as H-bonding at all.[12] One way to establish such an interaction beyond certitude is if the OH group was placed in *extreme* proximity to a neighboring covalently bound fluorine atom, making a strong H-bonding interaction literally unavoidable. With only a slight amount of modification our fluoronium precursor should be attenable to such an interaction.[13] Alcohol **47** ("*in*-alcohol") seemed to be an attractive candidate for a new study of extreme interactions involving fluorine (Figure 3.2). For example, at B3, the optimized structure clearly reveals an unusually strong interaction between O-H and F.[14] The calculated H---F distance is only 1.58 Å, and the distance between O and F is predicted to be 2.54

Å (use of a newer functional paired with a triple-ζ basis set [ωB97XD/cc-pVTZ] that is noted for an accurate account of dispersion effects yields a similar result: 1.59 Å; 2.53 Å).[15] The H-bond itself is roughly linear (170°), and the system, remarkably, does not attempt to relieve strain by bending much. On the other hand, at HF/6-311++G**, the situation is quite different. The H-bond is apparently much weaker; it is highly bent (OH---F bond angle = 104°); the H---F distance is 2.0 Å, and the C_s symmetry of the B3LYP structure is disrupted. Evidently, the account of electron correlation taken by the hybrid DFT methods is significant to the predicted structure of **47**.

3.3 Synthesis.

We decide on saturated *out*-alcohol **41** as a suitable starting point for the synthesis of **47**; the goal then would be to epimerize the *out*-OH group to the *in*-position. Oxidation of **41** with PCC proceeds slowly (presumably due to steric hindrance) over 24 h to afford ketone **58** in 75% yield. In turn, subjecting **58** to $LiAlH_4$ for 2 h in THF at reflux affords alcohol **47** in 32% yield after workup (Fieser method) and column chromatography on silica gel. The reaction requires harsh conditions for a ketone reduction, as models indicate a poor potential hydride attack angle that deviates significantly from the optimal Bürgi-Dunitz trajectory).[16]

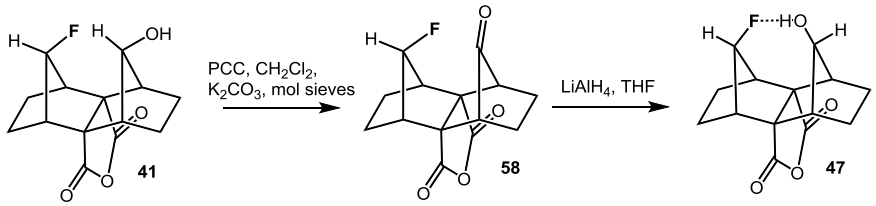

Scheme 3.1 Synthetic pathway for the generation of **47**.

3.4 Spectroscopic data.

IR spectroscopy. In order to document the H-bond, an IR study was undertaken. In fact, the free OH stretch of **47** was observed at 3620 cm^{-1} in DCM, (CH_2Cl_2 concentrations ranging from 10^{-3} to 10^{-2} M). Contrast this with alcohol **41** (employed as an appropriate intramolecular non-hydrogen bonded reference in dilute solution) whose free OH stretch appears at 3614 cm^{-1}. Turning to other solvents, in benzene **41** is red-shifted from **47** by 45 cm^{-1}, presumably due to its propensity for π-cloud-OH interactions.

Additionally, in MeCN, **41** is predominately H-bound to solvent, whereas **47** is not.[17] In π-electron-poor benzotrifluoride ($PhCF_3$), the π-cloud induced shift is virtually gone; the absence of a significant shift is also observed in CCl_4. In cyclohexane (CyH), a very non-interactive solvent and about as close to the gas phase as we can get,[18] the shift also virtually disappears (Table 3.1). Keep in mind that OH groups are almost invariably red-shifted upon strong H-bonding,[19] so these findings are quite unusual.

Table 3.1 IR study of the OH stretches of **41** and **47**.

Solvent	**41**	**47**
CH_2Cl_2	3614	3620
PhH	3591	3636
$PhCF_3$	3636	3633
CCl_4	3638	3639
CyH	3658	3659

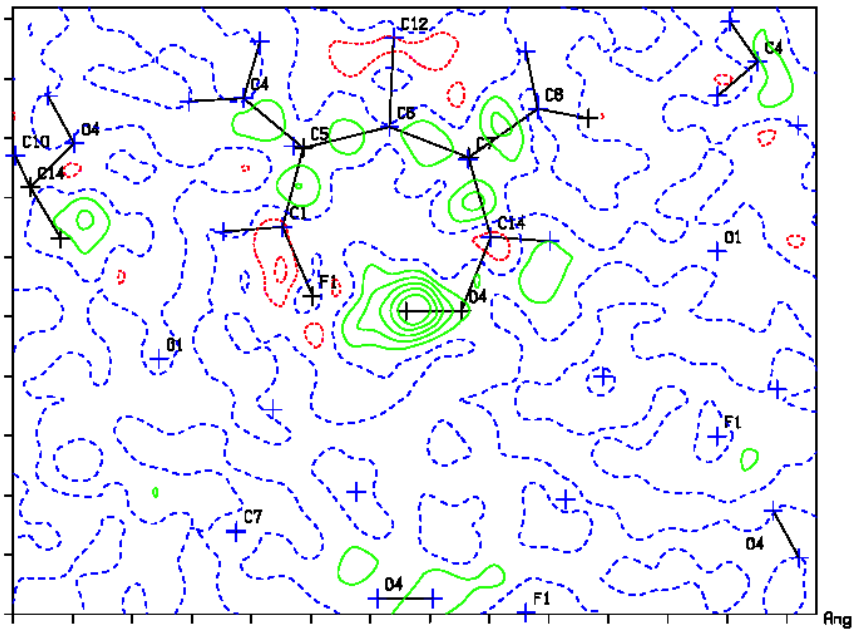

Figure 3.3 Difference Fourier map drawn in the plane defined by O4 H4 F1. The position of H4 is indicated by the contoured green circles near O4.

X-ray crystallography. The investigation of the structure of **47** through X-ray crystallography shows clear evidence of the strength of the hydrogen bonding interaction. When the *in*-hydrogen was fully refined (resulting in a difference Fourier map, Figure 3.3, that showed the position of the hydrogen clearly) the structure yielded bond lengths in fairly good agreement with the calculated values. The O-H bond in the structure was measured at 0.93 Å (calc. 0.96 Å) and the H---F distance is 1.58 Å (calc. ωB97XD/cc-pVTZ 1.59 Å); the O---F distance is 2.51 Å (calc. 2.53 Å). The O-H---F angle is given as 171° which fits closely with the calculated value (170°) as well. Investigation of the packing diagram generated from the crystal (Figure 3.4) reveals the robustness of the hydrogen bonding interaction; the alcohol hydrogen is not observed to have any furcating or otherwise short contact interactions.[20] On the other hand, the packing diagram of the crystal structure of *out*-**1** reveals several close, polyfurcating interactions of its alcohol hydrogen with neighboring oxygen atoms.

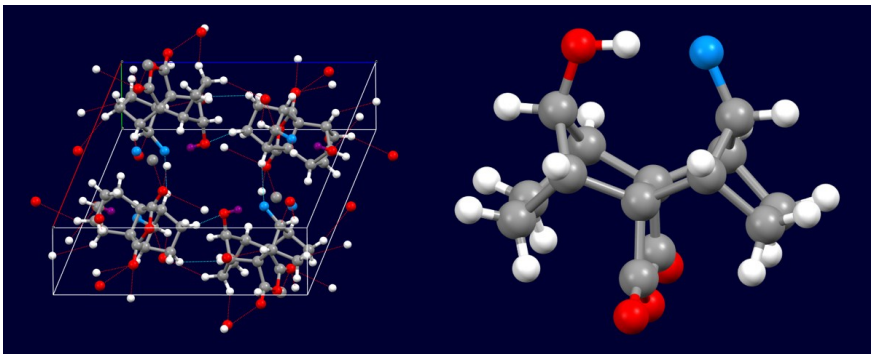

Figure 3.4 Packing diagram of **47** (left), alcohol protons are colored purple, and crystal structure of **47** (right).

NMR spectroscopy. Examination of the ^{1}H NMR spectrum of **47** immediately suggested some unusual features that aid in clarifying the situation. A sharp multiplet at 4.8 ppm (-OH) encompassing strong coupling between H and F was observed (68 Hz). The one-bond coupling between F and H is calculated at 76 Hz (B3LYP/6-311++G**); perhaps more than any factor, this would be indicative of a strong interaction.[21] The one-bond H-F coupling of the weaker, bent alternative structure predicted at HF/6-311++G** is only 18 Hz. Coupling to the proton vicinal to the oxygen was also seen, representing very slow exchange with the $CDCl_3$ solvent. Even in the presence of several equivalents of D_2O, this slow exchange was maintained. Computationally, the sequential placement of water molecules in this vicinity of

the O-H---F bond resulted in only very slight distortions to its geometry. On the other hand, **41**, *has no discernable alcohol proton visible in the NMR spectrum under identical conditions and concentrations indicating fast exchange with water.* In anhydrous $CDCl_3$, **41** displays its hydroxyl proton at 1.6 ppm, more than 3 ppm upfield from **47**. Coupling to fluorine is negligible, suggesting a predominately through-space interaction for the H-bond of **47**, which is, surprisingly, of the same magnitude as the fluorine's strong coupling to the geminal proton.

Labelling experiment. Clearly, the alcohol hydrogen on **47** is tightly held and led to the attempt to replace it with a deuterium and observe what effects such a substitution would have through NMR spectroscopy. Deuteration of **47** was achieved by dissolution in MeOD with the aid of gentle heat under a nitrogen atmosphere. The solvent was removed *in vacuo* and the deuterated product was redissolved in CD_2Cl_2 for the NMR experiments. In keeping with our hypothesis, the deuterated **47** was found to undergo exchange in solution ($CDCl_3$ saturated with H_2O) at a fraction (less than 0.001 times) of the rate of **41**. The ^{19}F spectrum shows a large isotopic shift δ(F---DO) – δ(F---HO) of -0.37 ppm, which is of the same value as the isotope shift for $[F\text{-}H\text{-}F]^-$,[22] known as the strongest documented H-bond.[23] Additionally, the ^1H and ^2H spectra show a large negative isotopic shift (-0.17 ppm). Together, these results, along with the large downfield shift (3.2 ppm), and solvent exchange behavior are evidence of a strong, almost linear H-bond.[24] Comparatively, the IR spectrum is fairly uninformative in a classical sense, barring a four-fold increase in the extinction coefficient of the OH stretch of **47** compared to **41**.[25]

3.5 DFT calculations.

The nature of the hydrogen bond in **47** can also be evaluated by the application of QTAIM parameters (B3).[26] For example, the electron density (ρ) at the BCP is appreciable (0.052). The question of strain is germane as well; **41** is predicted to be more stable than **47** by 3.7 kcal/mol at B3. On the other hand, *in*- and *out*-difluoride isomers, **57a** and **60** respectfully, which contain significantly less hydrogen bonding capability, are separated by 13.1 kcal/mol. These molecules can be thought of as computational controls; they are sterically fairly similar to **47** and **41**. Thus the significant attenuation in the gap between **47** and **41** is largely attributable to the H-bond. Alternatively, the C_s-symmetric bond rotamer of **47** may provide another semi-quantitative measure[27] – it is 7.1 kcal/mol less stable than **47** itself, and its calculated OH---F

though-space coupling is only 11 Hz. Once again, these data point to **47** as possessing a significant H-bond.

3.6 Control Reactions.

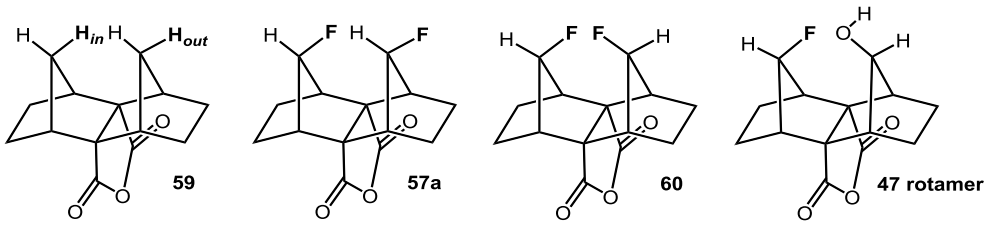

Figure 3.5 Structures of hydrogen bond controls used in calculations.

Could this be an example of what Jemmis et al. term a "no-shift" H-bond, i.e. one in which OH bond-shortening and bond-lengthening factors precisely cancel?[5] Excellent overlap between a lone pair (*n*) on F and σ* OH should command a red shift. Nevertheless, the predicted OH bond lengths are close (0.962 Å for **47** vs. 0.961 Å for **41**). The lack of elongation in the OH bond of **47** may be due in part to strain; after all, the rigid nature of the cage places the OH group in close proximity to the fluorine. It must be said that the choice of references can be somewhat subjective, especially when considering an intramolecular H-bond. Although **47** and **41** match up spectroscopically, calculationally several DFT methods predict a 20-30 cm^{-1} red shift upon H-bond formation. It is illustrative to compare **59** as a control in which red-shifting H-bonding tendencies have been minimized, yet a substantial proximity-based "jousting" interaction (with an attendant blue-shift) remains (Figure 3.5). At B3, the *in*-C-H bond (1.083 Å, 25.5% s-character in hybrid) is shorter than the *out*-C-H (1.094 Å, 23.2% s) by 0.011 Å. The coupled vibrations of the *in*-C-H bonds are predicted to be blue-shifted by 50 cm^{-1} (asym) and 93 cm^{-1} (sym) from the closest CH vibrations in the molecule. To summarize, the low energy structure of **47** seems to lie at the equilibrium distance at which blue and red shifts cancel. However, depending upon reference compounds, a very slight blue shift H-bond may be inferred, reminding us that the "no-shift" aspect is virtual rather than exact.

While those systems serve as good intramolecular controls, how does this interaction compare to *inter*molecular bonding systems. Alcohols **61a-d** (Figure 3.6) were thus compared as alternative intermolecular references as well (imagine excising the C-F bond and its support from *in*-**1**, but leaving behind the strained norbornane motif). These controls are also predicted to show little or no shift of the OH

stretch by DFT calculations. In CCl_4, **61a** and **61b** display free OH stretches at 3631 cm^{-1} (consequently a very slight blue shift separates *in*-**1** from these controls; whereas **61c** displays at 3635 cm^{-1}, and 7-norbornanol itself (**61d**) at 3633 cm^{-1}.[28] Thus, it appears that our putative strong interaction exhibits very little, if any, OH stretch perturbation in non-interactive solvents, compared with relevant controls.

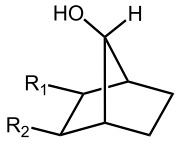

61a R_1 = Me, R_2 = H
61b R_2 = Me, R_2 = Me
61c R_1 = Cy, R_2 = H
61d R_1 = R_2 = H

Figure 3.6 Controls for intermolecular hydrogen bonding interactions.

One can also compare the large red shifts observed when control **41** interacts through intermolecular H-bonding with basic solvents and additives. In other words, chemically, the OH groups in **41** and **47** are very different. For example, titration of a solution of **47** with DMAP afforded little change in the OH stretch of the IR spectrum up and beyond 5 equiv. On the other hand, the OH stretch of **41** shifts greatly in the presence of excess DMAP to become a broad, strong band centered around 3000 cm^{-1}, indicating classical intermolecular hydrogen bonding and a red shift of ca. 600 cm^{-1}.

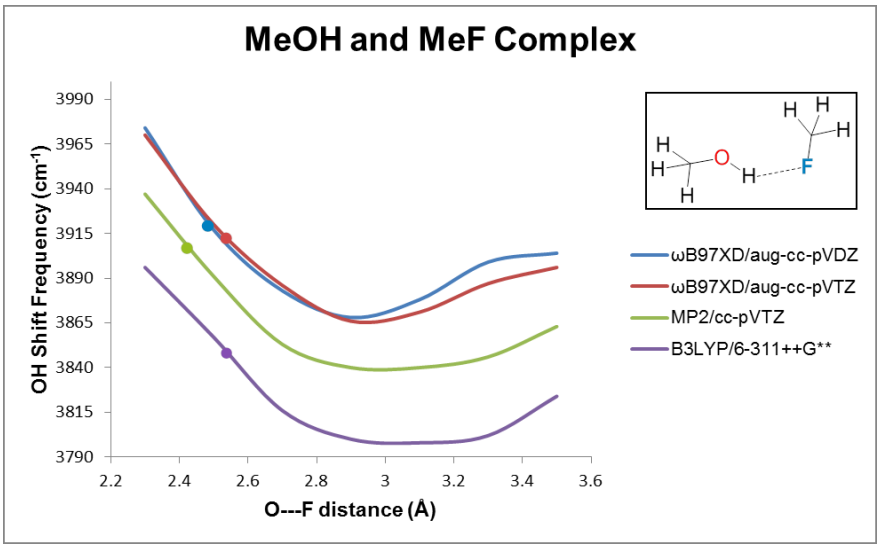

Figure 3.7 Effect of O---F distance on the predicted OH stretch of the MeOH-MeF complex. Predicted MeOH shift is marked with a solid dot.

As a control to judge the no-shift aspect of the O-H-F interaction, we subjected the simplest model system, the complex of fluoromethane (MeF) and methanol (MeOH), to calculation at a level known to handle hydrogen bonding in an exemplary fashion (ωB97XD/aug-cc-pVTZ).[29] At equilibrium, the complex shows an H---F distance of 2.07 Å, and an F---O distance of 2.92 Å (bond angle 144°). Varying the F---O distance of the complex provides an illuminating insight; at large distances, the OH stretch approaches that of calculated free MeOH at 3914 cm^{-1} (Figure 3.7). As the distance shrinks (and the complex strengthens) a red shift occurs in the OH stretch that peaks at near the equilibrium distance of the complex (2.92 Å). As the F---O distance is further shortened, an increasing blue shift trend appears. At around 2.5-2.6 Å, the complex reveals cancelling red and blue shifts resulting in a "no-shift" interaction (relative to MeOH) which, not coincidentally, is close to the O---F distance in **47** by both calculation and crystal structure. At 2.5 Å, the interaction is predicted to have a higher density at the BCP (0.035) than in the equilibrium structure (0.018). Repeating the process at the ωB97XD/aug-cc-pVDZ level of theory resulted in a similar result, albeit with slightly higher frequencies at larger F---O distances. Finally, when the rigid structure of **47** is loosened (e.g. in congeners **62** and **63**), a red shift is calculated, even though the magnitude of the H---F interaction decreases (Figure 3.8); this result is in line with our prediction for the MeF-MeOH system as well.

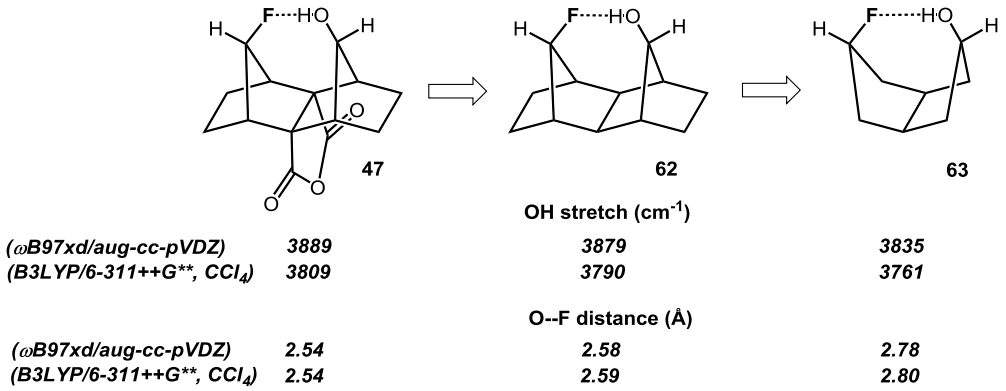

Figure 3.8 Effect of O---F distance on the predicted OH stretches of **62** and **63**.

3.7 Conclusion.

In conclusion, the cage system contains an unusually strong asymmetric hydrogen bond between an OH donor and a covalent F acceptor. The structure has been extensively characterized by NMR (coupling

constants, isotopic chemical shift perturbations, proton exchange rates and calculations) and crystallographic studies, all of which are consistent with a strong interaction. On the other hand, **47** shows little to no perceptible shift in the OH stretch of the IR spectrum relative to non-hydrogen bound standards in non-interactive solvents, an example of a putative "no-shift" H-bond, in which blue and red shifts virtually cancel relative to controls.

3.8 References.

[1] Allerhand, A.; Schleyer, P. v. R. *J. Am. Chem. Soc*. **1963**, *85*, 1715-1723.

[2] a) Hermansson, K. *J. Phys. Chem. A* **2002**, *106*, 4695-4702. b) Hobza, P.; Havlas*,* Z. *Chem. Rev.* **2000**, *100*, 4253-4264.

[3] Reed, A. E.; Weinhold, F. *J. Chem. Phys*. **1983**, *78*, 4066-4073.

[4] Alabugin, I. V.; Manoharan, M.; Peabody, S.; Weinhold, F. *J. Am. Chem. Soc.* **2003**, *125*, 5973-5987.

[5] Joseph, J.; Jemmis, E. D. *J. Am. Chem. Soc.* **2007**, *129*, 4620-4632.

[6] Nolasco, M. M.; Ribeiro-Claro, P. J. A. *ChemPhysChem* **2005**, *6*, 496-502. A weak CH—O interaction has been identified as having little if any IR shift of the OH stretch. Besides the weakness of the interaction, coupling of C-H resonances makes interpretation difficult.

[7] a) For a comprehensive discussion on hydrogen bonding to fluorine see: Schneider, H., *Chem. Sci.*, **2012**, *3*, 1381-1394. b) Weak CF—OH interactions have been shown in dimeric trifluoroethanol formed in a supersonic jet: Scharge, T.; Luckhaus, D.; Suhm, M. A. *Chem. Phys.* **2008**, *346*, 167-175.

[8] Filler, R.; Saha, R. *Future Med. Chem*. **2009**, *5*, 777-791.

[9] a) Barbarich, T. J.; Rithner, C. D.; Miller, S. M.; Anderson, O. P.; Strauss, S. H. *J. Am. Chem. Soc.* **1999**, *121*, 4280-4281. b) Jakobsche, C. E.; Peris, G.; Miller, S. J. *Angew. Chem. Int. Ed.* **2008**, *47*, 6707-6711.

[10] Howard, J. A. K.; Hoy, V. J.; O'Hagan, D.; Smith, G. T. *Tetrahedron* **1996**, *52*, 12613-12622.

[11] Shimoni, L.; Glusker, J. P. *Struct. Chem.* **1994**, *5*, 383-397.

[12] Bartolomé, C.; Espinet, P.; Martin-Alvarez, J. M. *Chem. Commun.* **2007**, 4384-4386.

[13] Struble, M. D.; Scerba, M. T.; Siegler, M. A.; Lectka, T. *Science* **2013**, *340*, 57-60.

[14] The predicted frequencies of the OH stretches for **41** and **47** at B3LYP/6-311++G** and other hybrid DFT levels are not of much help; these predictions are well within the performance errors of hybrid DFT vibrational frequency predictions.

[15] a) Chai, J. D.; Head-Gordon, M. *Phys. Chem. Chem. Phys*. **2008**, *10*, 6615-6620. b) Thanthiriwatte, K. S.; Hohenstein, E. G.; Burns, L. A.; Sherrill, C. D. *J. Chem. Theory Comput*. **2011**, *7*, 88-96.

[16] Bürgi, H. B.; Dunitz, J. D.; Shefter, E. *Acta Crystallogr. B*. **1974**, *30*, 1517-1527.

[17] Levitt, M.; Perutz, M. F. *J. Mol. Biol.* **1988**, *201*, 751-754.

[18] The solubility of **41** in cyclohexane is low; in hexane it is almost zero.

[19] Takasuka, M.; Taneda, H. *J. Chem. Soc. Perkin II* **1980**, 486-492.

[20] Rozas, I.; Alkorta, I.; Elguero, J. *J. Phys. Chem. A* **1998**, *102*, 9925-9932.

[21] Takemura, H.; Kaneko, M.; Sako, K.; Iwanaga, T. *New J. Chem*. **2009**, *33*, 2004-2006. Other OH---F interactions have shown through-space couplings of less than 10 Hz, our observed coupling is approximately an order of magnitude above that.

[22] Schah-Mohammedi, P.; Shenderovich, I. G.; Detering, C.; Limbach, H. H.; Tolstoy, P. M.; Smirnov, S. N.; Denisov, G. S.; Golubev, N. S. *J. Am. Chem. Soc.* **2000**, *122*, 12878-12879.

[23] Wenthold, P. G.; Squires, R. R. *J. Phys. Chem.* **1995**, *99*, 2002-2005.

[24] a) Desiraju et al. have defined H-bonds as weak, strong, and very strong. The H-bond of **47** would seem to qualify as strong: Desiraju, G. R. and Steiner, T. *The Weak Hydrogen Bond in Structural Chemistry and Biology*, OUP, Chichester, **1999**. **47** also fits Jeffrey's definition of a moderately strong hydrogen bond (a definition that is also inclusive of most biologically relevant interactions), see: Jeffrey, G. A. *An Introduction to Hydrogen Bonding*, Oxford, New York, **1997**, chap. b) Lastly, for a discussion on short, strong H-bonds see: Remer, L. C.; Jensen, J. H. *J. Phys. Chem. A* **2000**, *104*, 9266-9275.

[25] Generally, red-shifted H-bonds have enhanced intensity OH stretches, whereas blue-shifted H-bonds display diminished OH stretch intensities. Jemmis et al. (ref. 5) predict that no-shift H-bonds should have slightly enhanced intensities, which is what we observe.

[26] Grabowski, S. J. *J. Phys. Chem. A* **2011**, *115*, 12789–12799.

[27] For a similar use of rotameric controls, see: Zarycz, N.; Aucar, G. A.; Della Védova, C. O. *J. Phys. Chem. A*. **2010**, *114*, 7162-7172.

[28] Gerteisen, T. J.; Kleinfelter, D. C. *J. Org. Chem.* **1971**, *36*, 3255-3259.

[29] a) Chai, J. D.; Head-Gordon, M. *Phys. Chem. Chem. Phys*. **2008**, *10*, 6615-6620. b) Thanthiriwatte, K. S.; Hohenstein, E. G.; Burns, L. A.; Sherrill, C. D. *J. Chem. Theory Comput*. **2011**, *7*, 88-96.

Chapter 4

A Tight Intramolecular Hydrogen Bond to a Non-Conjugated Olefin

4.1 Introduction.

Hydrogen bonds play a huge role in how the world works, from imparting unique properties to water to controlling the genetic code. Ever since they were first determined to be a viable chemical interaction, the effects of hydrogen bonding have been the subject of countless studies. Over the years a perfect definition of a hydrogen bond has remained elusive; one of the first was put forth by Pauling, who classified them as electrostatic **A**-H---**B** interactions wherein both **A** and **B** are electronegative atoms.[1] Later this was expanded upon by Pimentel and McClellan to consist of **A**-H---**B** interactions, wherein there is direct evidence of bond formation in which the hydrogen on **A** plays a key role.[2] This greatly expanded the definition of H-bonding, for now many weak or "nonclassical" H-bonds could be included. However, the openness of the definition is a mixed blessing, as the sheer number of hydrogen bonding-like interactions makes it difficult to nail down exact criteria for their formation. In addition to the classic OH---O interactions, such as in water, other classical and non-classical (weak) interactions have been intensely studied over the last decades, such as OH---F,[3] NH---N,[4] FH---F[5] and CH---π.[6] While a fair number of studies have investigated the more popular H-bonding interactions to aromatic π-systems such as pyridine,[7] arenes[8] and indoles,[9] there are relatively few published studies concerning non-conjugated double bonds. In this chapter the synthesis and study of a cage system, **64**, that displays a close interaction between an OH group and a tetrasubstituted double bond is reported. Spectroscopic and crystallographic evidence indicates a significant interaction that more closely mimics the orientation of a calculated optimal intermolecular interaction (**65**).

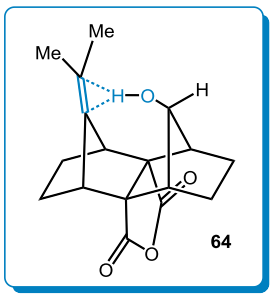

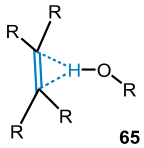

Figure 4.1 Intra- and intermolecular OH---π interactions.

4.2 Precedents.

Of the few studies that have been published on OH---π interactions in non-conjugated π-systems, all have documented fairly weak H-bonding interactions. The majority of cases have the alcohol group positioned too far away or situated poorly for the interaction from a geometric standpoint.[10] Some well-studied examples of weak OH---π interactions can be observed in 3-buten-1-ol[11] and *o*-allylphenol.[12,13] However, owing to the large degree of rotational freedom present in these molecules, the majority of them exist in an unbound state in solution. Several other studies have been undertaken to characterize the OH---π system in *syn*-7-norbornenol due to its conveniently placed alcohol group and relative lack of rotational freedom.[14,15] With its alcohol group positioned in close proximity to the double bond, a clear preference for the OH---π interaction is seen in the IR spectrum, an observation that is backed up by molecular modeling calculations. In addition, the molecule has an ideal control in its epimer *anti*-7-norbornenol, wherein the hydroxyl group is pointed away from the double bond. Previous studies, both experimental and theoretical, have confirmed the existence of a hydrogen bond, represented by a notable red shift in the IR spectrum (57 cm^{-1}) in comparison to *anti*-7-norbornenol in CCl_4.[16] However, because of the poor positioning of the alcohol in *syn*-7-norbornenol, which is at an awkward angle and a fair distance away, the interaction is still nonoptimal (the dihedral angle between the O-H bond and the C=C double bond (H-O---C(2)=C(3)) is about 81° at the ωB97XD/cc-pVTZ level of theory). What is more, the interaction is characterized by the presence of no BCP at suitable levels of theory. While this measure of the existence of hydrogen bonds is (in some cases, hotly) debatable, it does, in a certain way, represent H-bonding strength.[17] Ideally, a strong ROH---C=C interaction should have a dihedral angle of 0° resulting in the O-H bond and the C=C double bond lying in the same plane. In the previous chapter we discussed a strong OH---F hydrogen bonding interaction, where no notable shift was detected in the IR spectrum, compared to appropriate controls. We came to the conclusion that the "no-shift" was due to a mix of hydrogen bonding and bond compression.[3] Building on our previous work, we knew using a similar molecular scaffold as the latter would bring the OH group and the double bond into close contact as well as place them nearly orthogonal, perfect for hydrogen bonding overlap. The use of a double bond instead of a C-F would also free up space, reducing bond compression and allowing us to see the full strength of the hydrogen bond. In addition, the double

bond could be tetrasubstituted with electron donating aliphatic groups. The sum of all these factors should result in a more intense hydrogen bonding interaction.

4.3 DFT calculations.

We began our investigation of this putative tight OH---π bond by probing the interaction through molecular modeling calculations. The vibrational modes for both the *in*- and *out*-alcohols were predicted using the ωB97XD/cc-pVTZ basis set, because of its reputation for accurately predicting dispersion effects.[18] The calculated OH shifts place the *in*-OH of **64** red shifted, compared to the *out*-OH of **71**, with a difference of 167 cm^{-1}. This is an impressive (albeit predicted) red shift; over twice the difference between the *syn*- and *anti*-epimers of 7-norbornenol.[16] The calculation also places the alcohol hydrogen of the **64** only 1.974 and 2.076 Å from the olefin's bond ends, compared to the predicted 2.540 and 2.541 Å in *syn*-7-norbornenol, with the same method and basis set. To double check the accuracy of the method, the *anti*/*syn*-7-norbornenol red shift was calculated and found to be 67 cm^{-1} at the same level of theory. Another test was to compare the energy calculation of **64** to a non-hydrogen bound version of **64** where the OH bond is rotated 180°. The results predict **64** to be 7.30 kcal/mol more stable than the non-hydrogen bound version. Additionally, electron density (ρ) calculations using the QTAIM program indicate a BCP between the alcohol hydrogen and the olefin, $\rho = 0.036$.[19]

4.4 Controls.

For a better understanding of the strength of the interactions, intramolecular hydrogen bonds are often compared to analogous intermolecular hydrogen bonding interactions. From a computational standpoint, one control interaction is the intermolecular H-bond of methanol and ethylene.[20] This interaction and the related system of water and ethylene have been the topic of multiple computational studies.[21] However, we believe a model that is a better match for our cage molecule would be the complex of tetramethylethylene and MeOH (**65**, R = Me). This would take into account the electron donating capabilities of the methyl and aliphatic groups substituted on the double bond of **64**. For our investigation, the interaction of tetramethylethylene and MeOH was optimized using the same method and basis set as the previous

calculations (ωB97XD/cc-pVTZ). The predicted distances to the sp^2 carbons, 2.279 and 2.315 Å, are somewhat looser than those predicted for **64**. The predicted red shift for the control was 39 cm^{-1}.

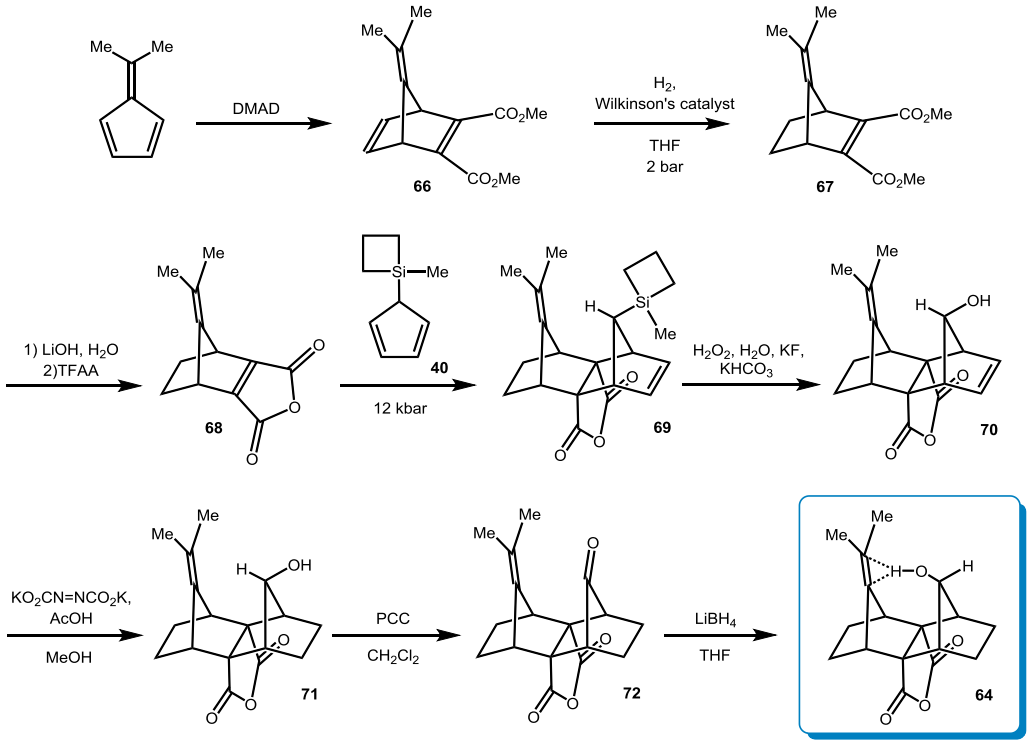

Scheme 4.1 Synthetic pathway for the generation of **64**.

4.5 Synthetic method.

In order to integrate the olefin into our sesquinorbornane scaffold, a new dienophile (**68**) was designed for the synthesis. The route begins with 6,6-dimethylfulvene, which was allowed to react neatly with dimethylacetylene dicarboxylate (DMAD) to yield the trienediester **66**. Wilkinson's catalyst was employed to reduce the least-substituted double bond, yielding **67**. This reduction was followed by saponification of the carbomethoxy groups with LiOH to form a dicarboxylic acid, which was then converted without workup into the corresponding anhydride using trifluoroacetic anhydride (TFAA). With this new dienophile in hand, it was treated with **40** at high pressure to perform the Diels-Alder reaction that makes sesquinorbornane scaffold **69**. This was followed by a Flemming-Tamao oxidation to convert the silane to alcohol **70** and a diimide reduction to reduce selectively the less substituted double bond. Similar to the *anti*/*syn*-7-norbornenol system, this *out*-alcohol (**71**) serves as an ideal control to study the strength of the

H-bonding interaction. Alcohol **71** was oxidized to a ketone (**72**) by treatment with PCC, and then reduced stereospecifically with $LiBH_4$ to form **64**.

4.6 Spectroscopic calculations.

X-ray crystallography. A single crystal of **64** was obtained through solvent evaporation from a solution in dichloromethane, and crystallographic measurements were performed using X-ray diffraction. The framework crystallographic analysis with the alcohol O-H bond constrained to 0.963 Å shows a very close OH---π interaction (predicted distances to the sp^2 carbons: 1.995 and 2.084 Å), which is in agreement to the predicted distances 1.974 and 2.076 Å at the ωB97XD/cc-pVTZ level of theory, as shown in figure 4.2. No signs of bifurcation of the OH bond were noted in the crystal packing.

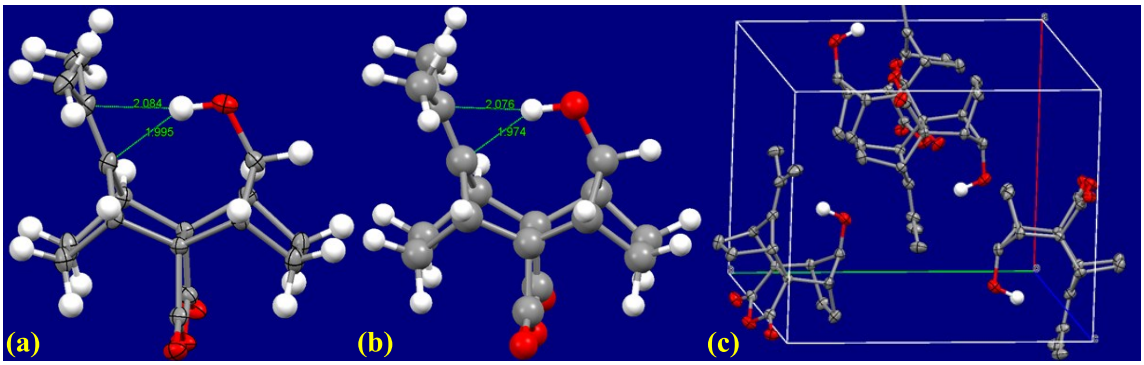

Figure 4.2 (a) Crystal structure of **64** determined from single crystal X-ray diffraction (50% thermal ellipsoids). The O-H bond distance was constrained to the value calculated in the DFT equilibrium calculation (0.963 Å). (b) Equilibrium structure calculation of **64** at ωB97XD/cc-pVTZ. (c) Crystal packing diagram of **64**. Except for the alcohol hydrogen, all hydrogen atoms have been removed for ease of observation.

IR spectroscopy. IR studies of **64** and **71** corroborate the molecular modeling predictions. When the two OH stretches were compared, it was immediately clear the bound alcohol of **64** has a far more intense OH stretch than the free alcohol of **71**. Also, the actual red shift in the IR spectrum was in fact greater than the prediction, measuring 188 cm^{-1}. These measurements were performed on dilute (10^{-2} M) samples in dichloromethane. When the solvent was changed to carbon tetrachloride, the interaction was unaffected as **64** was observed to have a red shift of 189 cm^{-1} compared to **71**, see Figure 4.3.

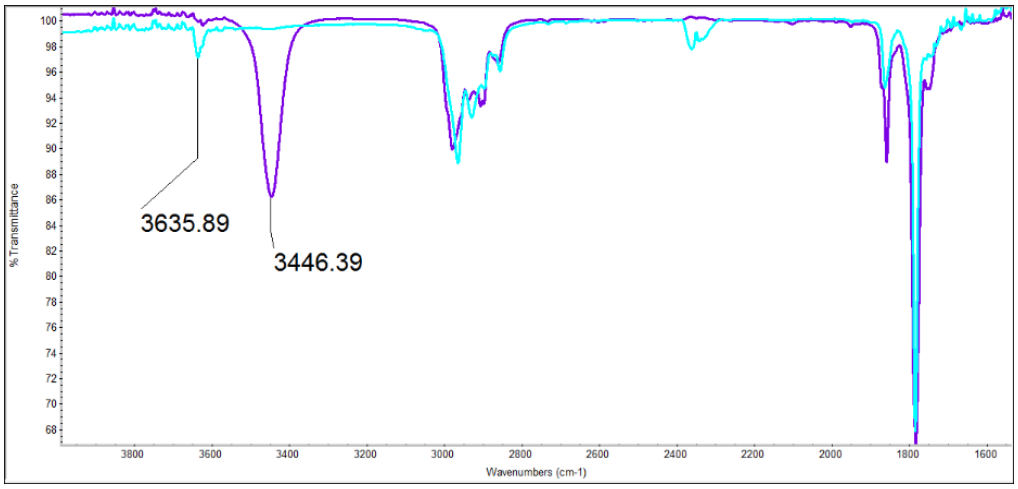

Figure 4.3 Overlay of the IR spectra of **64** (purple) and **71** (blue), in carbon tetrachloride, highlighting the large red shift in the alcohol stretching frequency.

NMR spectroscopy. In the ^{1}H NMR the alcohol hydrogen of **64** is found at 4.05 ppm; likely due to the deshielding effects of the C=C bond. Another example of this trend was observed in the proton geminal to the alcohol. In **64**, the geminal proton, 4.26 ppm, is pointed away from the olefin and effectively free from the influence of the C=C bond. However, in **71** the geminal proton is noticeably deshielded, compared to **64**, at 5.27 ppm. Another indication of how tight the hydrogen is held is the lack of exchange with the deuterated chloroform contaminated with traces of DCl. The integrations of the alcohol peak reveals that only a negligible amount of the proton in **64** exchanged, whereas the OH protons of **71** exchanged rapidly and completely.

4.7 Conclusions.

Our results show that **64** does indeed contain a tight hydrogen bonding interaction between the alcohol and the nonconjugated π-system. This is most evident in the IR spectrum where **64** is red shifted 188-189 cm^{-1} from the control system **71** and is shown to contain no free alcohol. In addition, our molecular modeling calculations show that **64** positions the alcohol far closer to the double bond compared to previously studied systems. This is a notable change when compared to the previous molecules studied, such as *syn*-7-norbornenol, whose bond distances were not too much different from the free-methanol/tetramethylethylene system. With the evidence from both molecular modeling and experimental

measurements it is clear that our system possesses a more significant hydrogen bonding interaction than previously seen, and thus is a more revealing probe of this phenomenon.

4.8 References.

[1] Pauling, L. *The Nature of the Chemical Bond*, 3rd ed.; Cornell University Press: New York, 1960.

[2] Pimentel, G. C.; McClellan, A. L. *The Hydrogen Bond*; Freeman: San Francisco, 1960.

[3] Struble, M. D.; Kelly, C.; Siegler, M. A.; Lectka, T. *Angew. Chem. Int. Ed.* **2014**, *53*, 8924-8928.

[4] Grunenberg, J. *J. Am. Chem. Soc*. **2004**, *126*, 16310–16311.

[5] Del Bene, J. E.; Alkorta, I.; Sánchez-Sanz, G.; Elguero, J. *J. Phys. Chem. A* **2012**, *116*, 9205-9213.

[6] a) Takahashi, O.; Kohno, Y.; Nishio, M. *Chem. Rev*. **2010**, *110*, 6049-6076; b) Brandl, M.; Weiss, M. S.; Jabs, A.; Suhnel, J.; Hilgenfeld, R. *J. Mol. Biol.* **2001**, *307*, 357– 377.

[7] Lomas, J. S. *J. Phys. Org. Chem.* **2012**, *25*, 620-627.

[8] a) Banerjee, P.; Chakraborty, T. *J. Phys. Chem. A*. **2014**, *118*, 7074-7084; b) Dušan P. Malenov, D. P.; Janjic´, G. V.; Veljkovic´, D. Z.; Zaric´, S. D. Comp. Theor. Chem. 2013, 1018, 59-65; c) Saggu, M.; Levinson, N. M.; Boxer, S. G. *J. Am. Chem. Soc.* **2011**, *133*, 17414–17419; d) Mohan, N.; Vijayalakshmi, K. P.; Koga, N.; Suresh, C. H. *J. Comput. Chem*. **2010**, *31*, 2874-2882; e) Gergely Tóth, G.; Bowers, S. G.; Truong, A. P.; Probst, G. *Curr. Pharm. Des*. **2007**, *13*, 3476-3493.

[9] a) Sasaki, H.; Daicho, S.; Yamada, Y.; Nibu, Y. *J. Phys. Chem. A*. **2013**, *117*, 3183-3189; b) Steiner, T.; Koellner, G. *J. Mol. Biol.* **2001**, *305*, 535– 557.

[10] Oki, M.; Iwamura, H.; Onoda, T.; Iwamura, M. *Tetrahedron* **1968**, *24*, 1905-1921.

[11] Bakke, J. M.; Bjerkeseth, L. H. *J. Mol. Struct*. **1998**, *470*, 247-263.

[12] Berdyshev, D. V.; Glazunov, V. P.; Novikov, V. L. *J. Appl. Spectrosc*. **2009**, *76*, 630-640.

[13] Rademacher, P.; Khelashvili, L.; Kowski, K. *Org. Biomol. Chem*. **2005**, *3*, 2620-2625.

[14] a) Marchand, A. P.; Ganguly, B. *Struct. Chem.* **2000**, *11*, 241-244; b) Rademacher, P.; Khelashvili, L.; Kowski, K. *Org. Biomol. Chem*. **2005**, *3*, 2620-2625; c) Brown, R. S. *Can. J. Chem.* **1976**, *54*, 3206-3209.

[15] Bjerkeseth, L. H.; Bakke, J. M.; Uggerud, E. *J. Mol. Struct.* **2001**, *367-368*, 319-338.

[16] Takasuka, M.; Tanida, H. *J. Chem. Soc., Perkin Trans. 2* **1980**, 486-492.

[17] Grabowski, S. J. *J. Phys. Chem. A* **2011**, *115*, 12789–12799.

[18] a) Chai, J. D.; Head-Gordon, M. *Phys. Chem. Chem. Phys*. **2008** , *10*, 6615–6620; b) Thanthiriwatte, K. S.; Hohenstein, E. G.; Burns, L. A.; Sherrill, C. D. *J. Chem. Theory Comput.* **2011**, *7*, 88–96.

[19] AIMAll (Version 13.05.06), Keith, T. A., TK Gristmill Software, Overland Park KS, USA, 2013 (aim.tkgristmill.com).

[20] Tarakeshwar, P.; Choi, H. S.; Lee, S. J.; Lee, J. Y.; Kim, K. S.; Ha, T.; Jang, J. H.; Lee, J. G.; Lee, H. *J. Chem. Phys.* **1999**, *111*, 5838-5850.

[21] Engdahl, A.; Nelander, B. *J. Phys. Chem.* **1986**, *90*, 4982-4987.

Chapter 5

Investigation of the Mechanism of the Fluoronium Intermediate

5.1 Introduction.

While the labeling experiment in chapter 1 shows substantial evidence that the hydrolysis of the fluoronium precursor **42** proceeds through an S_N1 path, the evidence is only circumstantial. In an effort to bolster our claims we have subjected the system to a series of experiments to obtain more information on its mechanism. Such methods include rate studies, control experiments, molecular modeling calculations and KIE studies.

5.2 Transition state calculations.

In order to predict isotope effects using DFT,[1] we need information about the putative transition states. We performed calculations to find potential transition states for the ionization of **42** and trapping of fluoronium **13** at several levels of theory. For example, a transition state for the ionization of triflate **42** (at B97, H_2O solvent model) was found to reveal some interesting features. The distance of the ionizing C-O bond is 2.37 Å; the structure also shows a forming C-F bond as well (*d* = 2.20 Å). Thus the fluorine atom rapidly closes in on the carbon as the ionization proceeds.

Calculation of the transition states using other functionals (M06, PBEPBE) afforded comparable results in terms of geometry. The activation free energy for the process is calculated to be 26.5 kcal/mol at 55 °C (H_2O dielectric), with the cation resting in an energy well about 12.5 kcal/mol below (Figure 5.1). The thermochemistry of such calculated reaction pathways should be approached with a high degree of caution,[2] and mechanistic conclusions derived therefrom subject to experimental verification. A salient example of this danger is provided in the calculated (S_N1) mechanism of the reaction of water with triflate **42**. The transition state for trapping of fluoronium **13** by water was also modeled; the distances of the forming/breaking bonds were similar if not identical to the ionization of triflate **42** (C-F = 2.23 Å; C-O = 2.34 Å; B97, H_2O solvent model). At B97 (H_2O dielectric), the second, water-trapping step is predicted to be rate-determining. It is obvious that the difference in the charged nature of the transition states, and the

role of specific solvation combined with the continuum solvent model give rise to an erroneous conclusion in terms of the energy.

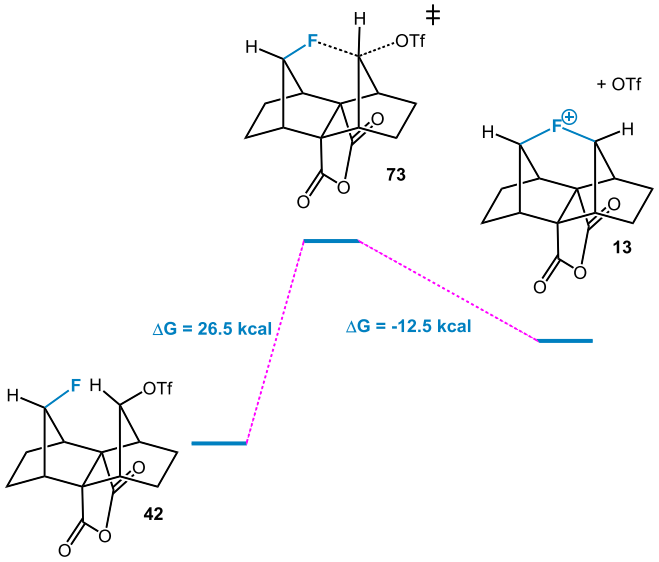

Figure 5.1 Calculated free energy of ionization for triflate **42** (B97, aqueous dielectric).

As mentioned in chapter 1, we proposed an "extended S_N2" reaction as a viable mechanistic alternative, a possibility seemingly ruled out by the labeling study. In addition, the stereochemical outcomes are inconsistent with this exotic form of the S_N2. What is more, we were unsuccessful at locating transition states that would describe this process. In fact, there is a very strong tendency for nucleophiles/Lewis bases to interact with the methano-bridges of system **13** through hydrogen bonding instead of engaging in incipient nucleophilic attack. For example, the depicted structure of a dihydrated version of cation **75** (B3) reveals this tendency (Figure 5.2).

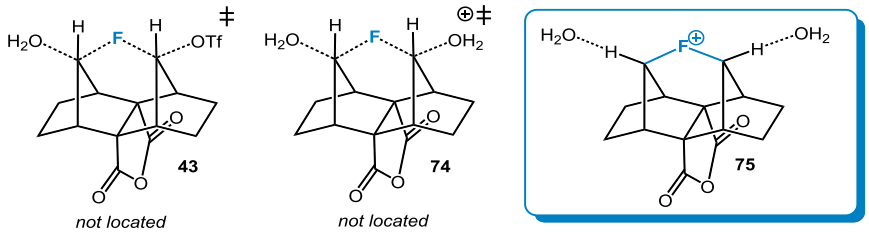

Figure 5.2 The hypothetical S_N2(e) transition states (not found) and a disolvated cation (minimum; found). Calculations at B3.

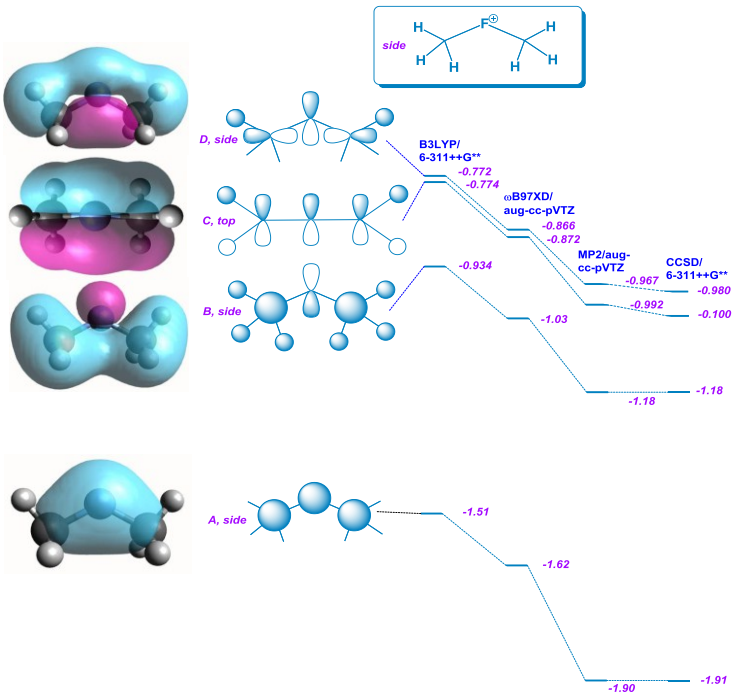

Figure 5.3 Calculated three-center bonding orbitals of dimethylfluoronium (C_{2v} symmetry) and their energy levels (eV) at several levels of theory (orbital C shown from top view, A, B, and D shown from side view).

Three-Center Bonding in a Model. Analysis of the C-F-C interaction in cation **13** is made somewhat difficult by the admixture of atomic orbitals (AOs) from the cage framework. If we remove the cage, we are left with the question of three-center bonding in the model system $[Me\text{-}F\text{-}Me]^+$ (imposed C_{2v} symmetry). Various levels of theory are in basic agreement on orbital topology and energy (Figure 5.3 depicts the four lowest lying molecular orbitals involve the three-center bonding of the C-F-C interaction). The lowest lying filled orbital A involves overlap of atomic s-orbitals. The next highest orbital B involves a p-orbital on fluorine, the 2s orbitals on the carbons and the 1s orbitals on the hydrogens, whereas the two higher energy orbitals C-D involve p-AO's on carbon and fluorine. The relative energies of the orbitals are carried over two DFT levels, one MP2, and one CCSD, providing us with a consistent picture.

Often in discussions of three-center bonding the question arises as to the viability of the so-called "classical," or two-center, alternative. In the case of the fluoronium system **13**, a classical alternative is not a stable minimum on the calculated potential energy surface. In order to estimate the energy of a hypothetical classical structure, we employed the procedure of Schleyer et al.[3] Namely, the corresponding

radical was optimized and then corrected by the computed vertical ionization energy. The resulting artificial cation was found to be 21 kcal/mol (B3) and 22.6 kcal/mol (B97) higher in energy than fluoronium **13** - no wonder it is not a minimum. It is a reasonable assumption that a carbocationic center will derive stabilization from any nearby lone pair of electrons (in this case from the fluorine atom).

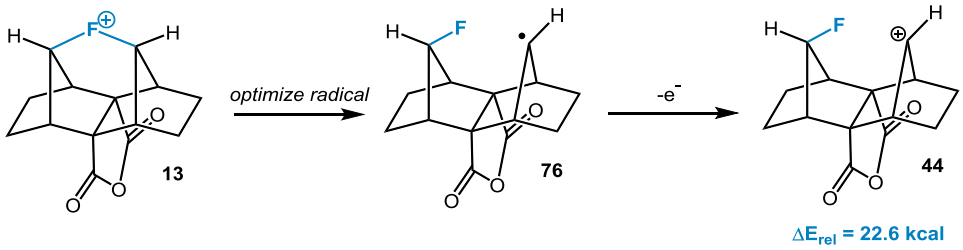

Scheme 5.1 Schleyer method for the calculation of the "classical" carbocation.

Although electron-counting schemes are arbitrary and sometimes hazardous to interpret, a trend can be discerned upon formation of the fluoronium from a model precursor such as **17** through a hypothetical hydride transfer (B97, vacuum). The fluorine atom becomes more positively charged, as do the two hydrogens on the methano-bridges. This gives some credence to the hydrogen bound, dihydrated cation **75**. On the other hand, the carbon atoms become more negatively charged, a pattern that may be ascribed to a natural consequence of three-center, four-electron bonding.

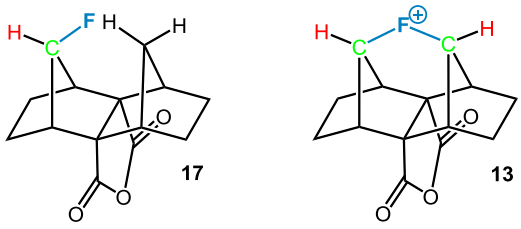

charges on F:
electrostatic -0.303
Mulliken -0.143
natural -0.395

charges on C:
electrostatic 0.328
Mulliken -0.260
natural -0.243

charges on H:
electrostatic 0.105
Mulliken 0.228
natural 0.176

charges on F:
electrostatic -0.178
Mulliken -0.051
natural -0.270

charges on C:
electrostatic 0.357
Mulliken -0.352
natural -0.275

charges on H:
electrostatic 0.177
Mulliken 0.320
natural 0.244

Figure 5.4 Comparison of charge disposition upon fluoronium formation (B97 vacuum; trend holds for other theoretical levels and with solvent models).

5.3 Rate studies.

Eyring Plot. We measured the activation free energy for the ionization of triflate **42** (70/30 v/v TFE/H_2O) in the temperature range 50-81 °C. An Eyring plot[4] (a plot of ln*k* v. 1/T) afforded a straight line whose slope corresponds to a ΔH_{act} of 14 kcal/mol. In addition, ΔS_{act} is -21 cal/molK and ΔG_{act} (55 °C) is 20.7 kcal/mol, which is less than that predicted by theory (26.5 kcal/mol); the enthalpy and entropy terms independently also differ substantially. The exceptionally negative entropy of activation deserves comment; although S_N1 reactions display negative values routinely,[5] this magnitude is unusually large. We attribute the large negative value to the ionizing role of the acidic fluorinated alcohol, which can effectively stabilize the developing negative charge on the departing triflate ion. This ionization ability has been shown by Berkessel to propagate through a mutually reinforcing and ordered network of solvent molecules (e.g. **73•solv**).[6] This organized transition state assembly would be expected to reduce entropy.

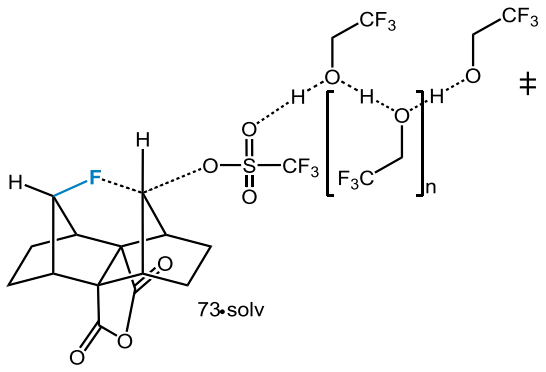

Figure 5.5 Solvation model of transition state **73**.

Grunwald-Winstein Test. This experiment is a fairly rigorous kinetic test for the operation of S_N1 and S_N2 mechanisms. Its basic form is as follows: $\log(k/k_o) = m\mathrm{Y}$, wherein *k* is a first order rate constant for a solvolysis in a solvent system of choice, and k_o is the same in a reference reaction (80% ethanol/water v/v). Y is a solvent "ionizing power" parameter, and *m* represents the sensitivity to the reactions of choice to ionizing power. Values of *m* that trend towards one or higher indicate a solvent response similar to an established S_N1 model reaction, whereas *m* values of 0.25-0.35 indicate S_N2 reactions. As our hydrolytic precursor **42** is a triflate, in order to ensure accuracy we employed the kinetic analysis employing the Y_{OTf} parameter set, which is based on solvolyses of 2-adamantyl triflate, a substrate rigorously established to

react through a pure S_N1 mechanism. Along with the reference reaction (80% ethanol/water v/v), we chose (80% acetone/water v/v) as its Y value of 0.243 suggested an easily measurable rate in our system.[7] It should be noted that both the reaction of choice and the reference were conducted in more nucleophilic (and thus less S_N1 favorable) media than the TFE solvolyses, thus ensuring a considerable margin of safety. The negative slope of plots of ln[triflate] versus time yielded *k* values that were inserted into the equation. The *k* values for triflate **42** were found to be 0.035 s^{-1} in 80% ethanol/water and 0.083 s^{-1} for 80% acetone/water. An *m* value of 1.54 was then calculated, strongly indicating an S_N1 reaction, with negligible nucleophilic solvent assistance, as expected. In comparison with 2-adamantyl triflate solvolysis, the present result is consistent with a later, and thus more product like transition state with considerable charge separation.

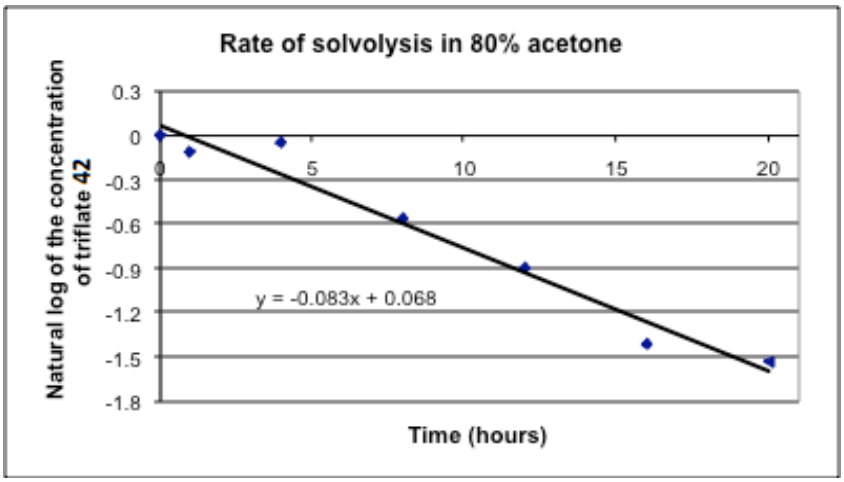

Figure 5.6 Rate study of the solvolysis of **42** in 80% acetone/water (v/v).

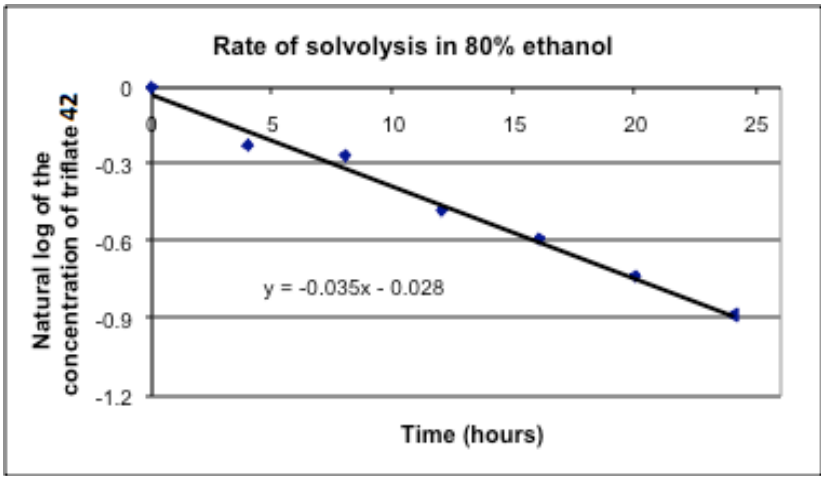

Figure 5.7 Rate study of the solvolysis of **42** in 80% ethanol/water (v/v).

Common Ion Effects. Common ion studies are often used to shed light on the role that ion pairs play in solvolysis reactions.[8] We chose LiOTf as a point of comparison; in the presence of varying quantities of (0.01 – 0.1M) LiOTf, the rate of reaction remains essentially the same within error. Consistent with this observation, recovered starting triflate **48** does not scramble its labels to any measurable extent; monitoring the solvolysis of triflate-d_2 **48**, we see no isomerization that would be indicative of external return. These results are not surprising – given the very low nucleophilicity of the triflate ion, it possesses little ability to compete with the water in the solution.

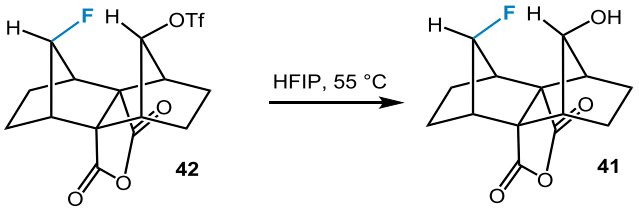

	k_{rel}
No additives	1
0.1M $In(OTf)_3$	1
2,6-(di-*t*-Bu)pyridine, (1.5 equiv)	34
2,6-(di-*t*-Bu)pyridine (1.5 equiv.), 0.002M $In(OTf)_3$	31
2,6-(di-*t*-Bu)pyridine (1.5 equiv.), 0.1M $In(OTf)_3$	5

Figure 5.8 Effect of base and $In(OTf)_3$ on the rate of solvolysis of **42**.

Solvolysis in the Presence of a Lewis Acid and a Hindered Base. This solvent dependent mechanistic "switch" prompted us to investigate other methods by which the S_N1 reaction coordinate could be altered. Two experiments immediately came to mind. The first endeavors to answer the question whether the addition of a base could lower the energy of the second transition state of the reaction by improving the nucleophilicity of the solvent molecules, as well as scavenging any triflic acid formed in the reaction (additional base has virtually no effect on the rates of solvolysis in aqueous media). The second experiment would be the addition of an alcohol-tolerant Lewis acid such as $In(OTf)_3$. In theory, the Lewis acid could coordinate to the triflate leaving group to aide in its removal, thus lowering the barrier of the first transition state. This in combination with a non-coordinating base could result in an even greater increase of the rate than with the base alone. For these experiments we chose to use HFIP as solvent and 2,6-di-*tert*-butylpyridine (DTBP) as the non-coordinating base. Initially it looked as though our theory was correct. In a conventional solvolysis reaction with **42** and the Lewis acid (0.1M $In(OTf)_3$, 65 °C) we

observed no discernable change in rate, compared to pure HFIP. Which was expected as the second step is rate determining. Then we attempted the same solvolysis reaction with base alone (1.5 eq. DTBP, 65 °C), and a large increase (34 times compared to pure HFIP) in rate was observed. However, when 0.002M $In(OTf)_3$ was added in addition to the base, the rate of reaction was found to decrease slightly to 31 times faster than pure HFIP. At much higher concentrations of Lewis acid (0.1M) the reaction rate decreased to five times that of pure HFIP. A possible explanation for this surprising result could be that deprotonated hexafluoroisopropoxide may be tied up through binding to In(III) (Scheme 5.2). This would counteract the effect of the base, and again make the nucleophile trapping step rate determining. Also, it is not out of the realm of possibility that liberated triflate ions from the Lewis acid may also play a role. These findings demonstrate that a change in rate-determining step in an S_N1 reaction can produce counterintuitive, if not peculiar, results (Figure 5.8).

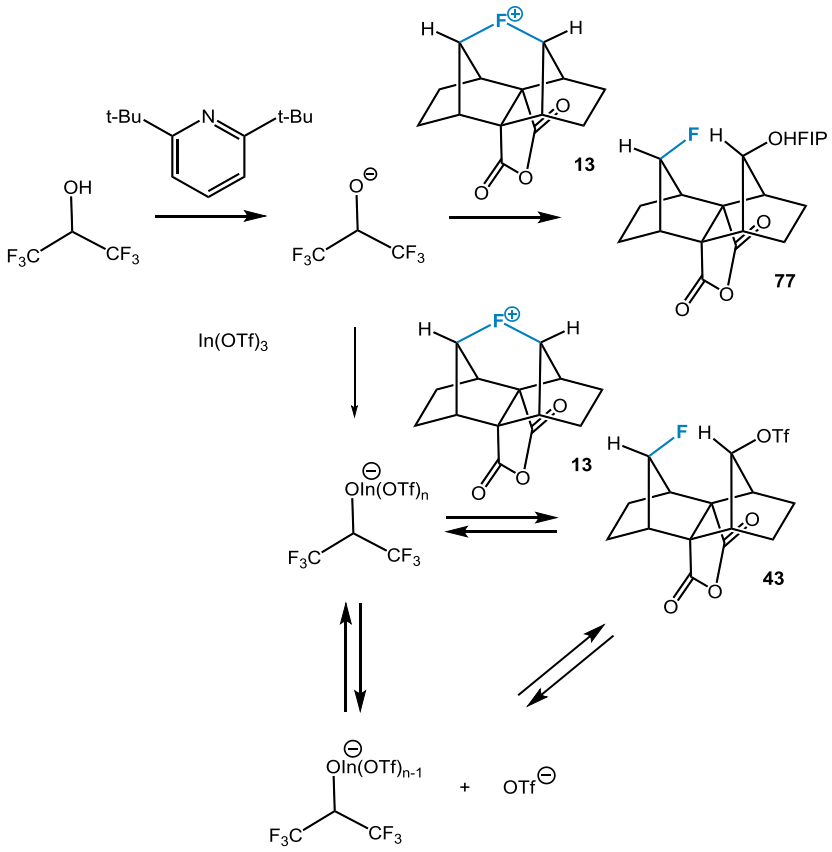

Scheme 5.2 Putative mechanism for the solvolysis of **42** in the presence of DTBP and $In(OTf)_3$, showing the trapping of the alkoxide.

These data can be summarized by comparison of qualitative reaction coordinate diagrams A-D (Figure 5.9); for simplicity's sake, ion pairs are neglected. In a lower nucleophilicity, higher ionizing medium (pure HFIP), the first step of the solvolysis reaction, loss of the triflate group (TS1‡), decreases in energy, whereas the second step, nucleophilic attack by the solvent (TS2‡), increases (A ➔ B). When a hindered base is added (2,6-di-*tert*-butylpyridine) the energy barrier of the second step drops significantly, such that the rate is greater than in the mixture of HFIP and water by almost a factor of two (B ➔ C). When $In(OTf)_3$ is added, quenching the alkoxide, the second step presumably increases in energy once again, and triflate is liberated. The fact that a large decrease in rate occurs in B ➔ C indicates that a common ion effect must be considered as well. This was shown to be unlikely as the addition of LiOTf (0.1M) to a solvolysis reaction in pure HFIP has no meaningful effect on the rate. In addition, the previously discussed analogous control reaction (0.1M $In(OTf)_3$) in pure HFIP also showed no appreciable change in the rate.

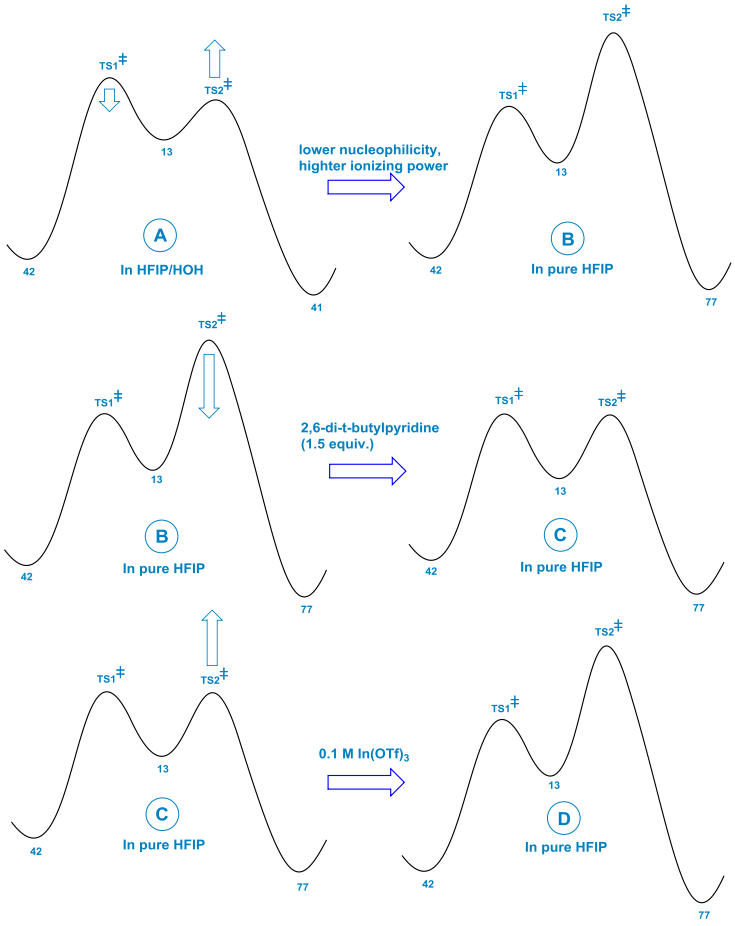

Figure 5.9 Alterations to the reaction energetics of the solvolysis reaction of **42** due to solvent effects and additives.

(5.1)

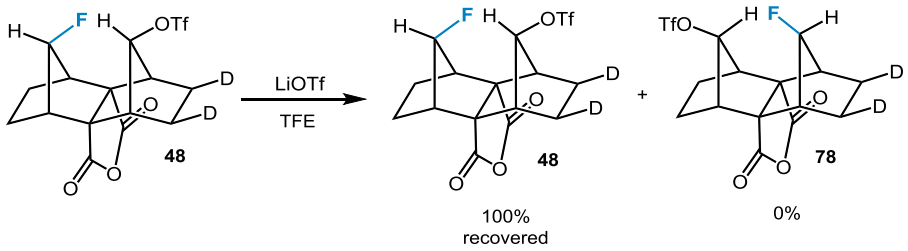

5.4 Isotopic labelling studies.

Solvolytic behavior of triflate 48 in pure polyfluorinated alcohols. As shown, hydrolysis and alcoholysis experiments were generally performed in mixtures of water and polyfluorinated alcohols. We most commonly employed TFE; rate trends in mixtures of TFE and various proportions of water comport with those expected for S_N1 reactions. Rates in mixtures of HFIP and water (70/30 v/v) are only slightly higher than those of analogous mixtures in TFE and perfluoro-*t*-butanol (PFTB) and significant conclusions are difficult to reach (Scheme 5.3). On the other hand, what about the pure alcohols themselves as reaction media? Polyfluorinated alcohols such as TFE are unusual solvents in several ways; for example, whereas the ionizing power increases in the order TFE < HFIP,[9] the dielectric constant decreases as TFE > HFIP.[10] Thus, as their ability to ionize substrates increases, their corresponding ability to dissociate ion pairs decreases. The properties of the pure solvents give rise to an interesting observation; in pure TFE, the rate of alcoholysis of **42** is 10 times greater than in HFIP,[11] and more than 1000 times greater than PFTB! This would suggest that the RDS of the triflate solvolysis has changed – instead of ionization, the RDS is now nucleophile trapping. Ingold et al.[12] first documented this behavior in the context of triarylmethyl halide solvolyses, and a subsequent convention settled on the (somewhat misleading) name S_N2C^+ to specify this mechanistic variant.[13] It is a less common phenomenon, and usually occurs in the context of highly stable and hindered carbocations. On the other hand, one can argue that hydrogen bonding of the acidic polyfluorinated alcohols to the anhydride group of triflate **42** could be responsible for inhibition of ionization. In light of Creary's results on the generation of α-keto carbocations from the respective triflates,[14] this seems much less likely, but must be considered.

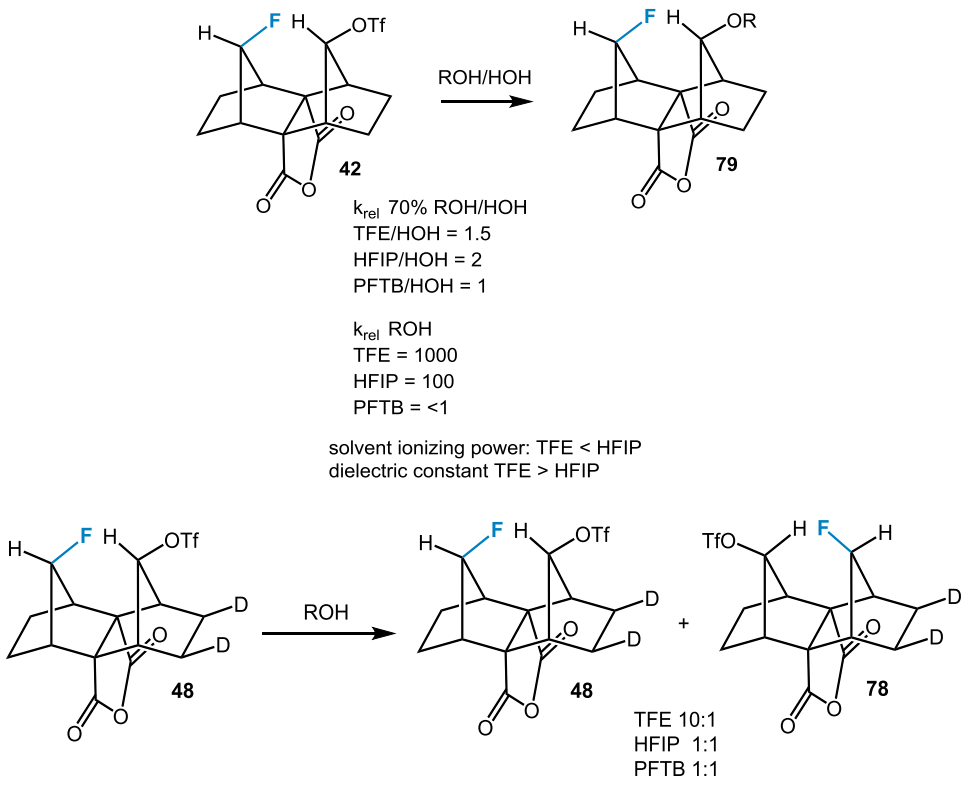

Scheme 5.3 Effects of solvent on solvolysis rate.

If we were seeing a change in the RDS, then a simple experiment would confirm the hypothesis. Under hydrolytic conditions (e.g. 70/30 v/v TFE/water), recovered quantities of labeled triflate **48** show no isotopic scrambling, consistent with the fast trapping of water by the cationic intermediate. However, when the reactions are conducted in pure TFE, evidence of a partial degree of scrambling is shown by NMR (~10%), in addition to formation of the ether product. When either HFIP or PFTB is employed, complete scrambling is observed in recovered triflate (**48**:**78** = 1:1), confirming that the cation-forming transition state is surmounted but the RDS has changed so that alcohol trapping is now rate determining (Scheme 5.3). These results illustrate the difference between solvents that foster ionization and those that promote dissociation; whereas water promotes both, the polyfluorinated alcohols are ionizing, but much less dissociating (smaller dielectric) than water. Hence "tight" ion pairs form in these media that can collapse back to the starting triflate. In aqueous media, however, dissociation is rapid and irreversible (i.e. lack of a common ion effect). Finally, the nucleophilicity of the pure alcohols is low, thereby increasing the barrier of the second step. In the case of PFTB, steric hindrance becomes a very large player as well.

Kinetic and Equilibrium Isotope Effects. Back in our original labeling experiment in chapter 1, we used deuterium atoms as labels to differentiate between the two alcohol or ether products of a putative fluoronium intermediate for purposes of integration. The deuterium atoms were positioned remotely to the $[C\text{-}F\text{-}C]^+$ array; thus integration resulted in a 1:1 ratio (within the error limits of our experiment at that time).

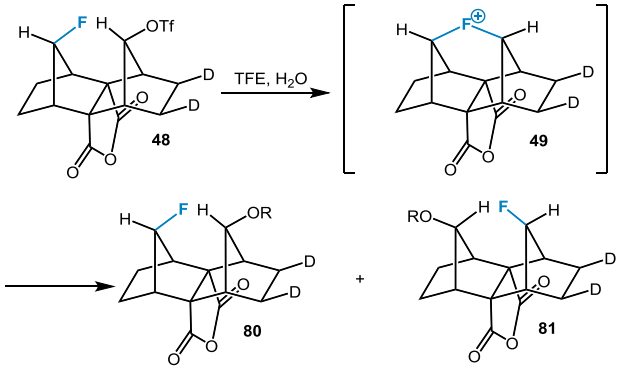

Scheme 5.4 Basic isotopic labeling study. Products are either alcohols or ethers depending on the presence of water.

It occurred to us, however, that even though the labels were remote, they may still exert a steric effect[15] in the transition state for both (S_N1) ionization of triflate **48** and the trapping of cation **49** by water. In fact, triflate-d_2 **48** ionizes 1.04 times faster than **42** (k_H/k_D = 0.963±0.003) as indicated by careful integration of product mixtures. This measurement is in rough concord with isotope effect calculations at (B97 and B3), in which the free energies of labeled and unlabeled transition states for ionization of **42** and **48** were compared in a water dielectric (k_H/k_D = 0.90 and 0.95, respectively at 328 K).

Owing to deuterium atoms being effectively "smaller" than hydrogens, trapping of water proximally to the deuterium atoms should also be favored. Thus, the ratio of products **80:81**, Scheme 5.4 (R=H), is measured at 0.93. The calculated isotope effect for trapping of water likewise predicts the same direction in close agreement to the experimental ($k_{distal}/k_{proximal}$ = 0.93 and 0.94 at B97 and B3, respectively at 328 K). Most importantly, these product ratios do not change with conversion, whereas the isotope effect for consumption of triflate **48** trends towards 1.00 at 100% conversion. In the case of water trapping, the isotope ratios are the same as measured at 10% conversion; this observation is in line with the trapping of a symmetrical intermediate.

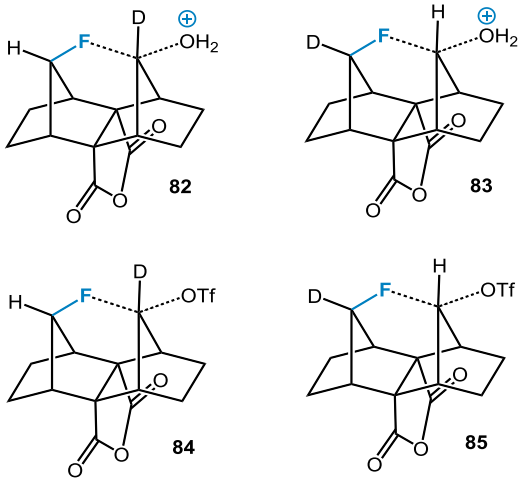

Figure 5.10 Isotopomeric transition states for C-F-C labeled molecules.

More interesting and relevant would be the introduction of deuterium labels on the carbon atoms anchoring the $[C\text{-}F\text{-}C]^+$ bond; this, however, represented a synthetic challenge. We know that *out*-alcohol **41** (Scheme 5.5) can be oxidized to ketone **58**, and reduced again with LAH to effect an epimerization to *in*-alcohol **47** (see chapter 3).[16] By using $LiAlD_4$ (LAD), a deuterium label can be introduced α- to the OH group to form *in*-alcohol **85** (34% yield, >98% D incorporation). It should be noted that the anhydride of the caged system is virtually inert to hydrolysis or reducing agents;[17] the trajectory needed for nucleophilic attack is precluded by steric interference from C-H bonds residing on the ethano-bridges.

At this point a fortuitous discovery was exploited; in an attempted triflation of *in*-alcohol **47**,[16] we instead isolated *out*-triflate[18] **42** in high yield (94%). Apparently the *in*-triflate **86**, being more strained (calculated activation free energy of ionization = 22.3 kcal/mol (B97, 40 °C, CH_2Cl_2 dielectric), ionizes very rapidly, and retraps the triflate ion in the *out*-position. Thus, we can effectively use this *in situ* triflation to epimerize the *in*-labeled alcohol **87** back to the *out*-position. Note however, that this triflation/rearrangement produces a mixture of label isomers **88** and **89** in the ratio of 1.14:1. If we can turn our attention back to the transition state **84** for trapping of triflate ion by the fluoronium, we can see why. The calculated isotope effect 1.07 (B97, 40 °C, CH_2Cl_2 dielectric) and more accurately at B3 (k_{dist}/k_{prox} = 1.12, 40 °C, CH_2Cl_2 dielectric) is congruent with what we observed, and represents a normal α-secondary deuterium isotope effect (Scheme 5.5). What is more, the predicted transition state (B97, CH_2Cl_2 dielectric) for ionization of the *in*-triflate **86** is a fascinating structure in its own right; it reveals a highly unusual S_Ni reaction with very evident frontside participation of fluorine (C-F distance = 2.71 Å, C-O

distance = 2.20 Å). A QTAIM analysis reveals a BCP between F and C in the transition state, indicating some type of interaction. Interestingly enough, another BCP is predicted to exist between F and the triflate ether oxygen.

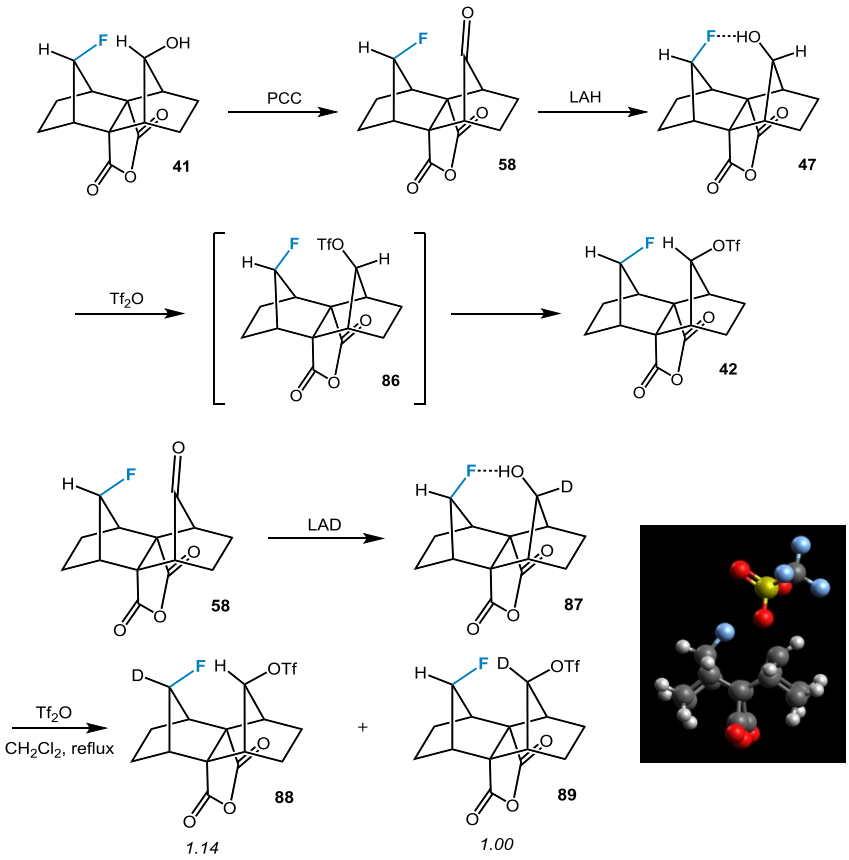

Scheme 5.5 *In*-to-*out* isomerization upon attempted triflation of alcohol **87** and the installation of isotopic labels in the C-F-C array. Picture: calculated transition state for ionization of **86** showing frontside participation of fluorine.

However, we must be careful in interpretation; if fluorine assists in the transition state, a *remote* isotope effect would be expected to diminish the phenomenological effect from the otherwise "limiting" value (which can be as high as ~1.4[19] for pure S_N1 reactions in related systems). A remote isotope effect on trapping of water also means a remote effect on ionization. An additional experiment, starting with the labeled triflates **88** and **89**, allows us to separate the remote KIE from the α-secondary KIE upon ionization. To start, triflation of a 1:1.14:1.5 mixture of α-labeled isomers **91** and **92** and protio-**42** produces a perfectly corresponding ratio of labeled triflates that are then isolated. As we have established an S_N1 process and rate determining ionization, we can now take the liberty of measuring KIEs by internal

competition. A competition was set up between isomer **88**, isomer **89**, and unlabeled isomer **42** in the said ratio (1:1.14:1.5). Two significant kinetic isotope effects were measured; the first, representing the rate of consumption of labeled isomer **89** (geminal D) versus unlabeled triflate, was found to be k_H/k_D = 1.22±0.01, once again a significant α-secondary effect. For comparison, the α-secondary KIE for the solvolysis of 7-norbornyl triflate in TFE/H_2O is 1.13 at 65 °C.[20] On the other hand, in **88** k_H/k_D = 1.04±0.01 for the position geminal to the fluorine atom (removed through space from the position of the triflate group). The fact that a measurable *remote* KIE[21] exists is indicative of participation of the fluorine in ionization, once again consistent with the model. Therefore, if fluorine is participating in ionization, it participates that much more heavily in the cationic species, thus disfavoring a rapidly equilibrating set of classical isomers (Equation 5.2). One can argue though, that remote effect may be at least partly attributable to relief of steric strain upon ionization, although the computational model strongly favors direct participation of fluorine.

(5.2)

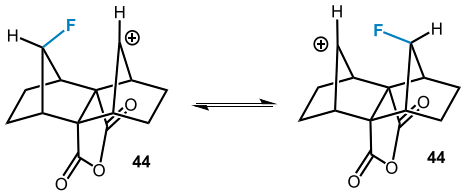

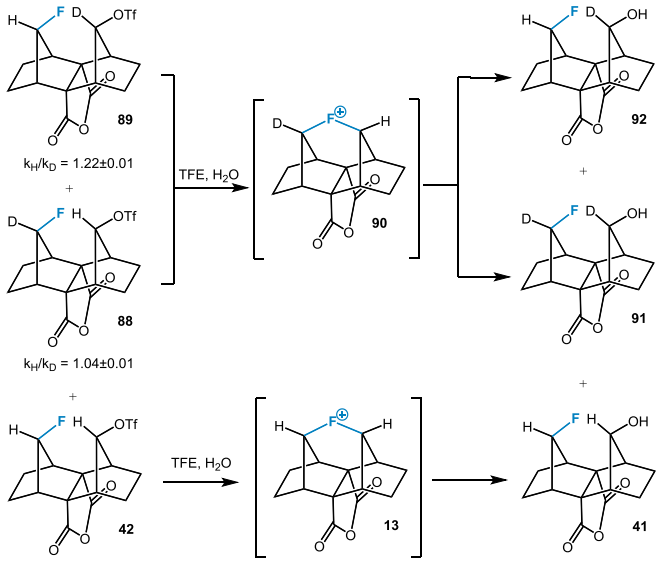

Scheme 5.6 Kinetic isotope effects for the hydrolysis reaction as a result of the isotopic labeling of the [C-F-C]$^+$ positions.

Predicted isotope effects were derived from analysis of the transition state of **90**, (B97, 55 °C, water dielectric) and computed to be k_H/k_D (α position) = 1.27 and k_H/k_D (remote position) = 1.07, roughly in line with what was found. Finally, isotope effects for the trapping of water by substrates **91** and **92** were found once again to be 1.14. These results are very important from a confirmatory standpoint – given stereochemically unique substrates (both *out*- and *in*-triflate isomers), we observe the exact same outcome, thus implying the exact same intermediate. Regardless of the starting ratio, the presence of a fluoronium intermediate commands an identical ratio of label isomers, which is what we observe.

We thought at this point in time that it would be good to calibrate the method for kinetic isotope effect calculations by applying various levels of DFT-based theory to the water-trapping reaction (Scheme 5.7). In general, most seem to be in fairly good agreement, including B3 and B97 (the latter chosen for its ability to take good account of dispersion effects).[22]

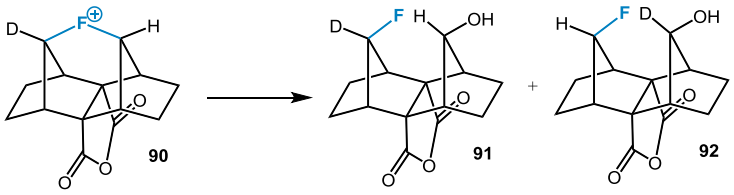

k_{dist}/k_{prox} = **91/92**

	k_{dist}/k_{prox}
experimental	***1.14***
B3LYP/6-311++G**	1.11
PBEPBE/DGTZVP	1.10
ωB97XD/6-311+G**	1.14
MPW1PW91/6-311++G**	1.10
B3PW91/cc-pVTZ	1.09

Scheme 5.7 Comparison of calculated isotope effects at various levels of theory (water dielectric, 55 °C).

Attempting to Force S_N2(e) Reactivity. Thanks to our labeling studies, a role for the S_N2(e) reaction has been ruled out in the hydrolytic reactivity of triflate **42**. However, what would happen if the reaction conditions strongly favored an S_N2(e) mechanism and disfavored an S_N1? Would that be enough to force the reaction to follow the S_N2(e) pathway? The answer seems to be no - employing a reactive S_N2 nucleophile (NaN_3, 15-crown-5) in a fairly non-ionizing solvent (benzotrifluoride) at 106 °C affords a reaction, but only in low conversion (~10%) over extended periods of time (4 days). Use of labeled triflate

48 confirms that this reaction proceeds through an S_N1 mechanism (~1:1 ratio of isotopomeric products (Equation 5.3). An examination of models indicates that the triflate **48** simply presents a very poor possible attack trajectory for S_N2 reaction. This result is also consistent with what is seen in the well-studied 7-norbornyl system; S_N2 attack at the 7-position[23] is disfavored sterically, in contrast to conventional secondary systems. To summarize, we have found no conditions in which an $S_N2(e)$ is observed, even when highly favored.

(5.3)

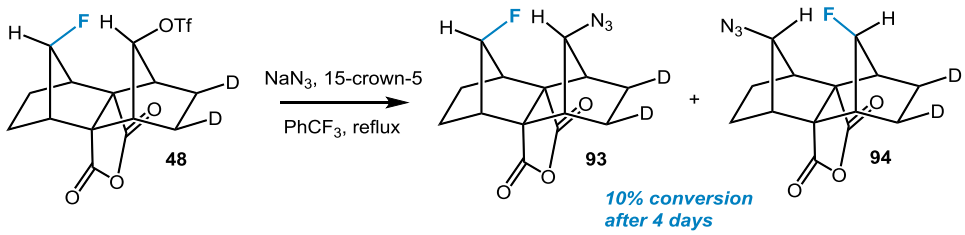

5.5 Potential role of equilibrium isotope effects.

One potential criticism of the overall model is that *in situ* protonation of alcohol **77** followed by ionization can produce isotopic scrambling in the product. When we subjected isotopomers **76**-**77** and **78**-**80** to calculation, we predict an equilibrium isotope effect[24] at B97 of 0.93, which is inverse to what is expected from a KIE (Scheme 5.8). That, in addition to the lack of scrambling in alcohol **54** when treated with strong acid at high temperatures (Equation 5.4), leads us to rule out equilibration as a source of isotope effects under all circumstances.

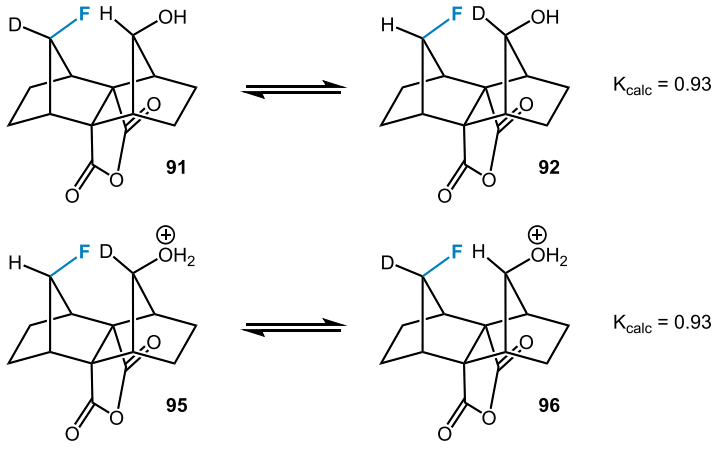

Scheme 5.8 Calculated equilibrium isotope effects for alcohols and oxoniums.

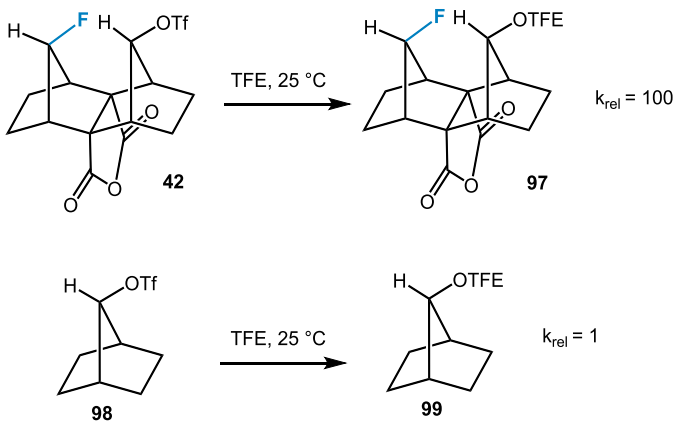

Scheme 5.9 Rate comparison of triflate **42** to 7-norbornyl triflate **98**.

(5.4)

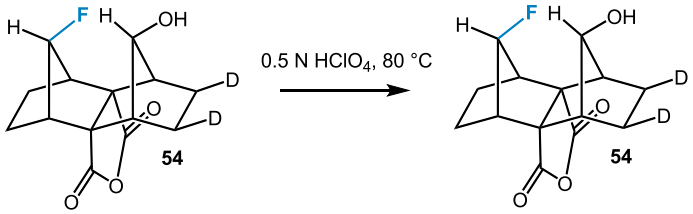

(N.R.)

5.6 Control reactions.

Fluorine Participation in the Transition State. The transition state models for hydrolysis all predict substantial fluorine participation. Fluorine's role, borne of its propinquity, would appear to be both inherently stabilizing as well as space-filling. This begs the question, what would happen to the rate if fluorine were absent from the system? The obvious comparison, for which rate data exist, is the 7-norbornyl triflate system (**98**). At 65 °C, triflate **42** solvolyzes in anhydrous TFE almost 100 times faster than does 7-norbornyl triflate.[69] Although implying a stabilizing role for the fluorine, one should bear in mind that system **42** also relieves strain upon ionization. The presence of the electron-withdrawing anhydride group in **42** is expected to retard the rate of hydrolysis of **42** with respect to **98**, leading to an underestimation in the effect that the fluorine plays in hydrolysis. The issue here is that the simple 7-norbornyl framework is structurally removed from that of system **42**, and is perhaps not an ideal control.

Comparison to μ-Hydrido Bridging. It is doubtful that an "ideal" control would exist for this system. Nevertheless, the most conservative control is one in which *only* the F atom is removed or replaced. A model system such as triflate **103** should provide an illuminating contrast. It is nearly identical

to triflate **42**, shorn of fluorine's participation. Instead, a hydrogen atom replaces fluorine, but the anhydride group and the same general amount of strain remain. Of course, hydrogen can provide stabilization to an S_N1 transition state through incipient μ-hydrido-bridging (and it is very likely that a cationic reactive intermediate in the hydrolysis of **104** is μ-hydrido-bridged) as Sorensen et al.[25] McMurry et al.,[26] and others have shown. μ-Hydrido-bridging is no longer a controversial topic and is known to provide an energetic benefit to numerous carbocationic systems; a comparative system would allow us to benchmark μ-hydrido-bridging versus fluoronium formation. In any case, the rate comparison of control **103** places a lower limit on what stabilization may be expected through fluorine participation. We found triflate **103** to be less reactive to hydrolysis than triflate **42** at 65 °C by a factor of 2.7, implying a modest stabilizing role for fluorine in the transition state for hydrolysis exceeding that for μ-hydrido bridging, as paralleled by our previous isogyric equations (Scheme 5.11).

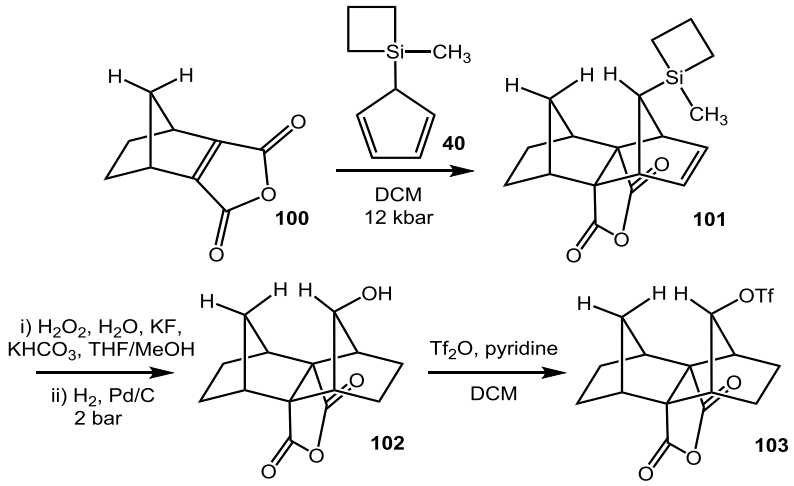

Scheme 5.10 Synthesis of μ-hydrido control **103**.

The synthesis of control **101** parallels that of triflate **42** (Scheme 1.5). Known dienophile **100**[27] is treated with silane **40** under high pressure (12 kbar) for 72 h; the silane is immediately cleaved by a Fleming-Tamao oxidation (15% yield). This is followed by hydrogenation with palladium on carbon (95% yield) and triflation (94% yield) to afford the product **103**, which can be purified by chromatography on silica. The synthetic method can be seen in Scheme 5.10.

The activation free energy for S_N1 ionization of **73** is computed to be about the same as that of triflate **104** at B3 (H_2O dielectric, TS for ionization of **103** at B97 was not found). Although there is no calculated free energy gap between them, a comparison of the transition state geometries is more illustrative and tells a different story. In both cases, anchimeric participation plays an evident role in stabilizing the transition states (F and H). Firstly, both the C-H and C-F bonds have lengthened a small amount in the transition states. However, in the case of **104**, the scission of the C-O bond has progressed much further (2.73 Å versus 2.37 Å for **73**). The X---H distance is lessened in **104** (X = H, 1.86 Å) v. **73** (X = F, 2.20 Å); in simple terms the H moves much more than F in its transition state. The conclusion is that **104** represents a somewhat "later" transition state.[28] While H and F both participate (anchimerically assist), F is apparently more effective than H in this role.

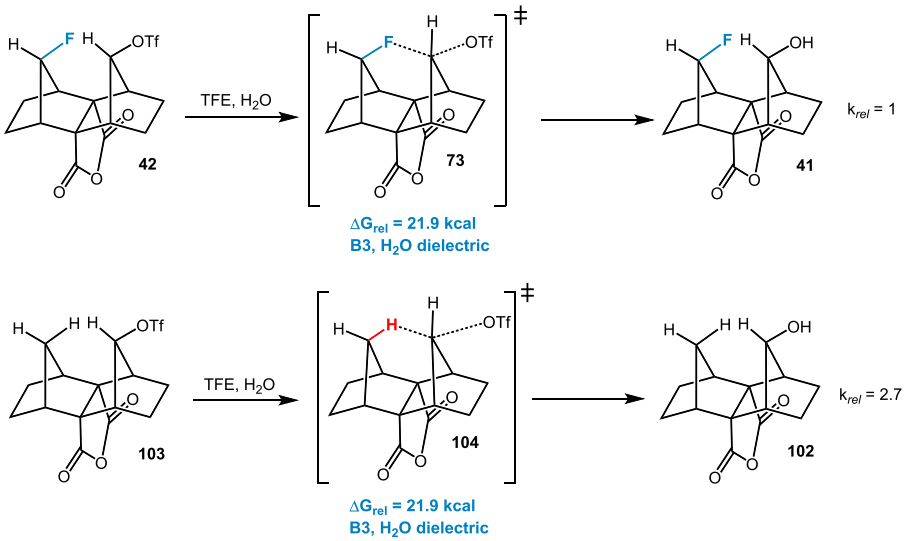

Scheme 5.11 Rate comparison of fluoro- to a μ-hydrido-bridging control.

5.7 Conclusion.

We have sought to expand upon our initial evidence with a comprehensive study involving several lines of experiment and argument to reach a more compelling conclusion about the generation of the putative symmetrical fluoronium ion **13** in solution. In turn: i) isotopic labeling studies show scrambling consistent with the trapping of a symmetrical intermediate; ii) rate measurements reveal the operation of an S_N1 mechanism through which a fluoronium ion must be generated; iii) in pure polyfluorinated alcohols, the RDS of the reaction changes from ionization to nucleophile trapping on a presumably hindered

carbocation; iv) KIE experiments are consistent with precedent and calculation in implicating participation by fluorine in the transition state for ionization of **42** (with unusual remote isotope effects reinforcing this conclusion) thus disfavoring the historically oft-postulated "rapidly equilibrating set of isomers" alternative; v) Starting with an epimeric precursor that hydrolyzes through a putative frontside S_Ni mechanism involving fluorine participation, KIE studies indicate that the identical intermediate is trapped (the fluoronium ion). vi) Isotopic distributions in the trapping of putative ion **90** by water are invariant to concentration and conversion and are also consistent with a symmetrical intermediate; vii) Comparisons with control compounds reveal probable anchimeric assistance in the transition state for the hydrolysis of **42**; for example, one experiment demonstrated fluorine's role from an energetic standpoint relative to commonly encountered μ-hydrido-bridged systems; viii) Computations at multiple levels of theory all agree fairly well on the structure of the fluoronium and the transition states leading thereto. Thus we can reach the notable conclusion that system **42** reacts solely through an S_N1 mechanism via a symmetrical fluoronium ion.

5.8 References.

[1] Fang, Y.; Gao, Y.; Ryberg, P.; Eriksson, J.; Kolodziejska-Huben, M.; Dybala-Defratyka, A.; Madhavan, S.; Danielsson, R.; Paneth, P.; Matsson, O.; Westaway, K. C. *Chem. Eur. J.* **2003**, *9,* 2696-2709.

[2] Plata, R. E.; Singleton, D. A. *J. Am. Chem. Soc.* **2015**, *137,* 3811-3826.

[3] Schreiner, P. R.; Schleyer, P. v. R.; Schaefer, H. F. III *J. Org. Chem.* **1997**, *62,* 4216-4228.

[4] Eyring, H. *J. Chem. Phys.* **1935**, *3,* 107-115.

[5] Winstein, S.; Fainberg, A. H. *J. Am. Chem. Soc.* **1957,** *79,* 5937-5950.

[6] Berkessel, A.; Adrio, J. A.; Huettenhain, D.; Neudoerfl, J. M. *J. Am. Chem. Soc.* **2006**, *128,* 8421-8426.

[7] Svensson, T.; Winstein, S. *J. Am. Chem. Soc.* **1972**, *94,* 2336-2347.

[8] a) Winstein, S.; Clippinger, E.; Fainberg, A. H.; Robinson, G. C. *J. Am. Chem. Soc.* **1954**, *76,* 2597-2598. b) Winstein, S.; Clippinger, E.; Fainberg, A. H.; Heck, R.; Robinson, G. C. *J. Am. Chem. Soc.* **1956**, *78,* 328-335.

[9] Reichardt, C.; Welton, T. *Solvents and Solvent Effects in Organic Chemistry*, 4th ed.; Wiley-VCH: Weinheim, Germany, 2010.

[10] Hong, D-P.; Hoshino, M.; Kuboi, R.; Goto. Y. J. Am. Chem. Soc. **1999**, *121*, 8427-8433.

[11] Seib, R. C.; Shiner, V. J. Jr.; Sendijarevic, V.; Humski, K. *J. Am. Chem. Soc.* **1978**, *100,* 8133-8137.

[12] Gelles, E.; Hughes, E. D.; Ingold, K. E. *J. Chem. Soc.* **1954**, 2918-2929.

[13] a) Kinoshita, T.; Ueda, H.; Takeuchi, K. *J. Chem. Soc. Perkin Trans. 2* **1993**, 603-604; these authors state that "the S_N2C^+-type mechanism can be represented by 'D_N + A_N' using the IUPAC Commission Recommendation System (IUPAC Commission on Physical Organic Chemistry, *Pure Appl. Chem.* **1989**, *61,* 23)." b) Ingold, C. K. *Structure and Mechanism in Organic Chemistry,* Cornell Univ. Press, Ithaca, N.Y., **1969**, 2nd ed., p. 470.

[14] Creary, X. *Acc. Chem. Res.* **1985**, *18,* 3-8.

[15] For studies on steric isotope effects: a) Melander, L.; Carter, R. E. *J. Am. Chem. Soc.* **1964**, *86,* 295-296. b) West, J. D.; Stafford, S. E.; Meyer, M. P. *J. Am. Chem. Soc.* **2008**, *130,* 7816-7817.

[16] Struble, M. D.; Kelly, C.; Siegler, M. A.; Lectka, T. *Angew. Chem. Int. Ed.* **2014**, *53*, 8924-8928.

[17] Similar behavior was observed in a related system: Bartlett, P. D.; Blakeney, A. J.; Kimura, M.; Watson, W. H. *J. Am. Chem. Soc.* **1980**, *102,* 1383-1390.

[18] Struble, M. D.; Scerba, M. T.; Siegler, M.; Lectka, T. *Science* **2013,** *340,* 57-60.

[19] Streitwieser, A. Jr.; Jagow, R. H.; Fahey, R. C.; Suzuki, S. *J. Am. Chem. Soc.* **1958**, *80,* 2326-2332.

[20] a) Gassman, P. G.; Hall, J. B. *J. Am. Chem. Soc.* **1984**, *106,* 4267-4269. b) Gassman, P. G.; Talley, J. J. *J. Am. Chem. Soc.* **1980**, *102,* 4138-4143.

[21] Fry, J. L.; Badger, R. C. *J. Am. Chem. Soc.* **1975**, *97,* 6276-6277.

[22] For a discussion of the use of newer functionals that complement B3LYP, see: Zhao, Y.; Truhlar, D. G. *Acc. Chem. Res.* **2008**, *41,* 157-167.

[23] For a notable study on the 7-norbornyl cation: Sunko, D. E.; Vancik, H.; Deljac, V.; Milun, M. *J. Am. Chem. Soc.* **1983**, *105,* 5364-5368.

[24] Smirnov, S. N.; Golubev, N. S.; Denisov, G. S.; Benedict, H.; Schah-Mohammedi, P.; Limbach, H-H. *J. Am. Chem. Soc.* **1996**, *118,* 4094-4101.

[25] a) Kirchen, R. P.; Sorensen, T. S.; Wagstaff, K. *J. Am. Chem. Soc.* **1978**, *100,* 6761-6763. b) Kirchen, R. P.; Sorensen, T. S. *J. Am. Chem. Soc.* **1979,** *101,* 3240-3243. c) Kirchen, R. P.; Okazawa, N.; Ranganayakulu, K.; Rauk, A.; Sorensen, T. S. *J. Am. Chem. Soc.* **1981**, *103,* 597-604.

[26] a) McMurry, J. E.; Lectka, T.; Hodge, C. N. *J. Am. Chem. Soc.* **1989**, *111,* 8867-8872. b) McMurry, J. E.; Lectka, T. *J. Am. Chem. Soc.* **1993**, *115,* 10167-10173. c) McMurry, J. E. Lectka, T. *Acc. Chem. Res.* **1992**, *25,* 47-53.

[27] Diels, O.; Alder, K. *Liebigs Ann Chem.* **1931,** *490,* 236-242.

[28] Hammond, G. S. *J. Am. Chem. Soc.* **1955**, *77,* 334-338.

Chapter 6

A C-F Bond Directed Diels-Alder Reaction

6.1 Introduction.

In fluorine chemistry a large amount of focus is put on how fluorine can decrease reactivity. This is perhaps best exemplified by fluorinated drugs that have shown a notable resistance to biological metabolism[1] and the low reactivity of perfluoropolymers like Teflon.[2] In some ways, these properties have led to a belief that the fluorine atom itself is unreactive and cannot be utilized in reactive chemistry like the other halogens. It is likely that the strength of the C-F bond (~110 kcal/mol) and the tight fashion in which it holds its lone pairs of electrons contribute to this misconception.[3] However, this is not always the case - C-F bond activations by transition metals,[4] silyl cations,[5] and even carbocations[6] are well-established processes; the nucleophilic displacement of benzylic, allylic, and tertiary C-F bonds are also commonplace.[7] On the other hand, aside from the fluoronium mentioned in the previous chapters, there are very few examples of C-F bonds themselves being used to direct reactivety through anchimeric assistance. One recent example is that a C-F bond positioned over the π-cloud of an arene ring can activate it toward electrophilic nitration.[8] In the search for other reactions with participating C-F bonds, we focused on signature processes in organic chemistry, such as the Diels-Alder (DA) reaction.

The DA reaction is an excellent way of forming C-C bonds, but it can result in several stereoisomers, depending on how the dienophile and diene approach each other (*endo/exo*), the reactants' symmetry, or some combination of both.[9] There have been attempts to increase the reaction's selectivity by relying on the anchimeric effect, and some success has been reported with alcohols, a commonly employed directing group.[10] Is it possible that a fluorine atom could act as a directing group as well? Herein we report a notably selective DA reaction between a fluorinated dienophile and a borole; calculations show that the interaction between B and F is a prime instigator in the reaction chemistry, and that by calculation its magnitude is maximized at (or very near) the transition state (TS).

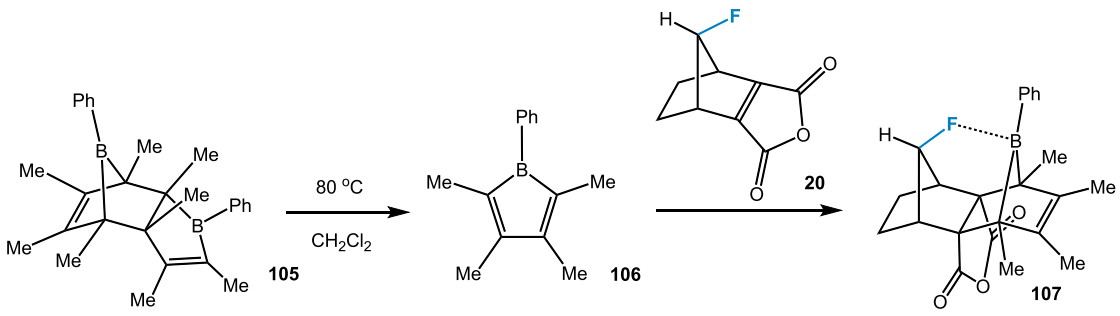

Scheme 6.1 Diels-Alder reaction of borole **106**.

6.2 Precedents.

Boroles (boracyclopentadienes) were first synthesized in 1969, but it is only recently that they have been seen as more than a novelty.[11] This is likely due to their antiaromatic nature, which results in a high degree of reactivity, especially toward DA reactions, as well as air and moisture sensitivity. We synthesized the borole dimer **105** in two steps from dimethylacetylene following the zirconacycle transfer method of Fagan and coworkers.[12] When heated at 80 °C, **105** readily converts into monomeric borole **106** (Scheme 6.1). We imagined that the Lewis acidic boron atom on formally antiaromatic borole **106** could interact in solution with a suitable Lewis base, such as the lone pairs of fluorine in a C-F bond, in an appropriately configured dienophile. This interaction could help position the borole and thereby improve reaction selectivity. It seemed that alkene **20** would be a good dienophile candidate, as an interaction between B and F in a hypothetical DA TS is stereoelectronically feasible, whereas that between B and the O on the carbonyls is not.

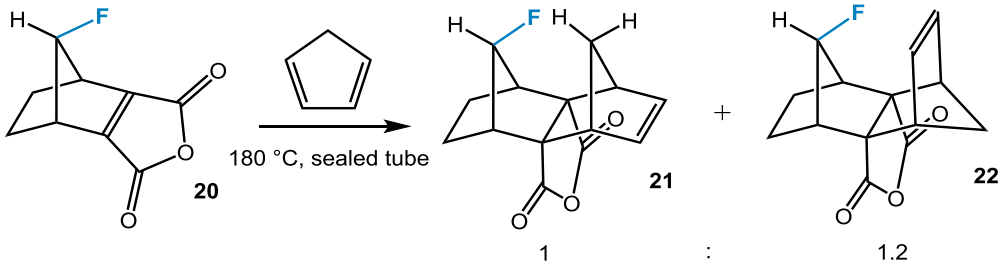

Scheme 6.2 Example of a typical Diels-Alder reaction with dienophile **20**.

6.3 Synthesis.

The borole dimer and the dienophile were both dissolved in CH_2Cl_2 and heated at 80 °C to facilitate the retro-DA reaction of the dimer. We observed that borole **106** reacts rapidly and smoothly to produce a moderate yield (45%) of diastereomerically pure adduct **107**. The other observed compounds proved to be starting material and decomposed borole; no other adducts were observed. In our experience, other DA reactions of dienophile **20** afford mixtures of stereoisomers, a fact which suggested that the reaction could be directed by the boron's coordination to the fluorine.[13] For example, the reaction of **20** with 1,3-cyclopentandiene occurs at 180 °C to afford a mixture of two diastereomers (Scheme 6.2).[13a]

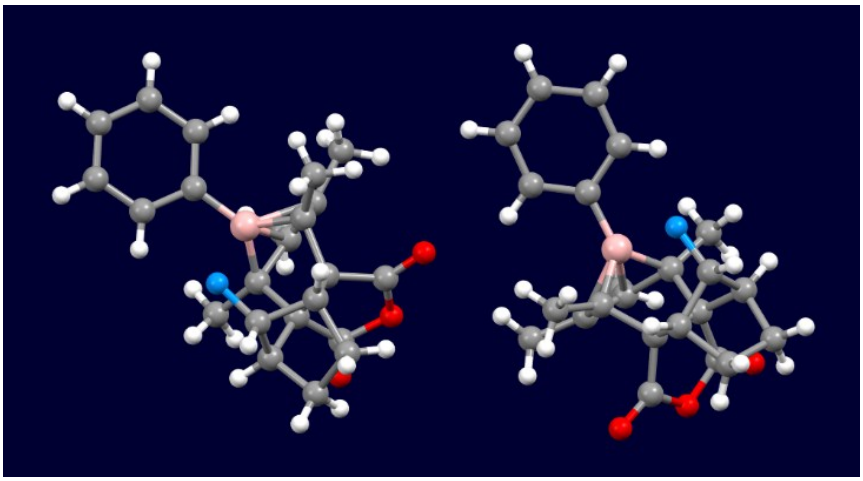

Figure 6.1 Crystal structure of **107** showing the two crystallographically independent molecules. Fluorine in blue; oxygen in red; boron in salmon. Note that the crystal is twinned.

6.4 X-ray crystallography.

Crystals of product **107** suitable for X-ray structure determination were grown from a mixture of CH_2Cl_2 and diethyl ether. The asymmetric unit contains two crystallographically independent molecules of **107** for which the phenyl rings are rotated in a different conformation. In the crystal, the two B---F distances are 2.5919(18) and 2.6095(18), depending on the conformation. Not surprisingly, a strong interaction between B and the vicinal C=C bond is noted. The boron is 1.896(2)/1.900(2) or 1.934(2)/1.936(2) Å away from the double bond, depending once again on which rotamer is observed. Although the crystal indicates bonding between the boron and the double bond, the carbon atoms still appear to be generally sp^2 hybridized. In fact,

the methyl groups seem to be tilted slightly upward toward the boron. This structure is isoelectronic to the 7-phenylnorbornenyl cation, and has been observed in a few other cases, such as in dimer **105**.[12,14] Numerous attempts were made to functionalize the vicinal double bond of **107**, but it was found to be unreactive to various substitution reactions, such as halogenation and hydrogenation. This is likely a combination of the bond donating electron density to the boron as well as steric hindrance from the methyl groups thereon and the partial coordination of fluorine.

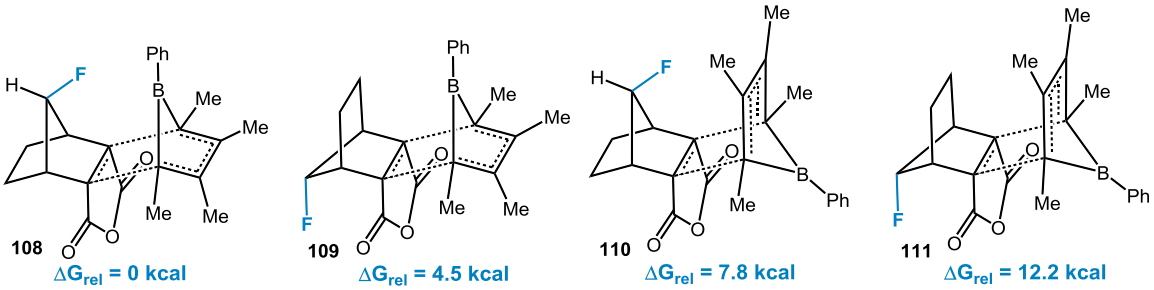

Scheme 6.3 Relative energy and activation energy of each TS pathway.

6.5 DFT calculations.

DFT calculations (6-311++G**/ωb97xd)[15] of four possible TSs for the reaction are shown in Scheme 6.3. As expected, TS **108**, leading to the observed adduct **107**, is almost 4.5 kcal/mol lower than the closest competitor **109**, presumably due in part to the interaction between B and F. Calculations also predict that the reaction proceeds in TS **108** through an unusual trajectory. Using DFT, the B---F distance was calculated at various lengths of the two C-C σ-bonds formed during the DA reaction. This allowed us to map the changes to the B---F interaction as the reaction proceeds (Figure 6.2). Initially as the two reactants approach each other, the B and the F are also drawn closer together. The smallest B---F distance, 2.27 Å, is predicted to be reached very close to or at TS **108**. Once the transition state is passed and product **107** begins to form, the F---B distance is predicted to lengthen again. The B---F interaction is evidently being diminished by a strong, through-space donating effect from the newly formed vicinal C=C double bond in the product. This results in the B---F distance in **107** being almost 0.33 Å longer than in TS **108**. The F---B interaction thus seems to "yo-yo" from tight in the TS to loose in the product wherein the donation from the C=C double bond takes precedence. An atoms-in-molecules analysis of **107** shows a BCP between B and F, which is indicative of a through-space interaction.[16] However, in TS **108** the BCP shows the same B---F relationship, only stronger.

The result is that the boron is unusually coordinated in product **107 -** weakly to the C-F bond, strongly in a through-space manner to the C=C bond, and covalently to three carbon atoms, to attain polyvalency.

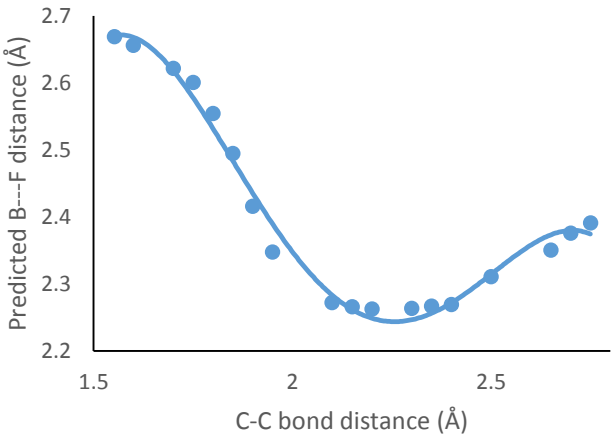

Figure 6.2 Predicted B---F distance from set C-C bond length during the C-C bond formation in TS **108**; curve fitted to a fourth order polynomial.

6.6 Competition reaction.

Having accumulated some evidence pointing to the B---F interaction providing a directing effect, we developed a competition experiment to quantify its *kinetic* consequences - that is, whether it actually accelerates the DA reaction. It is known that just about all other DA reactions of dienophile **20** require forcing conditions, either high temperatures or high pressures; on the other hand, borole **106** is an unusually reactive diene, so a faster rate is expected.[8,13] In a minimal amount of CH_2Cl_2 (3 mL), 0.2 equiv. borole dimer **105** was heated at 80 °C with 1 equiv. of the dienophile **20** and a second equiv. of control dienophile **112** in a sealed tube. In theory the borole dimer should yield 0.4 equiv. of **106**, however it was in practice less due to its extreme air sensitivity in our hands. Dienophile **112** is similar to **20** but has its fluorine pointed away from the double bond, so any DA product derived therefrom must form through a transition state bereft of fluorine participation. An assay of reaction progress after one day showed adduct **107** to be the *sole observed* DA derived product to the limit of detection. This result indicates that the B---F interaction has substantial effect on the rate (and selectivity) of the reaction vs. a closely configured control. In comparison dienophile

112, C-F---B coordination can only result in the formation of a nonproductive precomplex, and thus must play no role in reaction chemistry.

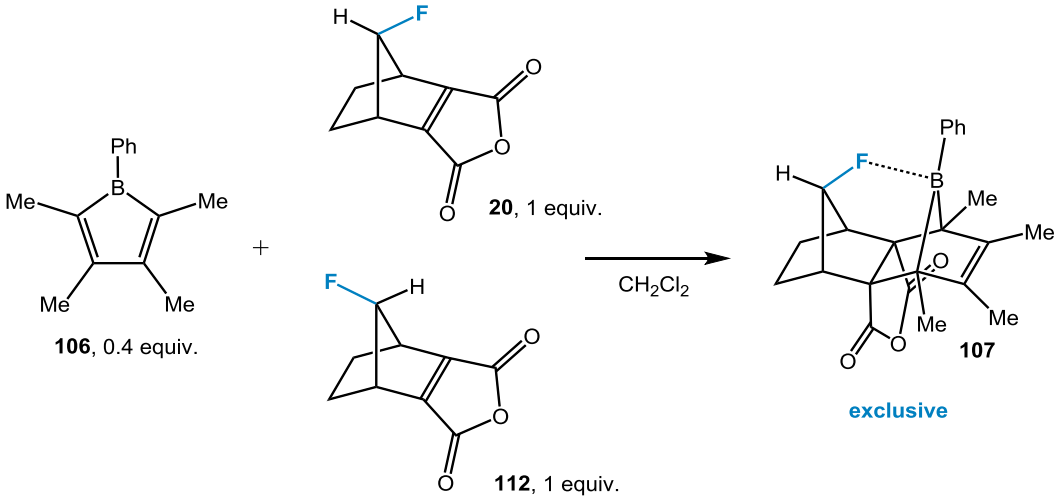

Scheme 6.4 *In*- vs. *out*-fluorine competition reaction.

6.7 Conclusion.

We have reported a highly selective DA reaction between a fluorinated dienophile and a borole. Interestingly, the source of the selectivity of this reaction appears to be a rare case of a fluorine on a C-F bond acting as a Lewis base and coordinating to the Lewis acidic p-orbital on the boron. In the TS the fluorine is predicted to act as a templating element in the reaction, by coordinating to the borole as it is suspended over the double bond. After the reaction is complete, the boron's empty p-orbital is drawn to the newly formed vicinal double bond. However, both DFT calculations and crystallography indicate that there still exists an interaction between fluorine and boron in the final product.

6.8 References.

[1] Ojima, I. *J. Org. Chem.* **2013**, *78*, 6358-6383.

[2] a) Biswas, S. K.; Vijayan, K. *Wear*, **1992**, *158*, 193-211. b) Wieleba, W. *Wear* **2002**, *252*, 719-729.

[3] a) O'Hagan, D. *Chem. Soc. Rev.* **2008**, *37*, 308-319. b) Lemal, D. M. *J. Org. Chem.* **2004**, *69*, 1-11.

[4] a) Amii, H.; Uneyama, K. *Chem. Rev.* **2009**, *109*, 2119–2183. b) Torrens, H. *Coord. Chem. Rev.* **2005**, *249*, 1957–1985. c) Aizenberg, M.; Milstein, D. *Science*, **1994**, *265*, 359-361. d) Clot, E.; Eisenstein, O.; Jasim, N.; MacGregor, S. A.; McGrady, J. E.; Perutz, R. N. *Acc. Chem. Res.* **2011**, *44*, 333-348. e) Burdeniuc, J.; Jedlicka, B.; Crabtree, R. H. *Chem. Ber.* **1997**, *130*, 145-154. f) Kiplinger, J. L.; Richmond, T. G.; Osterbergt, C. E. *Chem. Rev.* **1994**, *94*, 373-431.

[5] Meier, G.; Braun, T. *Angew. Chem. Int. Ed.* **2009**, *48*, 1546-1548.

[6] Ferraris, D.; Cox, C.; Anand, R.; Lectka, T. *J. Am. Chem. Soc.* **1997**, *119*, 4319-4320.

[7] Nova, A.; Mas-Ballesté, R.; Lledós, A. *Organometallics* **2012**, *31*, 1245-1256.

[8] Holl, M. G.; Struble, M. D.; Singal, P.; Siegler, M. A.; Lectka, T. *Angew. Chem. Int. Ed.* **2016**, DOI: 10.1002/anie.201601989.

[9] Martin, J. G.; Hill, R. K. *Chem. Rev.* **1961**, *61*, 537-562.

[10] Barriault, L.; Thomas, J. D. O.; Clément, R. *J. Org. Chem.* **2003**, *68*, 2317-2323.

[11] a) Eisch, J. J.; Hota, N. K.; Kozima, S. J. *J. Am. Chem. Soc.* **1969**, *91*, 4575-4577. b) Braunschweig, H.; Kupfer, T. *Chem. Commun.* **2011**, *47*, 10903–10914.

[12] a) Fagan, P. J.; Nugent, W. A.; Calabrese, J. C. *J. Am. Chem. Soc.* **1994**, *116*, 1880-1889. b) Fagan, P. J.; Burns, E. G.; Calabrese; J. C. *J. Am. Chem. Soc.* **1988**, *110*, 2979-2981.

[13] a) Scerba, M. T.; Bloom, S.; Haselton, N.; Siegler, M.; Jaffe, J.; Lectka, T. *J. Org. Chem.* **2012**, *77*, 1605-1609. b) Struble, M. D.; Scerba, M. T.; Siegler, M.; Lectka, T. *Science* **2013**, *340*, 57-60.

[14] Laube, T. *J. Am. Chem. Soc.* **1989**, *111*, 9224-9232.

[15] Chai, D.; Head-Gordon, M. *Phys. Chem. Chem. Phys.* **2008**, *10*, 6615-6620.

[16] Grabowski, S. J. *J. Phys. Chem. A* **2011**, *115*, 12789-12799.

Chapter 7

Experimental Methods

7.1 General methods.

Unless otherwise stated, all reactions were carried out under strictly anhydrous, air-free conditions under nitrogen. All solvents and reagents were dried and distilled by standard methods. ^{1}H and ^{13}C spectra were acquired on a Bruker Avance 400 MHz NMR in $CDCl_3$ at 25 °C; ^{19}F spectra were taken on a Bruker Avance 300 MHz NMR in $CDCl_3$. The ^{1}H and ^{13}C chemical shifts are given in parts per million (δ) with respect to an internal tetramethylsilane (TMS, δ 0.00 ppm) and/or and/or $CFCl_3$ (δ 0.00 ppm) standard. NMR data are reported in the following format: chemical shifts (multiplicity (s = singlet, d = doublet, t = triplet, q = quartet m = multiplet), integration, coupling constants [Hz]). IR data were obtained using an FT-IR with a flat CaF_2 cell. All measurements were recorded at 25 °C unless otherwise stated. Melting Points are uncorrected. HRMS calculations were performed on an ESI-ion trap mass spectrometer. Spectral data were processed with ACD/NMR Processor Academic Edition.[1]

7.2 Computational methods.

The Gaussian 09 package and Spartan 10 were used for all geometry optimizations.[2,3] The ^{19}F calculated chemical shifts were fitted to the empirical equation (at B3LYP/6-311++G**) $\delta_{calc} = -0.914\delta + 141.83$.[4] In most cases, geometry optimizations were determined using the ωB97XD/6-311+G** and the B3LYP/6-311++G** levels at various temperatures. In most cases optimized geometries and in all cases transition states were confirmed by vibrational analyses. Calculated electronic energies were converted to free energies through corrections obtained by vibrational analyses.

KIEs were calculated by the following method: the free energy of activation for ionization of isotopomers was compared to the free energy of activation for the protio-substrates. The isotopomeric free energies were calculated through comparison of vibrational analyses at specified temperatures of the ground states and transition states.

7.3 Experimental details for chapter 1.

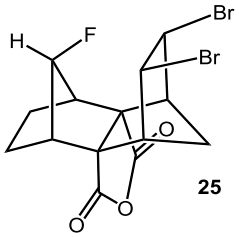

25

2,3-dibromo-12-fluorooctahydro-1,4:5,8-dimethano-4a,8a-(methanoxymethano)-naphthalene-9,11-dione (25). To a flame dried round bottom flask was added **22** (0.1 g, 0.40 mmol) in 10 mL of DCM. The solution was cooled to -78 °C and bromine (0.02 mL, 0.44 mmol) was added. The solution was then allowed to stir overnight at room temperature. The solution was quenched with a 10% solution of sodium thiosulfate (50 mL), extracted into DCM and the organic fractions were then washed with water and brine, dried with magnesium sulfate and concentrated under reduced pressure. The brominated product was isolated by recrystallization from DCM/hexanes to yield **25** as white crystals (0.142 g, 87%); ^{1}H NMR ($CDCl_3$) δ 5.01 (d, 1H, *J* = 60.8 Hz), 4.81 (m, 2H), 3.20 (m, 2H), 2.83 (s, 2H), 2.65 (d, 1H, *J* = 12.5 Hz), 1.89 (d, 2H, *J* = 9.6 Hz), 1.66 (d, 1H, *J* = 12.5 Hz), 1.45-1.37 (m, 2H); ^{13}C NMR ($CDCl_3$) δ 172.5, 100.4 (d, *J* = 213.0 Hz), 67.3 (d, *J* = 1.5 Hz), 55.5, 52.3 (d, *J* = 22.1 Hz), 41.3 (d, *J* = 14.0 Hz), 36.5 (d, *J* = 3.0 Hz), 23.2 (d, *J* = 9.6 Hz); ^{19}F NMR ($CDCl_3$) δ -179.46 (d, 1F, *J* = 60.8 Hz); IR 3053, 2915, 1865, 1785, (cm^{-1}, CaF_2, CH_2Cl_2)); HRMS (ESI+) calc for $NaC_{14}H_{13}Br_2FO_3$: 430.9093, found 430.9097.

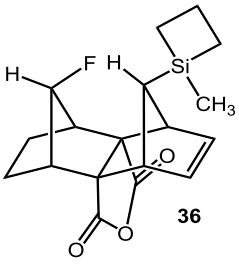

36

13-fluoro-12-(1-methylsiletan-1-yl)-1,2,3,4,5,8-hexahydro-1,4:5,8-dimethano-4a,8a-(methanoxymethano)-naphthalene-9,11-dione (36). Anhydride **20** (1.0 g, 5.49 mmol, 1 equiv) and silylated diene **40** (1.80 mL, 11.0 mmol, 2 equiv) were combined with methylene chloride (1 mL) in a 10 mL syringe. The resulting slurry was pressurized at 12 kbar for 2 days. The reaction was then recharged with fresh **40** (1.80 mL, 11.0 mmol, 2 equiv) and repressurized for 2 d. The resulting solution was evaporated to dryness and the residue was purified by gradient column chromatography on silica using 2%

EtOAc/hexanes as eluent, then 5% EtOAc/hexanes as eluent to yield **36** (0.42 g, 29%) as a white solid. ^{19}F NMR ($CDCl_3$): δ -169.16 (m, 1F), (calc. -168.83); the resulting wax was carried on directly to the Tamao-Fleming oxidation as it tends to undergo fairly rapid desilylation.

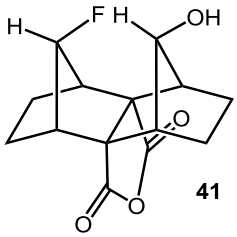

41

12-fluoro-13-hydroxyoctahydro-1,4:5,8-dimethano-4a,8a-(methanoxymethano)-naphthalene-9,11-dione (41). Silane **36** (0.35 g, 1.05 mmol, 1 equiv) was dissolved in a 1:1 solution of THF/MeOH, to which were added KF (0.12 g, 2.1 mmol, 2 equiv) and $KHCO_3$ (0.21 g, 2.1 mmol, 2 equiv). The resulting mixture was cooled in an ice bath and 30% H_2O_2 (1.8 mL, 15.8 mmol, 15 equiv) was added dropwise. The solution stirred overnight at room temperature. The solution was combined with EtOAc and water and extracted; the organic layer was washed with a 1M aqueous Na_2CO_3 solution and extracted. Aqueous layers were combined and back-extracted with EtOAc. Organic layers were combined, washed with brine and evaporated to dryness to give 0.26 g of the putative alcohol. The resulting product was immediately dissolved in EtOH and treated with Pd/C catalyst (0.03 g) and hydrogen gas at 2 bar in a Parr apparatus. The reaction was filtered through celite and concentrated *in vacuo* to yield alcohol **41** (0.25 g, 92%) as a white solid. ^1H NMR ($CDCl_3$): δ 5.67 (d, 1H, J = 18.3 Hz), 4.97 (d, 1H, J = 62.2 Hz), 2.61 (s, 2H), 2.43 (q, 2H), 2.16 (d, 2H, J = 9.4 Hz), 1.79 (d, 2H, J = 10.4), 1.61 (d, 1H, J = 4.3), 1.58-1.4 (m, 4H); ^{13}C NMR ($CDCl_3$): δ 173.74, 101.47 (d, J = 212.23), 75.88 (d, J = 47.57), 67.62, 45.42, 44.26 (d, J = 13.9), 24.34, 23.42 (d, J = 9.5); ^{19}F NMR ($CDCl_3$): δ -176.05 (ddt, J = 61.86, 18.6, 9.28, 1F). IR (CH_2Cl_2): 3613, 2963, 2901, 1856, 1783 cm^{-1}; HRMS (ESI+) calcd. for $NaC_{14}H_{15}FO_4$, 289.0852, found 289.0854.

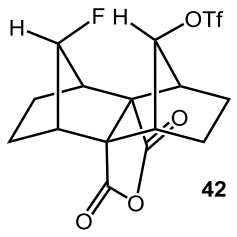

42

13-fluoro-9,11-dioxooctahydro-1,4:5,8-dimethano-4a,8a-(methanoxymethano)-naphthalen-12-yl trifluoromethanesulfonate (42). To a flame dried round bottom flask was added alcohol (**41**) (0.04 g,

0.15 mmol) dissolved in DCM (3 mL). The solution was treated with pyridine (0.07 mL, 0.86 mmol) and cooled to -78 °C. A 1M triflic anhydride solution in DCM (0.22 mL, 0.22 mmol) was added dropwise, and the solution was allowed to stir at room temperature for 1.5 h. The solution was washed with a cold 10% aqueous $NaHCO_3$ solution, then brine. The organic layer was isolated, dried with magnesium sulfate and concentrated under reduced pressure. The crude product was purified by flash chromatography on florisil with a 20% ethyl acetate and hexanes solution to yield **42** as white crystals (0.058 g, 97%); ^{1}H NMR (400 MHz, $CDCl_3$) δ 6.68 (d, 1H, *J* = 25.2 Hz), 5.05 (d, 1H, *J* = 61.6 Hz), 2.84 (m, 2H), 2.71 (s, 2H), 2.14 (d, 2H, *J* = 10 Hz), 1.86 (d, 2H, *J* = 9.4 Hz), 1.67 (d, 2H, *J* = 8.8 Hz), 1.49 (t, 2H, *J* = 8.8 Hz); ^{13}C NMR (400 MHz, $CDCl_3$) δ 171.9, 118.6 (q, *J* = 320 Hz), 101.29 (d, *J* = 212.3 Hz), 90.2 (d, *J* = 56.0), 66.49, 44.36 (d, *J* = 8.1 Hz), 44.18, 24.26, 23.2 (d, *J* = 9.6 Hz), ^{19}F NMR (300 MHz, $CDCl_3$) δ -75.33 (s, 3F), -177.03 (m, 1F); IR 3147, 1866, 1785 (cm^{-1}, CaF_2, CH_2Cl_2); HRMS (ESI+) calc for $NaC_{15}H_{14}F_4O_6S$: 421.0345, found 421.0341.

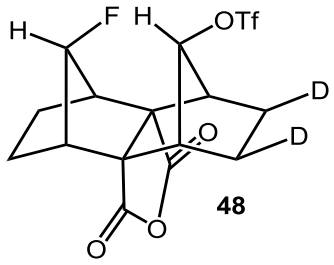

48

13-fluoro-9,11-dioxooctahydro-1,4:5,8-dimethano-4a,8a-(methanoxymethano)-naphthalen-12-yl-6,7-d_2 trifluoromethanesulfonate (48). To a flame dried round bottom flask was added alcohol **54** (0.15 g, 0.06 mmol, 1 equiv) dissolved in methylene chloride (3 mL). The solution was treated with pyridine (0.03 mL, 0.32 mmol, 5.7 equiv) and cooled to -78 °C. Triflic anhydride (0.06 mL, 0.06 mmol, 1.1 equiv) was added dropwise, and the solution was allowed to stir at room temperature for 1.5 h. The solution was washed with a cold 10% aqueous $NaHCO_3$ solution, then brine. The organic layer was isolated and concentrated *in vacuo* to yield triflate **48** as a waxy solid, which was used without further purification. ^{19}F NMR was used to confirm complete conversion to the triflate. ^{1}H NMR ($CDCl_3$): δ 6.67 (d, 1H, *J* = 25.8), 5.05 (d, 1H, *J* = 61.41), 2.84 (d, 1H, *J* = 2.1), 2.71 (s, 2H), 1.86 (d, 2H, *J* = 9.6), 1.65 (s, 2H), 1.51 (t, *J* = 8.9, 2H); ^{19}F NMR ($CDCl_3$): δ -75.34 (s, 3F), -177.07 (ddt, *J* = 65, 25.78, 8.2, 1F), (calc. -176.32); the triflate was found to decompose over time, so a ^{13}C NMR was not obtained.

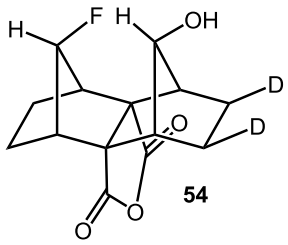

54

12-fluoro-13-hydroxyoctahydro-1,4:5,8-dimethano-4a,8a-(methanoxymethano)-naphthalene-9,11-dione-2,3-d_2 (54). The Fleming-Tamao reaction undertaken to make alcohol **41** was repeated on **36**, and the resulting product (0.25 g) was used in the next step without further purification. The product was added to a flame dried, three-necked round bottom flask equipped with a condenser, stir bar and stoppers. MeOH-d_1 (> 99% D, 40 mL) and dipotassium azodicarboxylate (4.76 g, 24.5 mmol, 26 equiv) were added to the flask (that was thoroughly pre-rinsed with deuterated solvent). The mixture was treated with acetic acid-d_1 (> 98% D 2.2 mL, 38.5 mmol, 40 equiv) via dropwise addition and stirred for 45 min. The reaction was then recharged with dipotassium azodicarboxylate (3.7 g, 18.8 mmol, 20 equiv) and acetic acid-d_1 (> 98% D, 1.7 g, 29.7 mmol, 31 equiv) and stirred for another 45 min. This process was repeated four more times, for a total of six additions, and the reaction was left to stir overnight. The reaction was quenched by slowly adding water until the solution ceased to bubble, and the product was extracted in EtOAc and evaporated to dryness. The resulting residue was purified by gradient column chromatography on silica starting with 20% EtOAc/hexanes as eluent, then switching to 70% EtOAc/hexanes to yield alcohol **54** (> 97% D incorporation, 0.18 g, 66.5%) as a white solid. The exo-diastereoselectivity was inferred from precedent and the fact that the endo reduction would be almost prohibitively sterically hindered. ^{1}H NMR ($CDCl_3$): δ 5.65 (d, 1H, J = 18.4 Hz), 4.96 (d, 1H, J = 62.4 Hz), 2.60 (s, 2H), 2.41 (s, 2H), 1.79 (d, 2H, J = 9.6), 1.61 (d, 1H, J = 4.3), 1.55-1.37 (m, 4H); ^{13}C NMR ($CDCl_3$): δ 173.76, 101.46 (d, J = 214.4 Hz), 75.87 (d, J = 47.6), 67.57, 45.34, 44.25 (d, J = 14.6), 23.94 (t, J = 47.7), 23.41 (d, J = 9.5); ^{19}F NMR ($CDCl_3$): δ -176.08 (ddt, J = 61.86, 18.6, 8.25 1F), (calc. -176.15). IR (CH_2Cl_2): 3613, 2963, 2901, 1856, 1783 cm^{-1}; HRMS (ESI+) calcd. for $NaC_{14}H_{13}D_2FO_4$, 291.0978, found 291.0971.

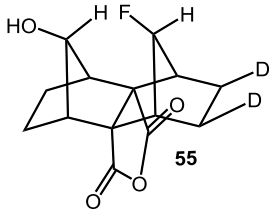

55

Fluoronium ion generation experiment: 12-fluoro-13-hydroxyoctahydro-1,4:5,8-dimethano-4a,8a-(methanoxymethano)-naphthalene-9,11-dione-6,7-d_2 (55) (identical conditions employed for runs with unlabeled 42). To a flame dried, round-bottom flask equipped with a condenser was added **48** (0.015 g, 0.04 mmol). 2,6-Lutidine (0.06 mL, 0.06 mmol) and 2,2,2-trifluoroethanol containing 20% water by volume (5 mL) was added and the solution was heated at 60 °C for 10 h. TFE was removed by rotary evaporation and the product was extracted with methylene chloride and concentrated *in vacuo* to yield a brown residue. This was further purified by gradient column chromatography on florisil, 100-200 mesh, with 5% EtOAc/hexanes as eluent, then 50% EtOAc/hexanes to yield alcohol **55** in an inseparable mixture of itself and **54** in a 1:1 ratio (96% yield). ^{13}C NMR ($CDCl_3$): δ 173.77, 101.48 (d, J = 213.7), 75.92 (d, 46.84), 67.58, 45.42, 44.18 (d, J = 13.9), 24.37, 23.3-22.7 (m); ^{19}F NMR ($CDCl_3$): δ -176.08 (ddt, J = 61.86, 18.6, 8.25 1F), (calc. -176.15); **55** was obtained as an inseparable mixture of itself and **54**. HRMS (ESI+) calcd. for $NaC_{14}H_{13}D_2FO_4$, 291.0978, found 291.0973.

7.4 Experimental details for chapter 2.

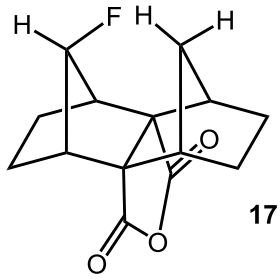

17

12-fluorooctahydro-1,4:5,8-dimethano-4a,8a-(methanoxymethano)naphthalene-9,11-dione (17). Compound **21** (0.097 g, 0.391 mmol) was dissolved in THF (5 mL). The solution was treated with Pd/C catalyst (0.01 g) and hydrogen gas at 2 bar in a Parr apparatus for 12 h. The mixture was then filtered through celite and concentrated under reduced pressure to yield **17** as white crystals (0.089 g, 91% yield);

mp = 188 °C; ^{1}H NMR ($CDCl_3$) δ 4.96 (d, 1H, *J* = 61.6 Hz), 3.15 (t, 1H, *J* = 12.3 Hz), 2.62 (m, 2H), 2.60 (s, 2H), 1.80 (d, 2H, *J* = 9.9 Hz), 1.75 (d, 2H, *J* = 9.1 Hz), 1.56-1.48 (m, 4H), 1.30 (dd, 1H, *J* = 11.7, 8.0 Hz); ^{13}C NMR ($CDCl_3$) δ 174.2, 101.4 (d, *J* = 213.7 Hz), 70.6, 44.3 (d, *J* = 15.37 Hz), 42.3, 38.7 (d, *J* = 38.1 Hz), 28.1, 23.5 (d, *J* = 10.2 Hz); ^{19}F NMR ($CDCl_3$) δ -173.04 (dm, 1F, *J* = 61.9 Hz); IR 3108, 2983, 2966, 2898, 1850, 1774, (cm^{-1}, CaF_2, CH_2Cl_2); HRMS (ESI+) calc for $NaC_{14}H_{15}FO_3$: 273.0903, found 273.0907.

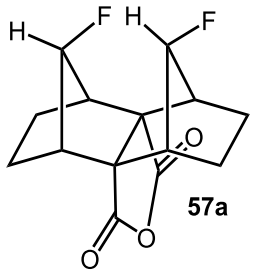

57a

12,13-difluorooctahydro-1,4:5,8-dimethano-4a,8a-(methanoxymethano)-naphthalene-9,11-dione (57a). A solution of **41** (21 mg, 0.08 mmol) in 5 mL of dichloromethane (DCM) was cooled to -78 °C with stirring. To the solution diethylaminosulfur trifluoride (DAST) (0.021 mL, 0.16 mmol) was added dropwise, and the solution was stirred for 1 h at -78 °C. The reaction was then quenched with saturated aqueous sodium bicarbonate (4 mL). The organic layer was separated, dried with magnesium sulfate, filtered through celite and the solvent was removed under reduced pressure. The crude product was purified by silica gel flash column chromatography with a 10% ethyl acetate and hexanes solution to yield **57a** as white crystals (5 mg, 23% yield); mp = 153 °C; ^{1}H NMR ($CDCl_3$) δ 6.32 (dd, 1H, *J* = 56.1, 18.0 Hz), 4.99 (d, 1H, *J* = 61.6 Hz), 2.68 (q, 2H, *J* = 4.8, 2.3 Hz), 2.64 (s, 2H), 2.12 (d, 2H, *J* = 11.9 Hz), 1.82 (d, 2H, *J* = 10.4 Hz), 1.56 (d, 2H, *J* = 4.5 Hz), 1.51 (t, 2H, *J* = 9.1 Hz); ^{13}C NMR ($CDCl_3$) δ 173.0 (d, *J* = 1.5 Hz), 101.22 (d, *J* = 213.7 Hz), 96.1 (q, *J* = 242.2, 53.4 Hz), 66.5 (d, *J* = 8 Hz), 44.3 (d, *J* = 14.6 Hz), 44.0 (d, *J* = 16.1), 24.3 (d, *J* = 5.9 Hz), 23.3 (d, *J* = 9.5 Hz); ^{19}F NMR ($CDCl_3$) δ –178.90 (dm, 1F, *J* = 60.8 Hz), –198.51 (dd, 1F, *J* = 55.7, 19.6 Hz); IR 3135, 2962, 2925, 2858, 1861, 1783, 1725, (cm^{-1}, CaF_2, CH_2Cl_2); HRMS (ESI+) calc for $NaC_{14}H_{14}F_2O_3$: 291.0809, found 291.0802.

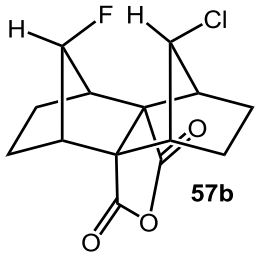

57b

12-chloro-13-fluorooctahydro-1,4:5,8-dimethano-4a,8a-(methanoxymethano)-naphthalene-9,11-dione (57b). To a solution of compound **42** (68 mg, 0.171 mmol) in 5 mL of dry N,N-dimethylformamide (DMF) was added sodium chloride (40 mg, 0.684 mmol). The solution was heated to 70 °C with stirring in a sealed tube and was allowed to react for 20 h. The solution was then poured into ice-cold water (20 mL) and extracted with EtOAc (3 x 15 mL). The organic layers were combined, dried with magnesium sulfate, filtered through celite and concentrated under reduced pressure. The crude product was then purified by silica gel flash column chromatography with a 20% ethyl acetate and hexanes solution to yield **57b** as white crystals (17.3 mg, 36% yield); mp = 135 °C; ^{1}H NMR ($CDCl_3$) δ 5.77 (d, 1H, *J* = 24.5 Hz), 5.02 (d, 1H, *J* = 62.0 Hz), 2.67 (q, 4H, *J* = 4.3, 1.9 Hz), 2.29 (d, 2H, *J* = 9.6 Hz), 1.84 (d, 2H, *J* = 10.7 Hz), 1.62-1.45 (m, 4H); ^{13}C NMR ($CDCl_3$) δ 172.8, 101.5 (d, *J* = 213.7 Hz), 68.4, 62.9 (d, *J* = 52.7 Hz), 47.0, 44.3 (d, *J* = 14.6 Hz), 24.9, 23.4 (d, *J* = 9.5 Hz); ^{19}F NMR ($CDCl_3$) δ −173.9 (ddt, 1F, *J* = 61.9, 24.7, 9.3 Hz); IR 3146.4, 3061.4, 2988.1, 2903.1, 1862.7, 1789.4, (cm^{-1}, CaF_2, CH_2Cl_2); HRMS (ESI+) calc for $NaC_{14}H_{14}ClFO_3$: 307.0513, found 307.0510.

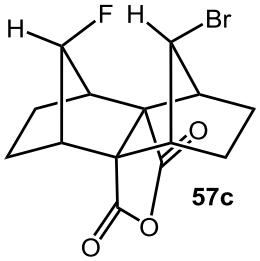

57c

12-bromo-13-fluorooctahydro-1,4:5,8-dimethano-4a,8a-(methanoxymethano)-naphthalene-9,11-dione (57c). To a solution of compound **42** (42 mg, 0.106 mmol) in 5 mL of dry acetone was added potassium bromide (51 mg, 0.424 mmol). The solution was heated to 70 °C with stirring in a sealed tube and was allowed to react for 48 h. The solvent was removed under reduced pressure and the resulting residue was dissolved in DCM (10 mL), and washed with water (2 x 10 mL). The organic layer was then dried with magnesium sulfate, filtered through celite and concentrated under reduced pressure. The crude

product was then purified by flash column chromatography on florisil 60-100 mesh with a 10% ethyl acetate and hexanes solution to yield **57c** as white crystals (9.1 mg, 26% yield); mp = 157 °C; ^{1}H NMR ($CDCl_3$) δ 5.84 (d, 1H, *J* = 24.8 Hz), 5.03 (d, 1H, *J* = 62.4 Hz), 2.72 (q, 2H, *J* = 4.6, 1.8), 2.68 (s, 2H), 2.33 (d, 2H, *J* = 9.6), 1.84 (d, 2H, *J* = 9.3), 1.61 (d, 2H, *J* = 8.8 Hz), 1.51 (t, 2H, *J* = 9.1 Hz); ^{13}C NMR ($CDCl_3$) δ 172.6, 101.6 (d, *J* = 214.4 Hz), 68.2, 54.0 (d, *J* = 51.96), 47.3, 44.2 (d, *J* = 14.6 Hz), 25.8, 23.4 (d, *J* = 9.5 Hz); ^{19}F NMR ($CDCl_3$) δ –173.71 (ddt, 1F, *J* = 61.9, 24.8, 8.3 Hz); IR 3152, 2962, 2926, 2853, 1865, 1783, (cm^{-1}, CaF_2, CH_2Cl_2); HRMS (ESI+) calc for $NaC_{14}H_{14}BrFO_3$: 351.0008, found 351.0015.

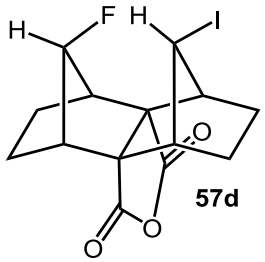

57d

12-fluoro-13-iodooctahydro-1,4:5,8-dimethano-4a,8a-(methanoxymethano)-naphthalene-9,11-dione (57d). To a solution of compound **42** (110 mg, 0.276 mmol) in 5 mL of dry acetone was added sodium iodide (165 mg, 1.1 mmol). The solution was heated to 70 °C with stirring in a sealed tube and was allowed to react for 20 h. The solvent was removed under reduced pressure and the resulting residue was dissolved in DCM (10 mL), and washed with water (2 x 10 mL). The organic layer was then dried with magnesium sulfate, filtered through celite and concentrated under reduced pressure. The crude product was then purified by silica gel flash column chromatography with a 20% ethyl acetate and hexanes solution to yield **57d** as white crystals that gradually turned brown when exposed to light (33.8 mg, 33% yield); mp = 167 °C; ^{1}H NMR ($CDCl_3$) δ 5.86 (d, 1H, *J* = 25.3 Hz), 5.03 (d, 1H, *J* = 62.9 Hz), 2.70 (s, 2H), 2.67 (s, 2H), 2.33 (d, 2H, *J* = 10.6 Hz), 1.83 (d, 2H, *J* = 10.1 Hz), 1.66 (d, 2H, *J* = 10.1), 1.52 (t, 2H, *J* = 8.6 Hz); ^{13}C NMR ($CDCl_3$) δ 172.4, 101.6 (d, *J* = 214.4 Hz), 67.5, 48.3, 44.3 (d, *J* = 14.6 Hz), 30.1 (d, *J* = 49.8 Hz), 27.4 (d, *J* = 2.2 Hz), 23.44 (d, *J* = 11.0 Hz); ^{19}F NMR ($CDCl_3$) δ -173.16 (ddt, 1F, *J* = 61.9, 25.8, 8.3 Hz); IR 3156, 2961, 2908, 1867, 1772, (cm^{-1}, CaF_2, CH_2Cl_2); HRMS (ESI+) calc for $NaC_{14}H_{14}IFO_3$: 398.9869, found 398.9873.

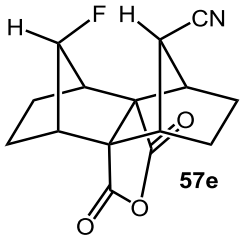

57e

13-fluoro-9,11-dioxooctahydro-1,4:5,8-dimethano-4a,8a-(methanoxymethano)-naphthalene-12-carbonitrile (57e). To a solution of compound **42** (22 mg, 0.056 mmol) in 5 mL of dry N,N-dimethylformamide (DMF) was added sodium cyanide (11 mg, 0.22 mmol). The solution was heated to 80 °C with stirring in a sealed tube and was allowed to react for 20 h. The solution was then poured into ice-cold water (20 mL) and extracted with EtOAc (3 x 15 mL). The organic layers were combined, dried with magnesium sulfate, filtered through celite and concentrated under reduced pressure. The crude product was then purified by silica gel flash column chromatography with a 20% ethyl acetate and hexanes solution to yield **57e** as white crystals (12.2 mg, 79% yield); mp = 174 °C; ^{1}H NMR ($CDCl_3$) δ 5.04 (d, 1H, *J* = 62.7 Hz), 4.56 (d, 1H, *J* = 30.8 Hz), 2.91 (q, 2H, *J* = 4.6, 1.8 Hz), 2.7 (s, 2H), 2.28 (d, 2H, *J* = 9.9 Hz), 1.87 (d, 2H, *J* = 9.3 Hz), 1.71 (d, 2H, *J* = 8.6 Hz), 1.56-1.49 (m, 2H); ^{13}C NMR ($CDCl_3$) δ 171.92, 118.7, 101.6 (d, *J* = 213.0 Hz), 69.6, 45.2, 44.3 (d, *J* = 13.9 Hz), 38.0 (d, *J* = 49.8 Hz), 26.0, 23.3 (d, *J* = 9.5 Hz); ^{19}F NMR ($CDCl_3$) δ -170.23 (ddt, 1F, *J* = 62.9, 30.9, 8.3 Hz); IR 3082, 2962, 2926, 2868, 2854, 1859, 1783, (cm^{-1}, CaF_2, CH_2Cl_2); HRMS (ESI+) calc for $NaC_{15}H_{14}FNO_3$: 298.0855, found 298.0859.

7.5 Experimental details for chapter 3.

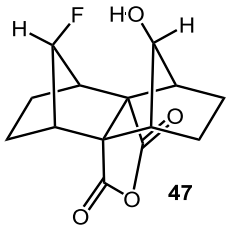

47

12-fluoro-13-hydroxyoctahydro-1,4:5,8-dimethano-4a,8a-(methanoxymethano)-naphthalene-9,11-dione (47). To a solution of **58** (26.5 mg, 0.01 mmol) in 3 mL of dry THF at 0 °C was added a 1M solution of lithium aluminum hydride (LAH) (0.2 mL, 0.02 mmol). The solution was removed from the ice bath and refluxed for 2 hours. The solution was cooled to 0 °C and quenched with water (8 μL), then 15%

aqueous NaOH solution (8 μL) and then water again (24 μL). The mixture was allowed to stir for one hour at room temperature before it was diluted with water and extracted with ethyl acetate (3 x 10 mL), dried and concentrated under reduced pressure. The crude product was purified by silica gel flash column chromatography with a 60% ethyl acetate and hexanes solution to yield **47** as white crystals (8.4 mg, 32% yield); ^{1}H NMR ($CDCl_3$) δ 5.17(d, 1H, *J* = 65.7 Hz), 4.81 (dd, 1H, *J* = 68.5, 11.4 Hz), 4.28 (dd, 1H, *J* = 11.6, 3.5), 2.94 (s, 2H), 2.66 (s, 2H), 1.89 (t, 4H, *J* = 10.9 Hz), 1.67 (t, 2H, *J* = 9.7 Hz), 1.53 (q, 2H, *J* = 15.7, 9.4 Hz); ^{13}C NMR ($CDCl_3$) δ 174.3, 103.8 (d, *J* = 209.3 Hz), 86.6, 70.7, 46.6, 44.6 (d, *J* = 13.2 Hz), 26.5, 24.2 (d, *J* = 11.0 Hz); ^{19}F NMR ($CDCl_3$) δ -180.79 (tt, 1F, *J* = 69.1, 10.3 Hz); IR 3620, 2963, 2914, 1861, 1780, (cm^{-1}, CaF_2, CH_2Cl_2); HRMS (ESI+) calc for $NaC_{14}H_{15}FO_4$: 289.0852, found 289.0856.

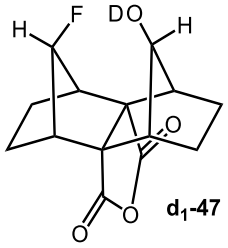

d_1-47

12-fluoro-13-(hydroxy-d)octahydro-1,4:5,8-dimethano-4a,8a-(methanoxymethano)-naphthalene-9,11-dione (d_1-47). Compound **47** was dissolved in *d_1*-methanol with light heat. The solvent was removed *in vacuo*. ^{2}H NMR (CH_2Cl_2) δ 4.64 (d, 1D, *J* = 10.1 Hz); ^{19}F NMR (CH_2Cl_2) δ -181.00 (t, 1F, *J* = 10.3 Hz); IR 2990, 2963, 2916, 2850, 2673, 1858, 1778, (cm^{-1}, CaF_2, CH_2Cl_2).

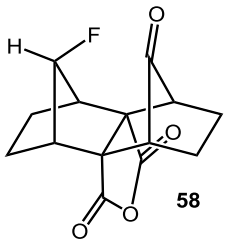

58

13-fluorooctahydro-1,4:5,8-dimethano-4a,8a-(methanoxymethano)naphthalene-9,11,12-trione (58). To a solution of **41** (412 mg, 1.55 mmol) dissolved in 25 mL dichloromethane, was added powdered 3Å molecular sieves (4.74 g) and potassium carbonate (2.03 g). The mixture was cooled to 0 °C and pyridinium chlorochromate (PCC) (501 mg, 2.32 mmol) was added with stirring. The mixture was removed from the ice bath and heated to reflux. The mixture was refluxed overnight, after which it was filtered through celite and concentrated under reduced pressure. The crude product was purified through

flash column chromatography on florisil 60-100 mesh with 20% ethyl acetate and hexanes solution to yield **58** as white crystals (308 mg, 75% yield); ^{1}H NMR ($CDCl_3$) δ 5.09 (dt, 1H, *J* = 56.0, 1.7 Hz), 2.74 (m, 2H), 2.53 (dd, 2H, *J* = 2.6, 1.9), 1.99 (d, 2H, *J* = 10.7 Hz), 1.88 (d, 2H, *J* = 9.6 Hz), 1.69 (q, 2H, *J* = 14.3, 5.8 Hz), 1.57 (m, 2H); ^{13}C NMR ($CDCl_3$) δ 204.7 (d, *J* = 6.6 Hz), 172.0, 102.2 (d, *J* = 205.7 Hz), 64.9 (d, *J* = 2.9 Hz), 44.9 (d, *J* = 15.4 Hz), 44.3 (d, *J* = 1.5 Hz), 22.1 (d, *J* = 9.5 Hz), 20.8; ^{19}F NMR ($CDCl_3$) δ -182.43 (dt, 1F, *J* = 56.7, 7.2 Hz); IR: 2984, 2901, 1864, 1781, (cm^{-1}, CaF_2, CH_2Cl_2); HRMS (ESI+) calc for $NaC_{14}H_{13}FO_4$: 287.0696, found 287.0698.

7.6 Experimental details for chapter 4.

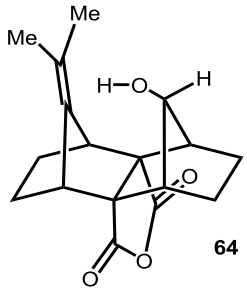

64

***in*-12-hydroxy-13-(1-methylethylidene)octahydro-1,4:5,8-dimethano-4a,8a-(methanoxymethano)-naphthalene-9,11-dione (64).** To a flame dried round bottom flask equipped with a condenser and stir bar was added **72** (0.074 g, 0.26 mmol) in 4 mL dry THF. To the solution was added a 2M lithium borohydride solution (0.52 mL) in THF. The solution was then refluxed for three hours. The solution was then quenched with a saturated solution of ammonium chloride and allowed to stir for an hour. The product was extracted into ethyl acetate, and the combined organic extracts were dried with $MgSO_4$ and concentrated under reduced pressure. The residue was purified by silica gel flash chromatography with a 30% ethyl acetate and hexanes solution to yield **64** as white crystals (0.0099 g, 13% yield); mp = 167-171 °C; ^{1}H NMR ($CDCl_3$) δ 4.25 (d, 1H, *J* = 12.9 Hz), 4.05 (d, 1H, *J* = 13.1 Hz), 3.09 (m, 2H), 2.38 (s, 2H), 1.83 (d, 2H, *J* = 8.8 Hz), 1.78 (s, 6H), 1.74-1.64 (m, 4H), 1.45-1.38 (m, 2H); ^{13}C NMR ($CDCl_3$) δ 173.7, 144.2, 125.3, 85.3, 70.2, 46.4, 42.0, 26.3, 24.7, 20.8; IR 3424, 3063, 2982, 1856, 1778 (cm^{-1}, CaF_2, CH_2Cl_2); HRMS (ESI+) calc for $NaC_{17}H_{20}O_4$: 311.1253, found 311.1257.

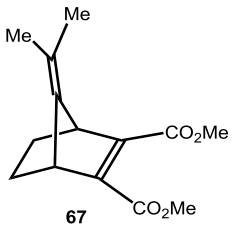

67

dimethyl-7-(1-methylethylidene)bicyclo[2.2.1]hept-2-ene-2,3-dicarboxylate (67). A solution of **66** (0.50 g, 2.01 mmol) dissolved in 20 mL of THF was treated Wilkinson's catalyst (75 mg, 0.081 mmol). The mixture was shaken in a Parr apparatus under hydrogen at 3.2 bar for two days. The mixture was then filtered through celite and concentrated under reduced pressure. The crude product was purified by flash chromatography on florisil with a 20% ethyl acetate and hexanes solution to yield **67** as a pale yellow oil, which solidified overnight into an amorphous solid (0.486 g, 96% yield); ^{1}H NMR ($CDCl_3$) δ 3.76 (s, 6H), 3.67 (m, 2H), 1.8 (d, 2H, *J* = 7.5 Hz), 1.53 (s, 6H), 1.38-1.28 (m, 2H); ^{13}C NMR ($CDCl_3$) δ 165.1, 144.1, 112.1, 52.1, 45.3, 25.5, 19.7; IR 3063, 2956, 2873, 1727, 1618, 1436 (cm^{-1}, CaF_2, CH_2Cl_2); HRMS (ESI+) calc for $NaC_{14}H_{18}O_4$: 273.1097, found 273.1097.

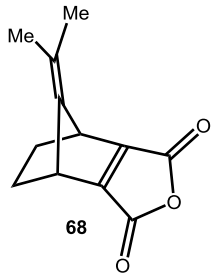

68

8-(1-methylethylidene)-4,5,6,7-tetrahydro-4,7-methanoisobenzofuran-1,3-dione (68). To a stirred solution of **67** (1.31 g, 5.23 mmol) in 50 mL of THF at 0 °C was added lithium hydroxide monohydrate (1.10 g, 26.2 mmol) in 50 mL of water. The solution was allowed to warm to room temperature and continue stirring for an hour. The solution was then acidified with 3M HCl, and extracted with EtOAc (3 x 50 mL). The organic extracts were combined, dried with $MgSO_4$, and concentrated under reduced pressure to yield the carboxylic acid, which was used in the following step without further purification. The carboxylic acid was dissolved in 150 mL of trifluoroacetic anhydride and refluxed for two days. The solvent was distilled off and the crude product was purified by flash chromatography on florisil with a 50% ethyl acetate and hexanes solution to yield **68** as a pale yellow oil, which solidified overnight into an amorphous solid (0.367, 34% yield); ^{1}H NMR ($CDCl_3$) δ 3.86 (s, 2H), 2.06-1.97 (m, 2H), 1.56 (s, 6H),

1.31-1.25 (m, 2H); ^{13}C NMR ($CDCl_3$) δ 159.9, 158.2, 147.7, 115.1, 40.8, 25.4, 19.6; IR 2984, 2949, 2876, 1839, 1768, 1728 (cm^{-1}, CaF_2, CH_2Cl_2).

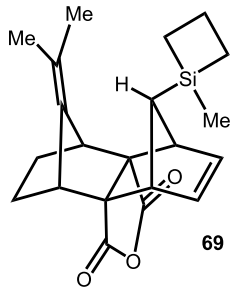

69

***out*-12-(1-methylsiletan-1-yl)-13-(1-methylethylidene)-1,2,3,4,5,8-hexahydro-1,4:5,8-dimethano-4a,8a-(methanoxymethano)-naphthalene-9,11-dione (69).** Anhydride **68** (1.28 g, 6.28 mmol) and silylated diene **40** (2.61 mL, 16 mmol) were combined with DCM (5 mL) in a capped 10 mL syringe. The resulting slurry was then pressurized for two days at 12 kbar. The resulting solution was concentrated under reduced pressure and the residue was purified by silica gel flash chromatography with a 5% ethyl acetate and hexanes solution to yield **69** as white crystals (0.41 g, 18% yield); mp = 156-158 °C; ^{1}H NMR ($CDCl_3$) δ 6.36 (s, 2H), 3.28 (m, 2H), 3.11 (m, 2H), 2.82 (s, 1H), 2.03-1.88 (m, 2H), 1.69 (d, 2H, J = 10 Hz), 1.64 (s, 6H), 1.57-1.50 (m, 2H), 0.93-0.75 (m, 4H), 0.16 (s, 3H); ^{13}C NMR ($CDCl_3$) δ 173.7, 142.7, 139.3, 119.5, 67.5, 51.8, 48.4, 42.2, 26.0, 20.7, 18.5, 14.9, -0.4; IR 2968, 2929, 2887, 1857, 1776, 1217 (cm^{-1}, CaF_2, CH_2Cl_2); HRMS (ESI+) calc for $NaC_{21}H_{26}O_3Si$: 377.1543, found 377.1544.

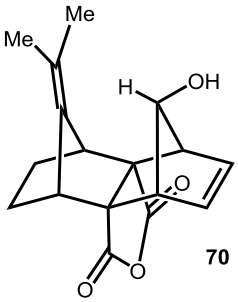

70

***out*-12-hydroxy-13-(1-methylethylidene)-1,2,3,4,5,8-hexahydro-1,4:5,8-dimethano-4a,8a-(methanoxymethano)-naphthalene-9,11-dione (70).** Compound **69** (0.41 g, 1.16 mmol) was dissolved in a 1:1 mixture of THF and methanol (50 mL) to which was added potassium fluoride (0.134 g, 2.31 mmol) and potassium bicarbonate (0.231 g, 2.31 mmol). The mixture was then cooled to 0 °C and 30% hydrogen peroxide (1.96 mL, 17 mmol) was added dropwise. The solution was stirred overnight at room

temperature. The solution was mixed with water to dissolve any salts and extracted once with ethyl acetate. The organic layer was washed with a 10% aqueous sodium sulfite solution. Aqueous layers were combined and extracted with ethyl acetate (3 x 50 mL). All organic fractions were combined, dried with $MgSO_4$, and concentrated under reduced pressure. The residue was purified by silica gel flash chromatography with a 30% ethyl acetate and hexanes solution to yield **70** as white crystals (0.29 g, 88% yield); mp = 174-177 °C; ^{1}H NMR ($CDCl_3$) δ 6.34 (s, 2H), 5.19 (s, 1H). 3.24 (m, 2H), 3.13 (m, 2H), 2.19 (s, 1H), 1.68 (s, 6H), 1.68-1.64 (m, 2H), 1.50-1.42 (m, 2H); ^{13}C NMR ($CDCl_3$) δ 172.3, 142.4, 135.2, 119.3, 83.7, 64.1, 54.1, 41.7, 25.7, 20.8; IR 3608, 3558, 3060, 2966, 2894, 1854, 1779 (cm^{-1}, CaF_2, CH_2Cl_2); HRMS (ESI+) calc for $NaC_{17}H_{18}O_4$: 309.1097, found 309.1098.

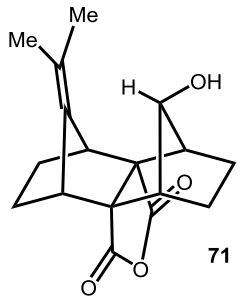

71

***out*-12-hydroxy-13-(1-methylethylidene)octahydro-1,4:5,8-dimethano-4a,8a-(methanoxymethano)-naphthalene-9,11-dione (71).** Compound **70** (0.450 g, 1.57 mmol) was added to a flame dried three-neck round bottom flask with large stir bar under nitrogen. Dipotassium azodicarboxylate (2.14 g, 11 mmol) was added and the solids were dissolved in methanol (80 mL). Glacial acetic acid (1.26 mL, 22 mmol) was added dropwise to the stirred mixture. The mixture was allowed to stir until complete consumption of the starting material was observed by TLC (2 hours). The mixture was slowly quenched with water until gas evolution ceased. The product was extracted with ethyl acetate (3 x 30 mL), and the combined organic extracts were dried with $MgSO_4$ and concentrated under reduced pressure. The residue was purified by flash chromatography on florisil with a 30% ethyl acetate and hexanes solution to yield **71** as white crystals (0.36 g, 79% yield); mp = 179-181 °C; ^{1}H NMR ($CDCl_3$) δ 5.28 (s, 1H), 2.97 (s, 2H), 2.41 (m, 2H), 2.05 (d, 2H, *J* = 9.2 Hz), 1.70 (s, 6H), 1.62-1.55 (m, 2H), 1.55-1.48 (m, 2H), 1.48-1.39 (m, 2H); ^{13}C NMR ($CDCl_3$) δ 173.6, 143.3, 118.0, 76.7, 65.8, 47.1, 42.6, 25.7, 23.8, 20.9; IR 3612, 2972, 2895, 1854, 1777 (cm^{-1}, CaF_2, CH_2Cl_2); HRMS (ESI+) calc for $NaC_{17}H_{20}O_4$: 311.1254, found 311.1254.

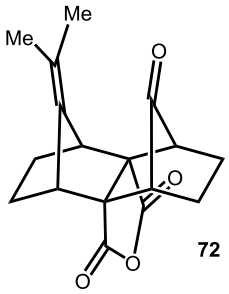

13-(1-methylethylidene)octahydro-1,4:5,8-dimethano-4a,8a-(methanoxymethano)-naphthalene-9,11,12-trione (72). To a flame dried round bottom flask equipped with a condenser and large stir bar, was added **71** (0.10 g, 0.35 mmol), crushed 3 Å molecular sieves (0.89 g) and potassium carbonate (0.38 g). To the mixture was added DCM (20 ml) followed by cooling to 0 °C. Pyridinium chlorochromate (PCC) (0.094 g, 0.438 mmol) was added and the solution was allowed to warm to room temperature before being refluxed overnight. The mixture was then filtered through celite and concentrated under reduced pressure. The residue was purified by silica gel flash chromatography with a 20% ethyl acetate and hexanes solution to yield **72** as white crystals (0.072 g, 72% yield); mp = 160-164 °C; ^{1}H NMR ($CDCl_3$) δ 2.99 (m, 2H), 2.26 (m, 2H), 1.87 (d, 2H, *J* = 10.8 Hz), 1.76 (d, 2H, *J* = 9.4 Hz), 1.68-1.6 (m, 4H), 1.60 (s, 6H); ^{13}C NMR ($CDCl_3$) δ 205.4,172.1, 134.7, 129.8, 62.3, 45.1, 43.3, 25.1, 21.1, 19.4 ; IR 2988, 2893, 1863, 1781, 1764 (cm^{-1}, CaF_2, CH_2Cl_2); HRMS (ESI+) calc for $NaC_{17}H_{18}O_4$: 309.1103, found 309.1106.

7.7 Experimental details for chapter 5.

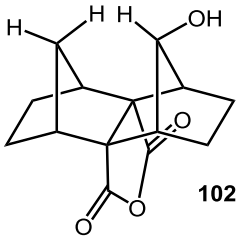

12-hydroxyoctahydro-1,4:5,8-dimethano-4a,8a-(methanoxymethano)naphthalene-9,11-dione (102). Alcohol **105** (0.116 g, 0.47 mmol) was dissolved in THF (20 mL) and palladium on carbon (0.02 g) was added. The mixture was hydrogenated on a Parr hydrogenator at 2.4 bar for five hours. The catalyst was removed by filtration through celite and the sample was concentrated under reduced pressure to yield **102** as white crystals (0.111, 95%); ^{1}H NMR ($CDCl_3$) δ 5.14 (s, 1H), 2.62 (s, 2H), 2.43 (m, 2H), 2.35 (d, 1H, *J*

= 11.9 Hz), 2.07 (d, 2H, *J* = 9.6 Hz), 1.64 (d, 2H, *J* = 10.6 Hz), 1.48 (d, 1H, *J* = 12.7 Hz), 1.49-1.39 (m, 4H); ^{13}C NMR ($CDCl_3$) δ 174.1, 78.0, 67.2, 46.8, 43.2, 43.0, 27.6, 24.1; IR 3055, 2977, 2901, 1861, 1781, (cm^{-1}, CaF_2, CH_2Cl_2)); HRMS (ESI+) calc for $NaC_{14}H_{16}O_4$: 271.0946, found 271.0941.

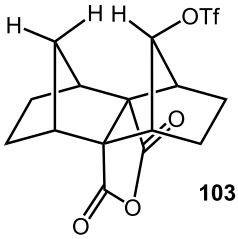

103

9,11-dioxooctahydro-1,4:5,8-dimethano-4a,8a-(methanoxymethano)naphthalen-12-yl trifluoromethanesulfonate (103). To a flame dried round bottom flask was added **102** (0.1 g, 0.40 mmol) dissolved in DCM (5 mL). The solution was treated with pyridine (0.18 mL, 2.30 mmol) and cooled to -78 °C. A 1M triflic anhydride solution in DCM (0.6 mL, 0.60 mmol) was added dropwise, and the solution was allowed to stir at room temperature for 1.5 h. The solution was washed with a cold 10% aqueous $NaHCO_3$ solution, then brine. The organic layer was isolated, dried with magnesium sulfate and concentrated under reduced pressure. The crude product was purified by flash chromatography on florisil with a 20% ethyl acetate and hexanes solution to yield **103** as white crystals (0.143 g, 94%); ^{1}H NMR ($CDCl_3$) δ 5.95 (s, 1H), 2.84 (m, 2H), 2.73 (m, 2H), 2.18 (d, 1H, *J* = 12.5 Hz), 2.07 (d, 2H, *J* = 9.6 Hz), 1.73 (d, 2H, *J* = 9.0 Hz), 1.67 (d, 2H, *J* = 8.8 Hz), 1.62 (d, 1H, *J* = 12.5 Hz), 1.51 (d, 2H, *J* = 8.9 Hz); ^{13}C NMR ($CDCl_3$) δ 172.1, 118.5 (q, *J* = 320 Hz), 90.9, 66.3, 45.8, 43.2, 42.9, 27.4, 24.0; ^{19}F NMR ($CDCl_3$) δ -75.40 (s, 3F); IR 2982, 2908, 1861, 1785, (cm^{-1}, CaF_2, CH_2Cl_2)); HRMS (ESI+) calc for $NaC_{15}H_{15}F_3O_6S$: 403.0439, found 403.0441.

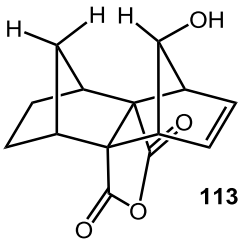

113

12-hydroxy-1,2,3,4,5,8-hexahydro-1,4:5,8-dimethano-4a,8a-(methanoxymethano)-naphthalene-9,11-dione (113). Anhydride **100** (0.5 g, 3.05 mmol) and silylated diene **40** (1.49 mL, 9.14 mmol) were combined with DCM (4 mL) in a capped 10 mL syringe. The resulting slurry was then pressurized for

three days at 12 kbar. The resulting solution was concentrated under reduced pressure and the residue was purified by silica gel flash chromatography with 5% ethyl acetate and hexanes to yield an inseparable mixture of the Diels-Alder products (1.06 g) as a white waxy solid. The mixture of isomers was then dissolved in a 50:50 mixture of THF and methanol (50 mL). Potassium fluoride (6.74 mmol) and potassium bicarbonate (6.74 mmol) were then added and the solution was cooled to 0 °C. Then 5.73 mL of 30% hydrogen peroxide was added dropwise to the flask. The solution was allowed to warm to room temperature and stirred overnight. The solution was quenched with a 10% solution of sodium sulfite (20 mL) and extracted four times with ethyl acetate. The organic layers were washed with water and brine, dried with magnesium sulfate and concentrated under reduced pressure. The crude product was purified by gradient column chromatography on silica gel with 30% then 50% ethyl acetate and hexanes to yield **113** as white crystals (0.116 g, 15%); ^{1}H NMR ($CDCl_3$) δ 6.39 (m, 2H), 5.04 (d, 1H, *J* = 11.7 Hz), 3.34 (m, 2H), 2.80 (m, 2H), 2.39 (d, 1H, *J* = 12.1 Hz), 2.21 (d, 1H, *J* = 11.7 Hz), 1.75 (d, 2H, *J* = 9 Hz), 1.56 (d, 1H, *J* = 12.1 Hz), (d, 2H, *J* = 9.3 Hz); ^{13}C NMR ($CDCl_3$) δ 172.6, 135.9, 84.9, 65.9, 54.1, 43.0, 41.5, 27.5; IR 3564, 3054, 2975, 2902, 1858, 1782, (cm^{-1}, CaF_2, CH_2Cl_2)); HRMS (ESI+) calc for $NaC_{14}H_{14}O_4$: 269.0784, found 269.0783.

7.8 Experimental details for chapter 6.

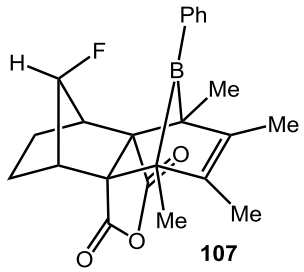

107

12-fluoro-1,2,3,4-tetramethyl-13-phenyl-1,4,5,6,7,8-hexahydro-1,4-borano-5,8-methano-4a,8a-(methanoxymethano)naphthalene-9,11-dione (107). To a sealed tube was added freshly made dimer **105** (0.971 g, 2.48 mmol) dissolved in 3 mL dry, degassed DCM and dienophile **20** (0.903, 4.96 mmol). The tube was sealed and heated at 80 °C for six hours. The solvent was removed in vacuo and the crude product was purified by flash column chromatography on florisil with a 5% ethyl acetate and hexanes solution to yield **107** as white crystals (0.8426 g, 45% yield); mp = 182 °C; ^{1}H NMR ($CDCl_3$) δ 7.26-7.20

(m, 3H), 7.18-7.09 (m, 2H), 5.11 (d, 1H, J = 56.7 Hz), 2.96 (m, 2H), 1.88 (m, 6H), 1.82 (d, 2H, J = 8.8 Hz), 1.48 (s, 6H), 1.42 (m, 2 H); ^{13}C NMR ($CDCl_3$) δ 173.0 (J = 0.7 Hz), 133.58, 133.55, 131.0 (J = 2.6 Hz), 128.0, 127.7, 103.5 (J = 206.0 Hz), 73.0 (J = 4.8 Hz), 42.1 (J = 15.5 Hz), 21.6, 21.4, 12.1, 11.5; ^{19}F NMR ($CDCl_3$) δ -189.1 (d, 1F, J = 56.8 Hz); IR 3055, 2963, 2932, 1856, 1772, (cm^{-1}, CaF_2, CH_2Cl_2).

7.9 References.

[1] ACD/ChemSketch Freeware, Version 12.01, Advanced Chemistry Development, Inc., Toronto, ON, Canada, www.acdlabs.com, 2012.

[2] Gaussian 09, Revision A.1, M. J. Frisch, et al. Gaussian, Inc., Wallingford CT, 2009.

[3] Spartan '10 Program, Wavefunction Inc., Irvine, CA.

[4] Merrick, J. P.; Moran, D.; Radom, L. *J. Phys. Chem. A* **2007**, *111*, 11683−11700.

Vita

Mark D. Struble was born in West Chester, Pennsylvania to Bob and Paula Struble. He graduated from B. Reed Henderson High School in 2007. Following that he obtained a B.S. in Chemistry from The Pennsylvania State University in 2011. While at Penn State he did undergraduate research in the lab of Dr. Bratoljub H. Milosavljevic, studying the agglomeration of gamma irradiated aqueous ovalbumin solutions. Additionally, he spent the summer of 2009 working at Stroud Water Research Center as part of a REU program. At Stroud he worked for Dr. Anthony K. Aufdenkampe, investigating spectroscopic methods for characterizing soil samples.

In the fall of 2011, he began his studies at The Johns Hopkins University in Baltimore. He soon joined the research group of Professor Thomas Lectka. His research focused on the synthesis of unique caged compounds and their resulting reactivity. Special attention was given to compounds containing fluorine. While he was at Hopkins he published no less than 7 papers. He was the recipient of the Gary H. Posner Fellowship (2013) and the Rudolph Sonneborn Fellowship (2015-2016), both from the chemistry department at JHU.

Following the completion of his graduate studies, he will be moving to Northwestern University as a Postdoctoral Fellow in the research group of Professor Samuel I. Stupp. There he will be engaged in the study of self-assembling organic materials and supramolecular chemistry.